Università degli Studi di Cagliari

PhD program in Life, Environmental and Drug Sciences

XXIX cycle

LIPOSOMES FOR siRNA AND SMALL MOLECULE DELIVERY

SSD: CHIM/09

PhD candidate: **Michele Schlich**

PhD program coordinator: **Prof. Enzo Tramontano**

Supervisor: **Prof. Francesco Lai**

Academic Year 2015-2016

Defended in April 2017

Section I

Liposomes for siRNA delivery

Chapter I

Introduction

Chapter II

RVG-modified liposomes for siRNA delivery to primary neuronal cells: evaluation of alpha synuclein knockdown efficacy

Section II

Liposomes for subcutaneous drug delivery

Section I

Liposomes for siRNA delivery

Chapter I
Introduction

1. RNA interference

RNA interference (RNAi) is a naturally occurring, efficient and specific pathway by which short double-stranded RNAs (dsRNA) mediate the inhibition of gene expression [1].

The mechanism of RNAi is exploited by cells to auto-regulate gene expression at a post-transcriptional level, and it has been demonstrated to have a crucial role in a plethora of physiologic cell processes, such as the down-regulation of transcription factors, protein degradation and signal transduction [2,3]. Moreover, RNA interference is an essential part of the immune response mechanism, being able to prevent the expression of viral genes [4,5].

In its essence, the RNAi mechanism is carried out in the cytoplasm, where the translation of a target messenger RNA (mRNA) is impeded due to its degradation. The mRNA to be targeted (or "silenced") is recognized by the base pairing with the antisense strand of the dsRNA, which activates a dedicated enzymatic machinery in charge for mRNA degradation [6].

The first report of RNAi was published by Napoli et al in the 1990 [7]. In the attempt to produce deep purple petunias, the authors overexpressed chalcone synthase, the enzyme responsible for the purple pigmentation, in the plants. Surprisingly, the transfected plants produced white flowers instead of purple ones, due to a reduction in chalcone synthase levels of over 50 folds compared to the wild type. This first, apparently controversial result, was followed by other researches on the gene-

suppressing action triggered by exogenous genetic material [8]. In 1998, RNAi was identified and described in animals by Fire and Mello, which were subsequently awarded the Nobel Prize in Physiology and Medicine, in 2006 [9]. Few years later, Tuschl et al provided the proof of RNAi-mediated silencing in mamalian cells, paving the way for its use as a tool for gene function research or as therapeutics [10].

1.1. Mechanism of gene silencing

The dsRNAs mediating RNAi can be classified in two groups: endogenous micro RNAs (miRNAs) or short interfering RNAs (siRNAs). These two dsRNAs have different origin, intracellular processing and mechanism of action, but they both ultimately lead to the degradation of the target mRNA and consequent inhibition of gene expression [1].

1.1.1. miRNA

The biogenesis of miRNA begins within the cell nucleus, where long primary micro RNAs (pri-miRNAs) are transcribed, typically by RNA polymerases II, from a wide variety of genes that may code for a cluster of different miRNAs, or for a miRNA and a protein [11]. The regulation of miRNA expression is still a relatively unexplored field, although in some cases it has been demonstrated that the target protein of a specific miRNA represses the expression of the miRNA itself, thus forming a feedback loop [12]. Structurally, pri-miRNAs are composed by a stem of approximately 33 imperfectly paired bases, ending in a hairpin-loop structure on one side, with flanking segments on the other side (**Figure 1.1**). Shortly after their transcription, pri-miRNAs are processed within the nucleus by Drosha, a RNAse III ribonuclease, to produce shorter pre-miRNAs, which are subsequently transported to the cytoplasm by the

karyopherin Exportin-5. Once in the cytoplasm, the pre-miRNAs are processed by the endoribonuclease Dicer, which removes the loop to yield a double stranded, functional miRNA of 21-25 base pairs [13]. The double stranded miRNA is subsequently unwound and the antisense strand (also called guide strand) is selected and loaded onto the RNA-induced silencing complex, RISC. The mechanism of strand selection is still being investigated, but the thermodynamic instability of the guide strand is supposed to have a role [14]. The miRNA strand loaded on the RISC has the function of selecting and binding to a complementary mRNA, which has been suggested to interact through its 3'UTR region [15]. The hybridization is known to be imperfect, and it has been shown that nucleotides 2 to 8 from the 5' end of the guide strand, also called the seed region, are essential for target recognition [16]. The precise molecular mechanism of silencing is still unknown. The hypothesis of gene silencing through ribosomal translational arrest or repression of initiation is the most supported, although also mRNA cleavage by an argonaute protein (Ago) taking part in the RISC has been detected [15,17]. The final result of this process is the post transcriptional gene silencing (PTGS) and, as a result, a lacking synthesis of the target protein.

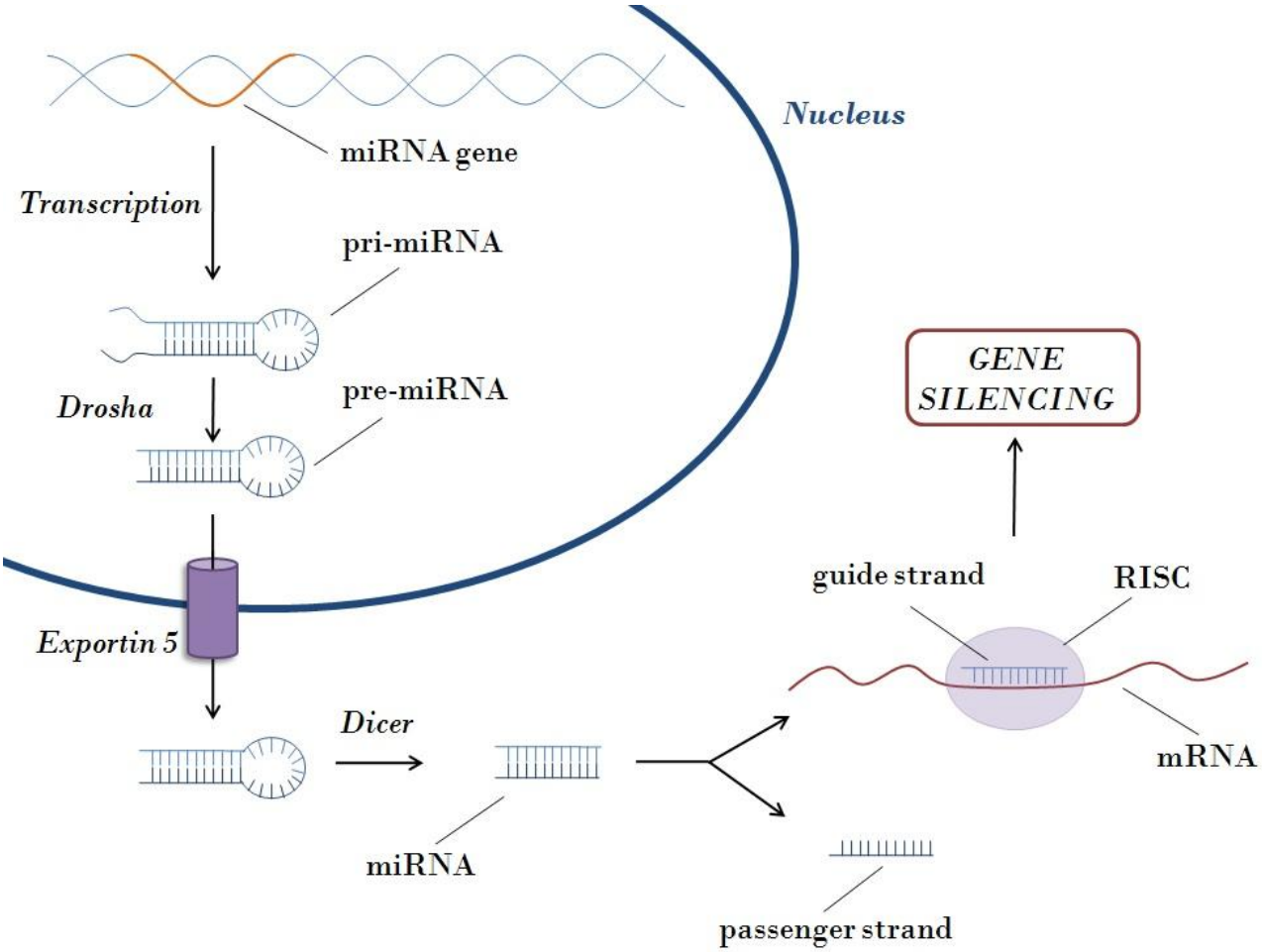

Figure 1.1. Schematic representation of the biogenesis, nuclear export and gene silencing mechanism of miRNA

1.1.2. siRNA

siRNAs derive from long, perfectly paired dsRNAs present in the cytoplasm. These dsRNA were initially thought to have an exogenous origin only, being taken up from the environment or deriving from viral infections. However, more recently, endogenous sources of dsRNA have been identified in animals [18]. In the cytoplasm, the dsRNAs are processed by Dicer which reduces them to form 21-23 bp long siRNAs. As for miRNAs, the double stranded siRNA is divided in the guide strand, to be loaded on the RISC, and the passenger strand, which is subsequently degraded. The siRNA-RISC complex binds to a complementary mRNA through a perfect pairing,

which induces the activation of Ago [11]. The PIWI domain of the Ago protein has a double-stranded RNA-guided hydrolytic function, which cleaves the target mRNA between the nucleotides that are base paired to siRNA residues 10 and 11[19]. Such a precise cut is followed by release of the truncated mRNA from the RISC, which could repeat its action on other targets, while the fragments of mRNA are attacked by cellular exonucleases to complete the degradation process [19].

1.1.3. Differences miRNA - siRNA

Although they both ultimately inhibit translation of mRNAs into their protein products, miRNAs and siRNAs show important differences.

Firstly, the miRNA biogenesis involve a nuclear processing, with consequent exportation to the cytoplasm through a dedicated transporter, while siRNA are formed directly in the cytoplasm [11,15]. These two class of short RNA duplexes share the use of Dicer to shape their final structure which will enter the RISC [20]. An additional difference is related to the mechanism of gene silencing: while siRNAs accomplish a perfect hybridization with the target mRNA, leading to a site-specific slicing by Ago, miRNA bases only partially binds to the mRNA counterparts, thus activating different mechanisms such as ribosomal arrest or translocation to P bodies [11,15]. As a result of this incomplete and promiscuous binding, a single miRNA is probably able to silence a large number of genes, while a siRNA has a higher specificity towards a single target mRNA.

1.2. Exogenous induction of RNAi

The mechanism of RNAi can be artificially induced by an exogenous agent, which is usually a siRNA or DNA encoding for a shRNA (short hairpin RNA)[21,22].

siRNAs are double stranded RNAs of 21-23 nucleotides, with a molecular weight of approximately 14 kDa, and a net negative charge deriving from their backbone of phosphate groups. They can be obtained by chemical synthesis thus allowing a precise control of the sequence needed, including chemical modifications where required, and a feasible scale up of the production [23].

Once delivered in the cytoplasm, siRNAs are able to trigger RNAi being directly loaded on the RISC, with no further processing. The gene knockdown, however, may be transient (up to 5-7 days) due to the dilution effect following cell proliferation and the degradation of siRNA by nucleases [24]. In fact, to predict the duration of the gene knockdown, the proliferation rate of the target cells, as well as the turnover rate of the target gene should be considered. In slowly dividing or non-dividing cells, the gene knockdown was reported to last for several weeks, with the siRNA stability being identified as the only limiting factor [25]. Conversely, in the case of proliferating cells, repeated administration of siRNAs are needed to maintain the silencing effect for a prolonged time.

The use of DNA (plasmidic or embedded in a viral vector) encoding for a shRNA (from now on called shRNA) could be an efficient alternative if a sustained block of the target gene expression has to be achieved. The DNA must be delivered within the nucleus and included in the host cell genome, posing its transcription under the control of a promoter suitable for the experimental needs [21,26].

The choice of the promoter would define which RNA polymerase isoform would transcribe the gene, and could allow the control of RNAi induction in a spatio-temporal manner [22]. The shRNA-encoding gene is transcribed in a pri-shRNA, which is processed by Drosha to yield a pre-shRNA, exported to the cytoplasm and further processed by Dicer to finally obtain the functional dsRNA, possessing similar

characteristics of a siRNA [27]. Exploiting the cellular transcription pathways to have a "siRNA factory within the cell" would turn in a stable and everlasting target gene silencing, which could be desirable for several applications (see paragraph 1.3). However, the need to deliver the DNA within the nucleus poses an additional barrier to be overcome by the delivery construct, and the approach might not be successful in quiescent and non-replicating cells [28]. Moreover, the intranuclear processing of shRNA could lead to a competition with the miRNA synthetic pathway, with unpredictable side effects deriving from reduced or abolished endogenous RNAi [29]. More in detail, it has been shown that the Exportin 5, which mediates the export of dsRNAs to the cytoplasm, is a rate-limiting component of the RNAi machinery, thus being suspected as the main factor for shRNA/miRNA competition [30,31]. Thus, a precise control of shRNA transcription, which could be achieved by tailoring the expression construct and exploiting tissue-specific promoters, is crucial to avoid the saturation of RNAi-involved enzymes [32].

Conversely, the siRNAs do not compete with the endogenous RNAi processes because they do not need any processing before entering the RISC [33].

1.3. Applications of artificially-induced RNAi

Artificially induced RNAi through siRNA or shRNA takes advantage of an endogenous biochemical pathway, and exploits it to destroy specific target transcripts and achieve gene silencing. As such, RNAi has been used to elucidate gene and protein functions, allowing the establishment of high-throughput screening formats [6]. However, the initial enthusiasm for the great potential of this approach is now reduced due to several limitations. For example, the relationship between the gene activity and the obtained phenotype has showed to be non-linear for many genes, thus impeding a

straightforward correlation between RNAi potency and macroscopic effects [34]. In several cases, RNAi has been exploited to produce transgenic animals, such as individuals characterized by a nearly-complete (knockdown) or partial (hypomorfic) suppression of a target gene [35,36]. In addition, RNAi could be used to generate *in vivo* models of disease, following the silencing of a gene which down-regulation is involved in the pathophysiology of the disease [37].

The therapeutic use of artificially induced RNAi has been foreseen right after RNAi discovery in mammals [10]. The great potential hold by this strategy relies on the fact that many diseases are related to the disregulation or the overexpression of a specific protein, and RNAi is potentially able to selectively silence any target gene, once the mRNA sequence is known. Oncology probably represents the greatest field of applications for therapeutic RNAi. In fact, the recent advances in the characterization of oncogenes involved in the development and progression of tumours, supply a large library of potential targets for RNAi, with several constructs under clinical evaluation [38]. Moreover, the silencing could be directed towards pro-survival genes, as well as genes involved in the multi-drug resistance of the tumour, which could turn in an improved efficacy of chemotherapy [39]. The therapeutic potential of RNAi is not limited to cancer treatment, and a great effort has been put in the evaluation of RNAi-based therapeutics for neurodegenerative, infectious and other disease with a genetic etiologic component [40,41]. In 2004, the first phase I clinical trial for a siRNA construct (bevasiranib) was initiated by Opko Health Inc [42]. Despite the current absence of approved siRNA-based medicines, more than 50 clinical trials of siRNAs for the cited applications have been or are being conducted since 2004, with several products reaching phase II and III [41].

2. RNAi delivery: challenges and opportunities

2.1. Barriers in the delivery of RNAi-based therapeutics

One of the most important issues for the therapeutic use of siRNAs and shRNAs, is represented by their unfavorable physico-chemical properties, which are directly linked to poor pharmacokinetics [39]. Ideally, the siRNA molecules systemically administered have to be stable in the circulation, effuse from the blood vessel to the surrounding tissue at the target site, cross the cell membrane and reach the cytoplasm to be loaded on the RISC and achieve gene silencing. Moreover, if the therapeutic construct is a shRNA, crossing the nuclear membrane is an additional requirement for the activity. Unfortunately, several barriers are hindering the siRNA path from the administration to the site of action. In the next paragraphs, an overview of the issues associated with siRNA delivery will be presented through a classification in kinetic and physical barriers.

2.1.1. Kinetic barriers

The first concern for siRNA delivery is the stability of the RNA itself. Once injected in the bloodstream, the siRNAs are quickly cleared by renal glomerular filtration due to their relatively small size, paired with the absence of an absorption transporter in the tubules [43,44]. Moreover, siRNAs are susceptible of enzymatic degradation, which is triggered by circulating and tissue ribonucleases (RNases) and lead to a short plasma half life [45]. RNases are a class of commonly occurring enzymes which are practically ubiquitous in the organism and rapidly trigger RNA hydrolysis through the interaction with the siRNA backbone [46]. In order to increase the circulation time, siRNAs have been chemically modified, conjugated or complexed with stabilizing

molecules (see paragraph 2.2). However, conjugated/complexed siRNA, have to avoid the uptake by the mononuclear phagocyte system (MPS), unless their final target cells are the macrophages themselves. Rather than by the siRNA itself, the phagocytic process is activated by the recognition of specific opsonin proteins absorbed on the surface of the exogenous agent [47]. Opsonins are a family of proteins present in the bloodstream which includes immunoglobulins, complement proteins, components of the extracellular matrix and other plasma proteins (e.g. albumin, laminin). The exact mechanism underlying the opsonization process is still not completely understood, however, it has been shown that size, charge and surface properties of the nanoparticles influence the degree and rate of opsonization [48].

2.1.2. Physical barriers

In the case of systemic administration routes other than intravenous injection (i.e. oral, subcutaneous), the first physical barrier to be overcome by the RNAi trigger is represented by the absorption in the bloodstream. This could be an hard task especially for orally administered siRNA constructs, which have to survive the harsh conditions of the gastrointestinal tract [49]. Conversely, huge effort is being put in the development of efficient subcutaneous delivery platforms for siRNA, as this administration procedure could be performed without trained professionals in a domestic setting. However, in order to reduce the complexity of delivery, the intravenous route is currently the most used in preclinical and clinical trials [50].

Once a stable, long circulating siRNA construct is intravenously injected, it has to face the obstacle represented by extravasation in the target organ (or tissue). Due to their nature of hydrophilic and negatively charged macromolecules, siRNA and shRNA can not cross the cell membranes by passive diffusion. This prevents them to get out from

the bloodstream by transcellular transport, unless they are chemically modified to circumvent this issue (see paragraph 2.2). Thus, getting out from the bloodstream is strongly dependent on the specific characteristics of the endothelium, such as the presence of fenestrations and their size. It is known that these structural features of the endothelium are highly variable depending on the perfused organ, thus implying that a uneven distribution in the different districts would be achieved after iv administration [50]. The next barrier, after having crossed the endothelium and the extracellular matrix, is the cell membrane. Again, the hydrophilic character and the high molecular weight of siRNA and shRNA prevent their uptake by passive diffusion. Moreover, the negatively charged phosphate backbone cannot favorably interact with the anionic heparan sulfate proteoglycans on the cell surface [51]. Usually, the cell uptake is triggered by the inclusion of the RNAi-agent in a nanocarrier or by conjugation. In those cases, the major mode of internalization is endocytosis, which would turn in the formation of an intracellular vesicle (endosome) entrapping the RNAi therapeutic cargo [51]. In this scenario, it is essential for the siRNA/shRNA construct to escape from the endosome and reach the cytoplasm to avoid lysosomal degradation. Once in the cytoplasm, the siRNA could finally mediate the RNAi and silence its target gene, while, if a shRNA has to be administered, it still have to cross the nuclear membrane, which represent the last physical barrier to be overcome by this type of agents [21,39].

2.2. Approaches for siRNA delivery

As described in the previous sections, the systemic administration of unmodified naked siRNA or shRNA is not sufficient to achieve a biological response due to serious delivery and stability issues. Thus, great effort is being put in the research of the most

convenient strategy to increase the pharmacokinetic performances of those agents without altering their ability to trigger RNAi. In the following sections, the main approaches reported in the literature will be reviewed, posing greatest attention on the non-viral delivery through the use of nanocarriers.

2.2.1. Chemical modification of siRNA

The options for the structural modification of siRNA are essentially of two types: one concerns the substitution of one or more atoms on the phosphate-sugar backbone, while the second involves the conjugation of siRNA with another molecule through the formation of a new covalent bond (usually between the passenger strand and the conjugated entity)[52].

The first strategy is often employed to increase the nuclease resistance of siRNA, and can be accomplished by the substitution of the phosphate moiety with a phosphorothioate or boranophosphate or by the introduction of an alternative group in position 2' of the sugar (i.e. 2'-O-methyl, 2'-deoxy, 2'-fluoro, 2'-methoxyethyl, locked nucleic acids) [53]. The rationale behind these modifications lies in the fact that additional groups in the siRNA structure introduce a steric hindrance, which prevents the interaction between the RNase active site and the chemically modified siRNA, thus impeding the enzyme-catalysed hydrolysis. However, much care has to be put in understanding the structure-activity relationship of modified siRNA, since some modifications may reduce the silencing efficiency due to a impeded recognition by the RISC, or may lead to toxicity [54]. Nowadays, the effect of several modifications at different sites of the siRNA backbone are described, and many companies in the field of oligonucleotides synthesis have their own proprietary modification patterns [54,55].

On the other hand, the conjugation of siRNA to another molecule is often exploited to obtain a new chemical entity (conjugate) possessing some advantageous properties of the conjugated molecule and maintaining the RNAi activity of siRNAs. The new covalent bond between the two can be formed exploiting a variety of reactions and linkers, and several molecules (polymers, peptides, lipids, targeting ligands) have been used to prepare siRNA-conjugates [52]. For instance, the chemical conjugation of cholesterol or other lipids has shown to increase the liver accumulation and the cell uptake due to the more lipophilic character of the conjugate as compared to the naked siRNA [56]. To prolong the circulation time and avoid the uptake by the MPS cells, siRNA-PEG conjugates have been synthesized and tested *in vivo* [57]. This strategy exploits the well-known ability of the hydrophilic polymer PEG (polyethyleneglycole) of shielding the circulating exogenous agent to avoid the opsonization and subsequent phagocytosis [58]. Moreover, a targeting ligand could be covalently linked to the siRNA, which would benefit of the receptor-mediated endocytosis triggered by the conjugated molecule, leading to an increased cell uptake [59].

2.2.2. Viral delivery

Viral vectors have been used as a research tool to transfer genetic material into mammalian cells for more than 30 years. More recently, it has been suggested that the same principle could have been used to induce the stable expression of a shRNA by the target cell [60]. This approach exploits the ability of viruses to insert their genetic material in the host cell's nucleus. Thus, the viral genetic material can be engineered to encode the required shRNA, which would be transported within the nucleus of the target cell, transcribed by the host's transcriptional machinery and

subsequently exported to the cytoplasm for gene silencing [61]. Currently, there are five types of viral vectors which are used for shRNA delivery, namely retrovirus, lentivirus, adenovirus, adeno-associated-virus (AAV), and baculovirus.

Each different viral delivery system has some advantageous properties which are related to its inherent ability of genetic transducer and to its mechanism of action. For instance, retroviruses have the advantage of inducing a stable transfection, which can be inherited by daughter cells and could be of particular interest for the treatment of chronic infections and cancer [39]. Conversely, adenoviruses are characterized by a less stable silencing activity due to the lack of a stable integration in the host's genome. In addition, adenoviruses lack a definite tissue tropism and tend to accumulate in the liver, where they may induce toxicity. Basing on these features, the use of adenoviral vectors could be the right choice when a transient silencing activity is needed and the liver is the main target organ for the RNAi therapy [61]. Lentiviruses have the peculiar ability of transfecting non-dividing cells, thus being an intriguing option for neuronal delivery [62]. Despite the many advantages, the use of viral vectors is associated with their potential of inducing an immune response, which could lead to severe acute toxicity [63]. Moreover, if the mechanism of transfection include the integration in the host cell's genome, as in the case of retroviruses, there is the risk for insertional mutagenesis and carcinogenesis [61]. On the other hand, adenoviruses and adeno-associated viruses are not mutagenic, since they deliver their genetic material with no insertion in the host's genome. However, since many common human infections are triggered by adenoviruses, the patient immune system could have developed neutralizing antibodies that could inactivate the adenoviral vector, interfering with its delivery task [64]. Conversely, adeno-associated viruses are not known to be related to any disease and, because of their low

immunostimulatory activity and their safety profile, they have been used in over 100 gene therapy clinical trials for cancer, neurodegenerative disorders and other genetic diseases [65].

Despite the great attractiveness of viral vectors, in many cases confirmed by promising human data, serious concerns still exist regarding the potential for immune response, the neutralization by circulating antibodies and the scalability of the production, which require further consideration.

2.2.3. Non-viral delivery

The alternative to viral vectors consist in a wide variety of non-viral vectors for siRNA and, to a lower extent, to shRNA delivery. These delivery platforms are based on non-covalent interactions between the nucleic acid and a number of molecules and/or macromolecule, with the great majority being polymers or lipids [66]. Depending on the physico-chemical properties of the lipidic or polymeric material, the siRNA could be encapsulated within a shell-core structure, adsorbed on the surface of a nanoparticle or complexed through electrostatic interactions [67]. The last strategy, which is the most widely used, requires that at least one component of the non-viral vector displays a net positive charge, which is exploited to establish electrostatic interactions with the anionic siRNA in order to obtain a self-assembled nanoparticle [68].

The inclusion of siRNAs in a non-viral vector would help solving the delivery and stability issues related to the systemic administration of the RNAi trigger. Nevertheless, particular care has to be put in the rational design of the delivery platform in order to achieve the correct organ and cellular localization and to maintain the silencing efficacy without causing toxic effects. It is out of the scope of

this thesis to provide a comprehensive overview of all the non-viral vectors for siRNA delivery, which have been excellently reviewed elsewhere [66,69]. Thus, in the following section, the main approaches for non viral delivery will be reported, focusing on how the delivery platform improve the pharmacokinetic properties of siRNAs, and on the main features to be considered in the design of a non-viral nanocarrier.

First of all, encapsulation of siRNA within a liposome or a polymeric nanoparticle would protect the nucleic acid from enzymatic digestion by circulating RNAses after systemic administration [70]. The complexation with a cationic polymer, or lipid would lead to the same protection, as long as the siRNA is not exposed on the external surface of the nanovector and available for nuclease attack. The **surface charge** of the delivery vector plays a crucial role in its fate *in vivo*. A cationic nanoparticle would be able to stimulate nonspecific endocytosis through the interaction of its positively charged moieties with the anionic components of the cell membrane [68]. This effect is particularly beneficial *in vitro*, where ideally all the cultured cells have to be transfected and no tissue-specificity is required [68]. However, in an *in vivo* setting, the use of cationic nanoparticles require further consideration. In fact, the positive charge would quickly attract serum albumin and other opsonins, which can be adsorbed on the surface of the delivery vector, modifying its size, shape and even reversing its Z potential [71]. Moreover, as previously discussed, the opsonin-labeled nanoparticles will be cleared from the circulation by the MPS, thus activating an immune response and ultimately impeding the induction of RNAi in the target tissue [72]. A widely used strategy to shield the positive surface of the liposomes/polymeric nanoparticles is represented by the coating with an hydrophilic polymer. **PEGylation**

of cationic nanoparticles has shown to significantly increase half life in the circulation, avoid opsonization and MPS uptake. PEG is undoubtedly the most used hydrophilic polymer to confer "stealth" properties, and it has been extensively studied in details such as the effect of the chain length and coating method used (post insertion or pre insertion) [73]. Other approaches to avoid the positive surface charge are being explored, such as the formation of asymmetric liposomes, where the inner layer is composed by cationic phospholipids (complexing the siRNA) and the outer layer by neutral and anionic lipids [74]; or the formation of anionic liposomes encapsulating a siRNA-polymer positive complex [75]. Despite the beneficial effect on the circulation time and nonspecific uptake, the lack of a positively charged surface will dramatically reduce the **cell uptake** in the target tissue too, and an extensive *in vivo* screening would be required to find the ideal compromise between the two properties. A convenient way to overcome this issue is to further decorate the surface of the nanocarrier with a ligand able to trigger a receptor- or adsorption- mediated endocytosis. The difference between the two processes relies on the involvement of a ligand-receptor binding in the former case, while an unspecific interaction between the targeting molecule and the cell membrane is associated to the latter [76]. In order to trigger the **receptor-mediated endocytosis** of non-viral vectors, several types of ligands, such as sugars, peptides, small molecules, aptamers, antibodies or antibody fragments, have been conjugated on the surface of nanocarriers [77]. Exploiting such pathway for the uptake of siRNA vectors may result in targeted delivery to a specific organ or tissue, in addition to the increased cell uptake in the desired cell population. However, the endocytotic process would lead to the internalization of the siRNA delivery platform within an intracellular vesicle called endosome. While entrapped in the endosome, the siRNA is not able to trigger RNAi, and it would be inexorably

degraded as the endosomal vesicle fuses with the lysosome and the pH drops [78]. Thus, the non-viral vector have to be equipped with a component which could efficiently trigger the **endosome escape** and release of the siRNA in the cytoplasm. Many different lipids, polymers and peptides have been claimed to mediate endosome escape of nanoparticles, and some mechanism of action have been proposed [79]. For instance, protonable polyamine-containing polymers are known to trigger endosomal escape through the so called **proton-sponge effect**. Briefly, during the maturation process of the endosome, protons and their counter-ions are pumped inside the vesicle with the aim of reducing the pH. However, the protonable polymer entrapped within the endosome would capture the protons and induce the entry of more ions, which are followed by water because of osmotic imbalance. Eventually, the osmotic pressure causes the rupture of the endosome, leading to the release of its content in the cytoplasm [80]. Another mechanism of endosome escape relies on the ability of certain amphipathic lipids, such as DOPE or other **helper lipids**, to interact with the phospholipids composing the endosomal membrane. Although the exact process has not been elucidated yet, the fusion of the lipid nanocarrier with the endosome membrane has been hypothesized, and a cytoplasmatic release of the siRNA has been shown when a helper lipid was included in the formulation [81]. Finally, the inclusion of a **fusogenic peptide** in the formulation could be beneficial for the endosome escape of non-viral siRNA delivery systems. These peptides are developed to mimic the endosomal disruptive properties of fusogenic sequences of viral fusion proteins, which can undergo a conformational change at acidic pH, exposing their hydrophobic domains and inducing the fusion with the endosome membrane [82].

The great attractiveness of non-viral delivery systems rely on their potentially unlimited possibilities for modification, the ease of manufacturing and the safety

profile. Regarding this last point, special care has to be put in the choice of components which have to be non toxic and inert, but also biodegradable and should not lead to accumulation in the organism. The first nanoparticle-based siRNA therapeutic to undergo a phase I clinical trial was CALAA-01 [ID: NCT00689065], in 2008 [83]. CALAA-01 nanoparticles are composed of a PEGylated cyclodextrin-based polymer, decorated with a human transferrin protein as a targeting ligand, and complexing a functional siRNA [84]. Since then, other non-viral delivery vectors such as SNALP® (stable nucleic acid lipid particles), AtuPLEX® (liposomes), LODER™ (poly-lactic co-glycolic acid nanoparticles) moved from the bench to the clinical trials phase, rising confidence for the potential success of the non-viral strategy and boosting the research and the investments in the field [85,86].

2.3. siRNA delivery to neurons

One of the most challenging field of application for the therapeutic RNAi is the treatment of neurological diseases. The potential of this approach has been investigated in prelinical models of spinocerebellar ataxia, amyotrophic lateral sclerosis, Huntington's, Parkinson's and Alzheimer's diseases [40,87]. However, the difficulty of siRNA delivery to the central nervous system (CNS) due to the presence of additional intra- and extracellular barriers, represents the main obstacle to the success of such approach. In the following paragraph, a brief overview of these barriers will be reported, as well as the main strategies applied to overcome them.

Firstly, the **blood brain barrier (BBB)** is an anatomical and functional barrier separating the CNS from the circulation, allowing the transfer of nutrients and certain small molecules only, thus representing an obstacle to the diffusion of most substances from the circulation to the CNS [88]. CNS delivery can be achieved through

various invasive techniques, such as disruption of the BBB, convection-enhanced delivery, intracerebro and intracerebro-ventricular infusion, all of which are linked to poor patient compliance, high cost and the risk for severe side effects [89]. A non-invasive alternative for brain delivery rely on the systemic administration of a drug delivery system, either possessing suitable physico-chemical features to trigger **adsorption-mediated transcytosis**, or being decorated with a homing device able to interact with a receptor on the endothelium of the CNS capillaries and induce the translocation to the brain parenchyma [90,91]. In the latter case, the targeted delivery system may be transported across the endothelial cell through a **carrier-mediated transport**, or endocytosed and released on the basal side exploiting the **receptor-mediated transcytosis** [92]. Indeed, several carrier proteins for essential nutrients (eg glucose, amino acids, vitamins) as well as receptors for peptides and proteins (insulin, transferrin, enkefalins), hormones (leptin), low density lipoproteins (LDL) and small molecules (glutathione), have been identified in the luminal side of the brain endothelial cells, and have been exploited for the brain delivery of targeted nanocarriers after transvascular delivery [93]. In addition, several viral, bacterial and even animal toxins which are known to have access to the CNS, were evaluated as potential targeting agents [94]. The structure-activity relationships of some of them were investigated in order to produce safer and more effective molecules, as in the case of the rabies virus glycoprotein (RVG), which structure was reduced to an only 29 amino acids peptide (**RVG peptide**) able to trigger a receptor mediated transcytosis through the neuronal acethylcholine receptor (nAChr), widely expressed in the brain endothelium [95].

The BBB structure and its functions may be modified in several pathological conditions, thus, the full understanding of such changes is essential for the design of a

brain-targeting vector which has to interact with a disease-modified BBB [96]. For instance, in the presence of a cancer of the CNS, the brain endothelium can be modified, to a different extent depending on tumour type and severity, in its morphology and function, resulting in the development of the **blood-brain tumour barrier (BBTB)** [97]. In the case of an high-grade brain cancer the BBTB is leaky in nature, allowing the uptake of the therapeutic agents in the tumor-affected areas. In contrast, the lower grade tumours, small lesions or isolated cancer cells may only show minor alterations in the permeability of the BBB [98].

Overcoming the BBB is nothing but the first issue to siRNA neuronal delivery. Once penetrated in the brain parenchyma, the RNAi construct will encounter a variety o cell types, including neurons, microglia and astrocytes, all of which possess different ability to interact and endocytose the nanocarriers. For instance, neuronal cells represent a particular challenge for the introduction of foreign genetic materials such as the siRNA [99]. The mechanism underlying the reduced permeability of neurons have not been elucidate yet, but this feature is shared with other post-mitotic cell populations [100]. Thus, if a specific cell type has to be targeted by the RNAi construct, additional care has to be put in the design of the vector to avoid the off-target cells, which would eventually reduce the dose of siRNA reaching its target through an unspecific uptake.

Chapter II
RVG-modified liposomes for siRNA delivery to primary neuronal cells: evaluation of alpha synuclein knockdown efficacy

Alpha-synuclein (α-syn) deposition in Lewy bodies (LB) is one of the main neuropathological hallmarks of Parkinson's disease (PD), the most common neurodegenerative disorder with motor symptoms. Of note, LB accumulation is considered as a causative factor for PD, thus suggesting that strategies aimed at reducing α-syn levels could be relevant for its treatment, especially because we still lack resolutive therapeutic strategies for healing subjects suffering from this disease.

In the present study we aimed to set up novel anionic liposomes as silencing RNA (siRNA) nanocarriers suitable for systemic delivery and specifically designed to efficiently reduce neuronal α-syn by RNA interference (RNAi). To this purpose we prepared anionic liposomes, with a mean diameter of 100 nm, loaded with a complex of siRNA-protamine for efficient α-syn gene silencing. The nanoparticles were characterized for their ability to load, protect and deliver the functional siRNA to mouse primary hippocamapal and cortical neurons as well as for their efficiency to induce gene silencing in these cells. In addition, the liposomes were decorated with a rabies virus glycoprotein (RVG)-derived peptide as a targeting agent to overcome the BBB and tested for stability in serum as well as α-syn gene silencing efficiency. Of note, the RVG-decorated liposomes were found to display suitable characteristics for future *in vivo* applications and were able to significantly reduce α-syn levels in both cortical and hippocampal neurons without altering cell viability. Collectively, our

results indicate that RVG-decorated anionic liposomes may represent an ideal delivery tool for further evaluation to achieve efficient α-syn gene silencing *in vivo* in mouse models of PD.

1. Introduction

Alpha-synuclein (α-syn) is a 140 amino acid protein abundantly expressed throughout the central nervous system (CNS) [101]. The protein is crucially involved in the regulation of neurotransmitter trafficking at the pre-synaptic region, where it exists in equilibrium between a soluble and a vesicle-bound form [102]. In particular, α-syn has been found to interact with synaptic vesicles as well as pre-synaptic membrane-associated proteins [103–105]. However, α-syn knockdown and null mice were viable, fertile and had normal motor behavior, suggesting that a compensative effect exists with the other forms of synucleins (β and γ) [106,107].

In 1997, α-syn was identified as the main protein component of Lewy bodies (LB) [108], eosinophilic inclusions that are among the main pathological hallmarks of Parkinson's disease (PD), PD dementia (PDD), dementia with Lewy bodies (DLB), LB variant of Alzheimer's disease (AD) and LB dysphagia. Numerous evidence points out that the deposition of the protein in the brain plays a pathogenic role in these disorders. Indeed, mutations and multiplications of the α-syn gene locus SNCA cause the onset of familial forms of PD and DLB and the progression of PD symptoms correlate with the topographical spreading of LB pathology in the brain [109]. Furthermore, studies in experimental models of PD have shown that α-syn accumulation and aggregation is neurotoxic, thus corroborating the above observations [105].

Thus, since clinical and experimental findings indicate that higher levels of α-syn promote its toxic potential [110,111], it is also reasonable to postulate that neuroprotective effects could be achieved by suppressing this protein expression in neurons.

In the last decade, RNA interference (RNAi) has been found to constitute a useful tool to reduce the expression of α-syn *in vitro* and *in vivo* through the administration of silencing RNA (siRNA) or short hairpin RNA (shRNA) vectors. A shRNA expressing lentiviral vector designed to silence human α-syn has been found to efficiently knockdown the target protein both *in vitro* in the human SH-SY5Y cell and *in vivo* in the striatum of human α-syn transgenic rats [112]. Nevertheless, the clinical use of viral vectors is hindered by the risk of immunogenicity and issues linked to large-scale production [87]. As an alternative, the use of naked siRNA was exploited to achieve specific and resilient silencing of α-syn in the hippocampus and cortex of mice after intracerebral infusion [113]. More recently, the potential of α-syn silencing has been investigated in non-human primates. Indeed, a chemically modified siRNA inoculated in the left substantia nigra of squirrel monkeys was found to induce a significant gene knockdown of the protein without triggering adverse reactions at the injection site [114]. Conversely, other authors detected dramatic neurotoxicity following intrastriatal infusion of adenoviral vectors embedded with SNCA shRNAs, with a sudden drop of tyrosine hydroxylase (TH) positive cells and dopamine levels observed at 4 weeks after administration [115]. What can be hypothesized following these results is that a "therapeutic window" of α-syn silencing may exist, with either too low or too high expression levels leading to toxicity. Another possible explanation for the above results may rely on the fact that adenoviral vectors injections can induce strong neuroinflammatory and immune cell activation [63]. These pathways

could very well contribute to the induction of noxious events that, coupled to the neuropathological alterations occurring in the injured brain of PD animal models, may transform α-syn gene silencing from beneficial to detrimental. Therefore, non-viral delivery of siRNA, rather than that of viral vector-associated shRNA delivery, seems to constitute a more promising and safe route to investigate for gene silencing in the human brain. This is reinforced by the fact that the use of shRNA can be associated with a broad spectrum of off-target irreversible effects on gene regulation.

Nonetheless, when focusing on the potential clinical translation of siRNA therapeutics for neurological disorders, the route of administration is of primary importance. In this regard, the previously cited works, although demonstrating the therapeutic potential of α-syn siRNAs, lack of an acceptable application route for the treatment of a large population of human patients, as the associated gene silencing is not permanent and could only be achieved through intracerebral infusion. Instead, brain-targeted delivery of siRNA by systemic administration (e.g. intravenous) would provide a non-invasive alternative with greater patient acceptability, reduced cost and without the risks associated with surgery.

Nonetheless, the fascinating potential of brain delivery after systemic administration of siRNA is undermined by limitations derived from the difficulties of crossing the blood brain barrier (BBB) as well as from the unfavorable physicochemical characteristics of siRNA. In fact, siRNAs are double stranded RNA, hydrophilic and anionic in nature, so they are unsuitable for permeability across both the cell membranes and the BBB [50]. In addition, naked siRNA can be quickly degraded by circulating RNAses and their fast renal elimination account for an extremely short (<5 minutes) plasma half life [22]. For this reason, several nanocarriers of different nature (polymeric, lipidic, peptidic…) have been recently used as siRNA encapsulating

agents in order to improve *in vivo* stability and targeted organ specific delivery [66,116] .

For instance, Cooper and coauthors included an anti-SNCA siRNA in exosomes whose surface was decorated with a rabies virus glycoprotein-derived peptide (RVG peptide) [117] that is known to function as a brain delivery agent. Indeed, the RVG peptide can bind the acetylcholine receptors on brain endothelial cells and then triggers a receptor mediated transcytosis that allows the nanocarrier to cross the BBB and results in widespread delivery in the brain parechyma [95,118]. RVG-modified exosomes effciently decreased the levels of endogenous and pro-aggregating α-syn after systemic administration in wild type (wt) or transgenic mice, respectively. In addition, the use of exosomes as drug delivery systems has been shown to hold great potential, especially for their intrinsic ability to mediate cell-to-cell material transfer and enhanced stability in the circulation. However, the variability in size and composition due to different cellular origins, the risk of immune suppression or activation and the lack of large scale isolation methods represents major obstacles for the clinical translation of exosomes as siRNA delivery vectors [119,120].

Liposomes share with exosomes the vesicular structure formed by a phospholipids bilayer, but they have the advantage of a synthetic origin, with the possibility of fine-tuning their properties through the selection of components and preparation method. In addition, the external surface of liposomes could be chemically modified to introduce a targeting agent to trigger the penetration of the BBB through the receptor-mediated transcytosis [121]. Cationic liposomes can bind the siRNA by electrostatic interactions to form lipoplexes, which have been extensively used as nanocarriers for RNA delivery [122]. However, cationic nanoparticles are well known

for their cellular toxicity, aggregation with serum proteins and unspecific uptake by different cells, posing serious concerns to *in vivo* use [123].

In the present work, we exploited the cationic nature of protamine, a naturally occurring low molecular weight protein, to form a condensed complex with anti-SNCA siRNA, which is then subsequently mixed with anionic and neutral lipids to form negatively charged, PEGylated liposomes. The nanovesicles were modified with a RVG peptide to facilitate CNS distribution after intravenous administration, providing the potential for a non-invasive and convenient delivery route. The ability of liposomes to load and protect siRNA was tested together with their ability to deliver siRNAs and to silence α-syn in mouse primary neuronal cell cultures.

The rationale behind this work was to obtain a nanocarrier for siRNA delivery, which could be suitable for future *in vivo* application, without the known undesirable features (eg positive charge, use of viral vectors…) and with the advantages of simplicity, reproducibility and safety of the formulation.

2. Experimental

2.1. Materials

Distearoylphosphatidylcholine (DSPC) and distearoylphosphatidylethanolamine-polyethyleneglycol-2000 (DSPE-PEG) were purchased from Lipoid (Ludwigshafen, Germany). Distearoylphosphatidylethanolamine-N-[maleimide(polyethylene glycol)-2000] (DSPE-PEG-Mal) was purchased from NOF Corporation (Tokyo, Japan). Cholesterol, protamine, LISS-Rhodamine, carboxyfluorescein -(FAM), chloroform, were purchased from Sigma (Milan, Italy). Amicon Ultra 4 (molecular weight cut-off: 30,000 Da) concentrators were from Merck Millipore (Darmstadt, Germany). The peptide RVG with a cysteine on C-terminal

(YTIWMPENPRPGTPCDIFTNSRGKRASNGC) was synthesized by GenScript (Piscataway, NJ).

The anti-SNCA siRNA (target sequence UGGCAACAGUGGCUGAGAA) and the negative control siRNA labeled with DY-547 (siGLO) were purchased from Dharmacon.

2.2. Protamine-siRNa complex formation and liposomes preparation

Liposomes were prepared using the thin-film hydration method. For the preparation of stealth liposomes (SL) a mixture of DSPC (4.7 μmol), cholesterol (2.7 μmol) and DSPE-PEG (0.4 μmol) was used. For the preparation of RVG-directed liposomes (RVGL), half of the DSPE-PEG was substituted by DSPE-PEG–Mal (0.2 μmol). The lipid mixture was dissolved in chloroform, which was then evaporated under reduced pressure at room temperature to obtain a lipid film. The vacuum was applied for 6 h to ensure total removal of any solvent trace. In a separate vial, protamine and siRNA (anti-SNCA or fluorescent negative control, siGLO) were mixed at given ratios in RNAse free PBS (pH 7.4) and incubated for 30 minutes at room temperature under gentle stirring to allow formation of the complex. The lipid film was hydrated under mechanical stirring with the protamine-siRNA complexes (1.75 μg/ml siRNA) at 65°C. The liposomes obtained were sonicated by a Soniprep 150 ultrasonic disintegrator (MSE Crowley, UK) for 3 minutes with a scheme of hits and pauses of 5 and 2 seconds, respectively. For the preparation of RVGL, RVG peptide (0.2 μmol) was incubated with maleimide grafted liposomes overnight at room temperature. RVGL were separated from uncoupled peptide by the means of centrifugal ultrafiltration (MWCO 30 KDa). For the preparation of fluorescein amidite (FAM) and Liss-Rhodamine labelled -stealth or -RVG liposomes, the lipophilic dye Liss-Rhodamine was included in the lipid mixture, while the hydration medium was composed of the hydrophilic

dye FAM only in PBS (pH 7.4). For the preparation of empty liposomes (EL), the same lipid composition of SL was used, while the hydration medium consisted of PBS (pH 7.4).

2.3. Liposome physicochemical characterization: mean size, polydispersity index and zeta potential

The average diameter, polydispersity index (PDI) and zeta potential (ZP) of the samples were determined by photon correlation spectroscopy (PCS) using a ZetasizerNano-ZS (Malvern Instrument, UK). Samples were backscattered by a helium–neon laser (633 nm) at an angle of 173° and a constant temperature of 25° C. The instrument automatically adapts to the sample by adjusting the intensity of the laser and the attenuator of the photomultiplier, thus ensuring reproducibility of the experimental measurement conditions. The PDI was used as a measure of the width of the size distribution. PDI less than 0.2 indicates a homogenous and monodisperse population. Zeta potential was estimated using the ZetasizerNano-ZS by means of the M3-PALS (phase analysis light scattering) technique, which measures the particle electrophoretic mobility in a thermostated cell.

2.4. Encapsulation efficiency

The percent entrapment of siRNAs within liposomes was determined through an indirect fluorimetric method. Briefly, SL or RVGL were subjected to ultrafiltration using Amicon Ultra centrifugal filters (cutoff 30000 Da) [124]. The unentrapped siRNA in the filtrate was quantified by the Quant-iT® RiboGreen RNA assay (Invitrogen) against a siRNA standard curve. The siRNA-RiboGreen fluorescence was

measured with a microplate reader (Synergy 4, Bio-Tek) using excitation and emission wavelengths of 495 and 525 nm, respectively.

2.5. Stability of vesicles in serum

SL and RVGL at 0.58 mg/ml total lipid concentration, were incubated in 10% fetal bovine serum (FBS) at 37°C under gentle agitation. At given time points, 200 µl of the incubation mixture was withdrawn and diluted with 800 µl distilled water. Size and polydispersity index were measured by PCS immediately after the dilution, at 37°C.

2.6. Nuclease protection assay

To monitor the degradation of liposomal siRNA by serum nucleases, SL and RVGL were prepared at a final siRNA concentration of 133 nM, and incubated with RNAse ONE™ (Promega) at 37°C. At stated time points 80 µl aliquots were removed, heated at 80°C for 5 minutes to inactivate RNAses, mixed with SDS (0.5%) to disrupt liposomes and stored at -80°C until gel electrophoresis was performed. All the samples were mixed with a 10X Blue juice, gel loading buffer (Invitrogen, CA, USA) and were added to the wells of 1% agarose electrophoretic gel, prepared with Tris borate EDTA (TBE) buffer and containing 6 µl of Sybr Green II™ (Thermofisher Scientific) per 100 ml solution. The electrophoresis was carried out 90 V for 45 min in TBE buffer. Unbound siRNA was used as a control. The bands were visualised by UV using DNR Bioimaging Systems MiniBis Pro and the software Image Lab 4.0.1. The relative amount of siRNA at each time point was quantified using the band at time 0 as a reference (100%).

2.7. Cell cultures

Primary cortical and hippocampal neuronal cell cultures were prepared from P0 newborn C57BL/6J mice. Brain cortices and hippocampi were dissected and mechanically dissociated in complete medium composed by Neurobasal A (Life Technologies, Milan, Italy) supplemented with 100 µg/mL penicillin, 100 µg/mL streptomycin (Sigma-Aldrich, Milan, Italy), 0.5 mM glutamine (EuroClone, Milan, Italy) and 1% B27 supplement (Gibco) and centrifuged. Cell count and viability assays were performed using the trypan blue exclusion test. For immunocytochemistry (ICC) or western blotting (WB) analysis, neurons were seeded either on poly-D-lysine-coated 24 well plates glass coverslides ($8x10^4$ cells/cm^2) or on poly-D-lysine coated Petri dishes ($4x10^5$ cells/cm^2), respectively. Cells were maintained at 37° C in a humidified atmosphere of 5% CO_2 and 95% O_2 in complete medium for 7 days *in vitro* (DIV) prior to liposome treatments.

2.8. Liposome treatment

Cells were maintained for 72 hours at 37° C in a humidified atmosphere of 5% CO2 and 95% O2 in complete medium with liposomes with 25 nM final concentration of siRNA for α-synuclein. For RVG empty liposomes were used at the same dilution as Stealth liposomes. Control cells were maintained for 72 h in fresh complete medium.
In a subset of experiments the cells were subjected to RNAi by using the conventional transfection agents INTERFERin (Polyplus) and Lyovec (InvitroGen).

2.9. Immunocytochemistry

For immunostaining experiments, cells were fixed by incubation for 10 min in 4% paraformaldehyde/4% sucrose made up in 1 M phosphate-buffer saline (PBS) pH 7.4

and then stored in PBS containing 0.05% sodium azide. Slides were incubated for 4 h at room temperature (RT) in blocking solution (1% w/v bovine serum albumin (BSA) plus 10% v/v normal goat serum (NGS) in PBS), then overnight at 4 °C with the primary antibody (SYN1, BD Bioscience) at the optimal working dilution. On the following day, cells were incubated for 1 h at RT with the fluorescent secondary antibody diluted in 0.1% Triton X-100 PBS plus BSA 1 mg/ml. Finally, cell nuclei were counterstained either with Dapi (Sigma-Aldrich), Hoechst 33342 (Sigma-Aldrich) or ToPro (Invitrogen) and the coverslips were mounted on glass slides by using Vectashield mounting medium for fluorescence (Vector Laboratories, Burlingame, CA, USA).

2.10. Antibodies

Alpha-syn was visualized by using SYN-1 monoclonal antibody (BD-Bioscience, Milano, Italy).

A mouse monoclonal anti-Neu-N antibody (Millipore) was used for recognising neuronal cells.

2.11. Statistical analysis

All the statistical analysis were carried out by using One-way ANOVA + Newman-Keuls post comparison test.

3. Results and discussion

3.1. Liposome preparation and characterization

The liposomes were prepared using the thin-film hydration method. Neutral (DSPC, cholesterol) and anionic (DSPE-PEG, DSPE-PEG-Mal) lipids were selected with the

aim of producing negatively charged vesicles. The EL were prepared by hydrating the lipid film with PBS pH 7.4 and were used to optimize the lipid ratios and their total concentration. The mean diameter of the selected EL was 105±5 nm with a Z-potential of -31±3 mV.

In order to exploit the negative charge of the liposomes as a driving force for siRNA loading, a cationic complex of siRNA and protamine was prepared. The protamine/siRNA mass ratio was optimized to achieve a stable positive charge and complete siRNA binding, this was checked by gel electrophoresis. A protamine/siRNA ratio of 1 was sufficient to complex all the siRNA and to form complexes with Z potential of 22±4 mV (**Figure 2.1**).

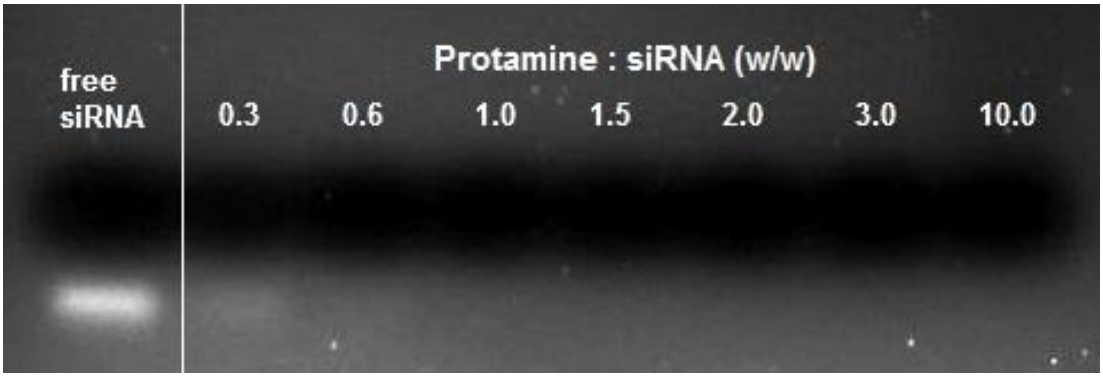

Figure 2.1. Electrophoretic gel of protamine-siRNA complexes at various weight ratios. Free siRNA (not complexed with protamine, first lane on the left) was used as a positive control

For the preparation of SL and RVGL, the lipid film was hydrated with a buffered solution containing siRNA-protamine complexes above the transition temperature of the main lipid. Therefore, the loading step was concurrent to the liposome formation, which was previously reported to achieve higher entrapment efficiency compared to the mixing of siRNA with preformed hollow liposomes [125]. To reduce liposome size and obtain small unilamellar vesicles (SUV), the formulations were subjected to

sonication by using a titanium probe sonicator. For the preparation of the RVGL, DPSE-PEG was partially substituted with DSPE-PEG-Maleimide and, after the sonication step, the RVG peptide was linked to the maleimide moieties exposed on the liposomal surface through the formation of a thioether bond. This reaction was carried out in PBS for 12 hours at room temperature under gentle stirring. To achieve the removal of the uncoupled peptide from the RVGL dispersion, the crude product was filtered by centrifugal ultrafiltration (MWCO 30 KDa), as previously described [126]. The purification step was necessary to rule out any possible competition of the free RVG with the RVGL for the receptor binding. Moreover, since the maleimide group slowly undergoes hydrolysis when in contact with water, it was essential to proceed quickly in the preparation of RVGL.

A monodisperse population of liposomal nanoparticles (PDI<0.2) was obtained, with no significant (P<0.05) difference in the size of the EL compared to the SL (105±5 nm and 108±8 nm, respectively). The size of the resulting liposomes before the reaction with the RVG peptide were similar to the size of SL, in agreement with the fact that the maleimide moiety does not induce aggregation nor destabilization of the bilayer. Conversely, the mean diameter of the RVGL measured after the RVG peptide link to the vesicular surface was slightly increased (121 ±4 nm), suggesting that the covalent binding with the maleimide occurred (**Table 2.1**). Moreover, the Z potential of RVGL significantly decreased after the reaction between the maleimide-grafted liposomes and the RVG peptide. A possible explanation could lie in the fact that the RVG peptide has a calculated isoelectric point of 8.8, which translates in a net positive charge at pH 7.4, reducing the Z potential to the value of -16±5 mV. The formulated vesicles were separated from the unencapsulated siRNA by means of centrifugal ultrafiltration to

determine the entrampent efficiency, which resulted in 89 ± 4% for SL and 86 ± 4% for RVGL.

	Mean Diameter	**PDI**	**Z potential**
EL	105±5 nm	0.129±0.019	-31±3 mV
SL	108±8 nm	0.131±0.023	-28±5 mV
RVGL - before RVG binding	106±5 nm	0.153±0.027	-30±4 mV
RVGL - after RVG binding	121 ±4 nm	0.168±0.022	-16±5 mV

Table 2.1. Mean diameter, polydispersity index (PDI) and Z potential of empty liposomes (EL), stealth liposomes (SL), RVG-tagged liposomes (RVGL)

3.2. Nuclease protection assay

One of the main bottlenecks in the clinical use of siRNAs is their poor stability due to enzymatic degradation. For this reason, the ability of the liposomal formulation to protect loaded siRNAs against RNAses over time was tested *in vitro*. The SL were co-incubated with RNAse ONE® at 37°C, and sampling from the mixture was carried out at given time points. After the heat-mediated inactivation of RNAses, the siRNA was released from the nanocarriers by the addition of SDS. The anionic surfactant SDS was chosen to achieve the dual goal of disrupting the lipid vesicles and releasing the siRNA from protamine complexes and allow its migration and visualization on the electrophoretic gel. As shown by **Figure 2.2**, the liposomal siRNA was efficiently protected from enzymatic activity for a significantly longer time compared to a naked siRNA (negative control, second lane), which was completely degraded after 10 minutes of incubation with RNAses. In **figure 2.2B**, the relative amount of intact siRNA over time is reported. The quantitative analysis was carried out assuming as 100% the intensity of the time 0 band. As can be seen by the graph, the black line (representing the liposomal siRNA) shows an initial burst of siRNA degradation (from

0 to 10 minutes), followed by a slowdown of the process rate. This could be ascribable to an immediate degradation of the unencapsulated siRNA, followed by a second phase, when the siRNA is slowly being released by the liposomes and thus becoming available for the enzymatic digestion. The brightest band present in all the SL lanes accounts for the signal of SDS, as confirmed by a control experiment with the surfactant alone (data not shown).

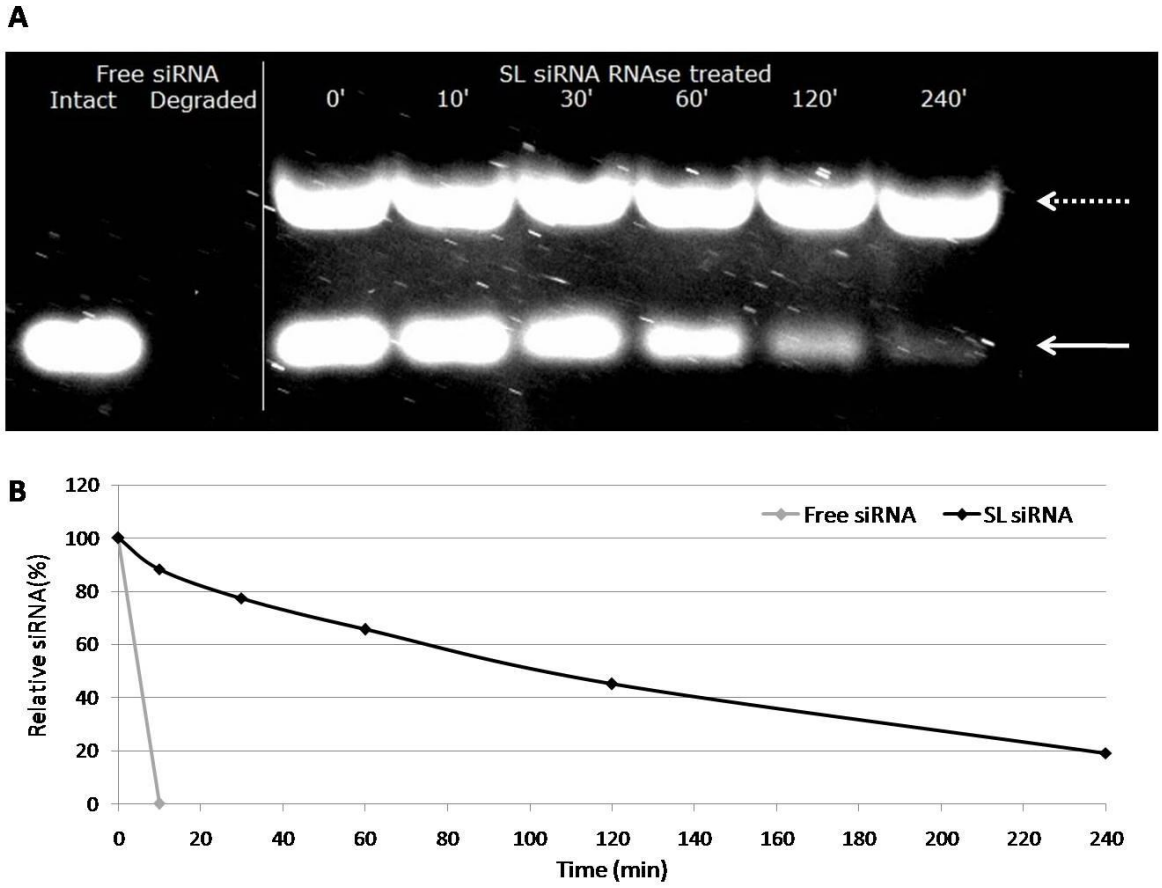

Figure 2.2. Nuclease protection assay. A) Electrophoretic gel: on the left, free siRNA was either directly loaded on the gel (first lane, Intact) or incubated with RNAses for 10 minutes (second lane, Degraded) and used as positive or negative control, respectively. On the right, SL at different incubation times with RNAses (0, 10, 30, 60, 120 and 240 minutes) were disrupted with SDS to allow the visualization of encapsulated siRNA on the gel (white arrow). The dotted arrow indicates the signal of SDS. B) The relative amount of intact siRNA is plotted against incubation time with RNAses. Black line: liposomal siRNA; grey line: free siRNA

3.3. Serum stability

With the aim of future *in vivo* applications of our liposomal nanocarriers for siRNA delivery, the SL and RVGL were tested for their stability in 10% foetal bovine serum. Indeed, although PEGylation should confer "stealth" properties and avoid opsonization, this assay was necessary to rule out the possibility of an interaction between the RVG residues exposed on the surface of RVGL and serum proteins, which would promote aggregation of the nanoparticles resulting in a dramatic increase in the mean diameter [58]. As expected, the SL did not show any significant increase in size after 24 hours of incubation with FBS. Interestingly, also the RVGL retained their initial diameter when exposed to FBS (**Figure 2.3**).

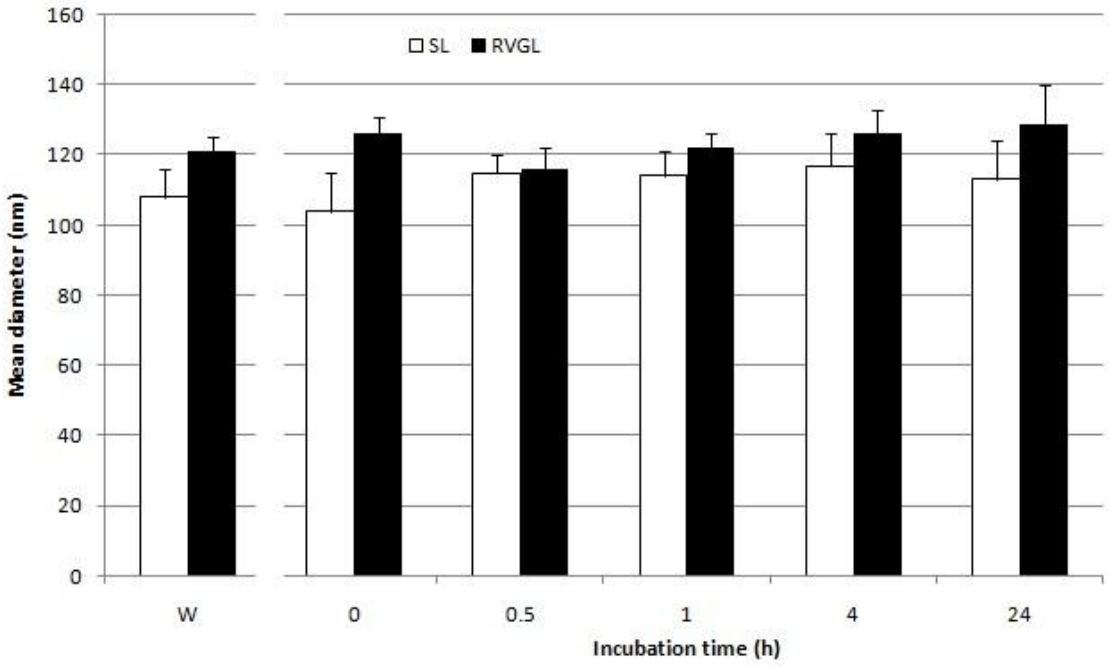

Figure 2.3. Vesicle stability in serum. The histogram represents the mean diameter of SL (white bars) or RVGL (black bars) after 0, 0.5, 1, 4 or 24 hours incubation in 10% FBS. W: mean diameter of SL and RVGL measured in water, to be used as a reference. Bars represent the mean ± standard deviation of at least three independent experimental determinations.

These results confirm that the length of the PEG chains and the used DSPE-PEG/DSPC/cholesterol ratio were optimal to protect the liposomes from serum protein adsorption. Of note, the stealth properties were not lost following substituting of half of the DSPE-PEG with DSPE-PEG-RVG for active targeting.

3.4 Uptake of liposomes and siRNAs by primary mouse cortical neurons

In order to study the *in vitro* uptake of RVG and stealth liposomes by neuronal cells we evaluated the internalization of FAM/Liss-Rhodamine labelled liposomes by primary mouse cortical neurons using confocal microscopy. Results show that neuronal cells were able to internalize both FAM/Liss-Rhodamine labelled-RVG or -stealth liposomes (**Figure 2.4A**). The presence of a marked FAM and Liss-Rhodamine-positive signal within cells in the higher magnification images confirms that several neurons were able to uptake large amounts of liposomes. In addition, the co-localization of the lipophilic and the hydrophilic dyes within the cells corroborate the hypothesis that liposomes can cross the cell membrane retaining their core-shell structure (**Figure 2.4A**, higher magnification). This observation correlates well with an uptake mechanism mediated by an endocytic pathway rather than by the fusion of the vesiscles with the cell membrane. The absence of FAM/Liss Rhodamine positivity in the control neurons treated with unlabeled RVG liposomes was indicative of the specificity of the positive fluorescence signal. Image analysis addressing the measurement of FAM-positive area (**Figure 2.4B**) showed the increased uptake of FAM/Liss-Rhodamine RVG-liposomes from primary cortical neurons when compared to unlabeled RVG liposomes, that didn't show positivity for fluorescence, and to FAM/Liss-Rhodamine loaded stealth liposomes.

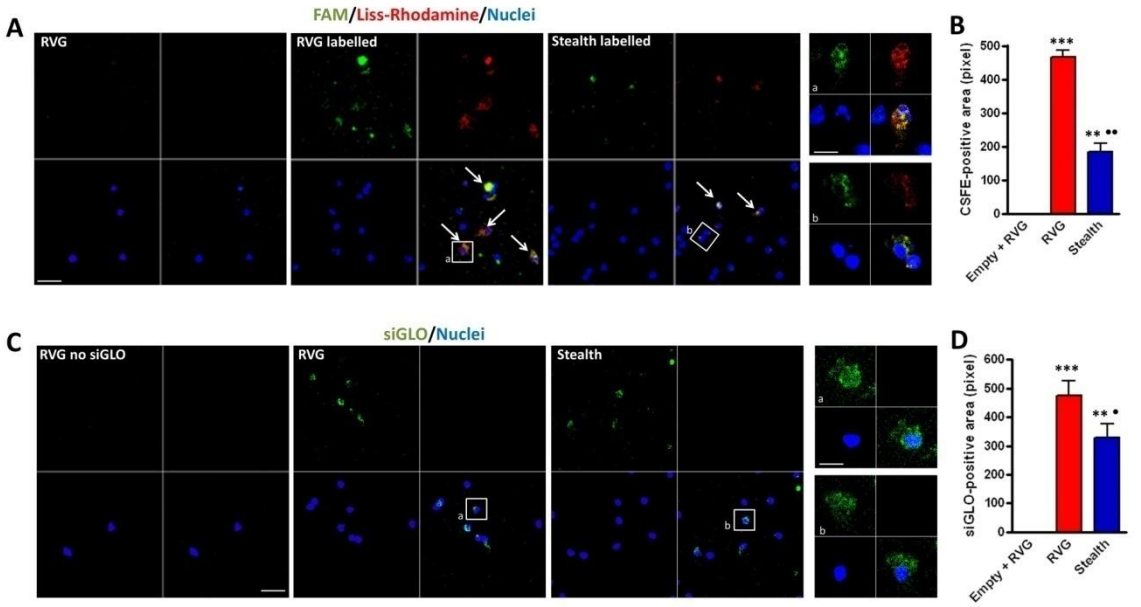

Figure 2.4. A. Representative photomicrographs showing confocal microscopy images of FAM/Liss-Rhodamine immunofluorescence in primary mouse cortical neurons exposed for 4 hours to control unlabelled RVG liposomes, FAM/Liss-Rhodamine-loaded-RVGL or -SL. Cell nuclei were counterstained with Hoechst 33342. The presence of green and red fluorescence is indicative of FAM and Liss-Rhodamine uptake, respectively. Scale bar: 50 μm; higher magnification scale bar: 15 μm.

B. The histogram is showing the mean ± s.e.m. of FAM-positive area in the primary cortical neurons treated with unlabelled RVGL, FAM/Liss-Rhodamine-labelled-RVGL or -SL. Neurons treated with the labelled RVG liposomes showed a marked increase of FAM-positive area (*** $P < 0.001$) when compared to unlabelled RVGL-treated neurons that were devoid of green fluorescence signal. The neurons treated with the labelled SL also showed a statistically significant increase of FAM-positive area when compared to unlabelled RVGL-treated cells (** $P < 0.01$) although this increase was significantly lower than that observed in labelled-RVGL treated cells (•• $P < 0.01$).

C. Representative photomicrographs showing confocal acquisitions from primary neuronal cell cultures treated for 4 hours with empty RVGL or RVGL and SL loaded with siGLO. The green fluorescence signal is indicative of the uptake of oligonucleotide duplexes from cells. Scale bar: 50 μm; higher magnification scale bar: 15 μm.

D. The histogram is showing the siGLO-positive area ± s.e.m. measured from primary neuronal cells cultures that were treated for 4 hours with empty RVGL or siGLO-

loaded RVGL and SL. Please note the statistically significant increase of siGLO-positive area in the neurons treated with siGLO-loaded RVG liposomes when compared to those treated with control RVG liposomes (*** $P < 0.001$). The neurons treated with siGLO-loaded SL also showed a significant increase of fluorescence-positive signal when compared to empty RVGL-treated cells (** $P < 0.01$). However, they showed a significantly lower positivity for siGLO when compared to the neurons that were exposed to siGLO-loaded RVG liposomes (• $P < 0.05$).

In addition, primary mouse cortical neurons were exposed to either RVG or stealth liposomes that had been previously loaded with siGLO green transfection indicator that is a fluorescent oligonucleotide duplex. Neurons treated with empty RVG liposomes were used as controls. We observed that neurons treated with siGLO-loaded RVG liposomes were able to uptake fluorescence labelled oligonucleotide duplexes, whose signal was concentrated within cell nuclei as evidenced in the higher magnification panels (**Figure 2.4C**). The neurons treated with siGLO-loaded stealth liposomes also showed positivity that however seemed to be more diffused and less localized within the nuclei (**Figure 2.4C**). This evidence suggests that, as expected, siRNA delivery by stealth liposomes had a slower uptake kinetic when compared to that mediated by RVG liposomes. The specificity of the fluorescence signal was confirmed by in the absence of positivity in the neurons exposed to siGLO-free RVG liposomes (**Figure 2.4C**). These data were confirmed by image analysis (**Figure 2.4D**) showing the presence of higher siGLO-positive area in siGLO-loaded RVGL when compared to siGLO-loaded SL.

To corroborate that liposomes were actually uptaken by neuronal cells and not by astrocytes, despite the low number of these cells in our primary neuronal cell cultures, these were exposed to either control empty RVG, FAM/Liss-Rhodamine-labelled RVG or FAM/Liss-Rhodamine-labeled stealth liposomes for 4 hours and then

fixed and immunolabelled with the specific marker NeuN that marks the nuclei of neuronal cells. In line with the above observations, we observed a higher uptake of FAM/Liss-Rhodamine labelled RVG and stealth-liposomes by NeuN-positive cells (**Figure 2.5A**), that was confirmed by the image analysis data addressing the number of NeuN/FAM-positive cells per mm^2 (**Figure 2.5B**).

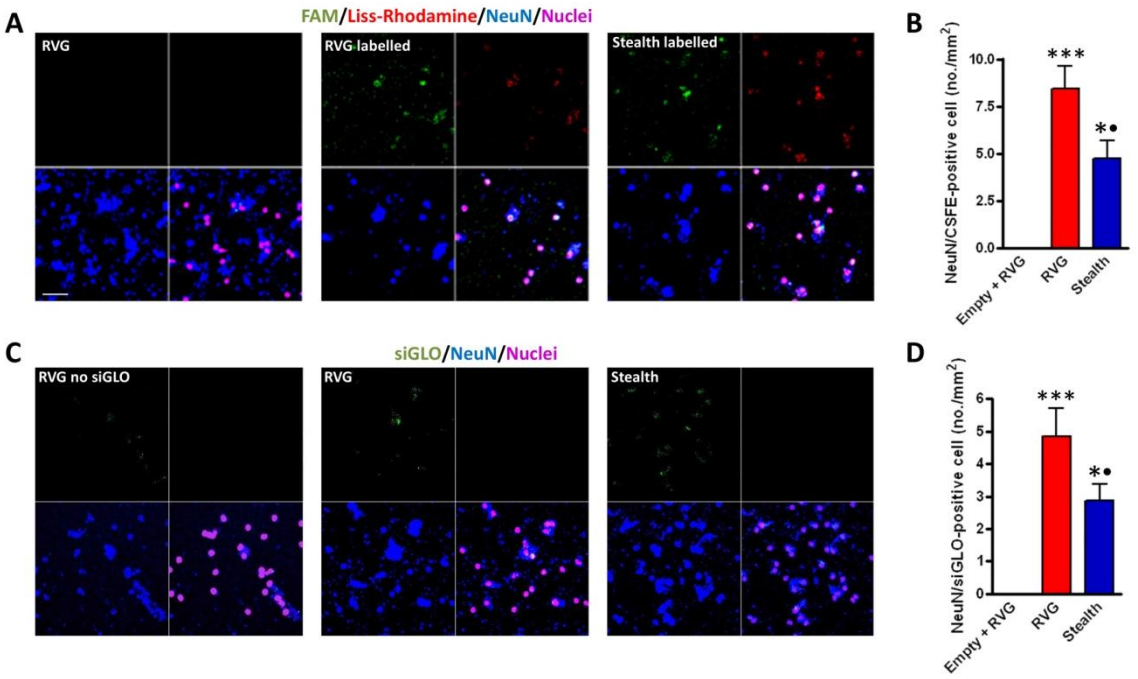

Figure 2.5. A. Representative photomicrographs showing confocal microscopy images of FAM/Liss-Rhodamine immunofluorescence in NeuN-immunopositive cortical neurons exposed for 4 hours to unlabelled RVGL, FAM/Liss-Rhodamine-loaded RVGL or SL. Scale bar: 50 µm.

B. The histogram is showing the mean ± s.e.m. number of FAM/NeuN-positive cells per mm^2 in the cortical neuon cell cultures exposed for 4 hours to unlabelled RVGL, FAM/Liss-Rhodamine-labelled -RVGL or -SL. A statistically significant increase in the number of FAM/NeuN-positive cells is evident in the cultures that were exposed to FAM/Liss-Rhodamine RVG liposomes (*** $P < 0.001$) when compared to unlabelled RVGL-treated neurons. The neurons exposed to FAM/Liss-Rhodamine SL also showed a statistically significant increase of FAM-positive area when compared to unlabelled RVGL-treated cells (* $P < 0.05$) although this increase was significantly lower than that observed in the cells treated with FAM/Liss-Rhodamine RVG liposomes (• P <

0.05).

C. Representative photomicrographs showing confocal acquisitions from NeuN-immunopositive neuronal cell cultures treated for 4 hours with empty RVGL or RVGL and SL loaded with siGLO. The green fluorescence signal is indicative of the uptake of oligonucleotide duplexes from cells. Scale bar: 50 μm.

D. The histogram is showing the mean ± s.e.m. number of siGLO/NeuN-positive neurons in the primary cortical cultures that were treated for 4 hours with empty RVG or siGLO-loaded-RVGL or -SL. The cells exposed to siGLO-loaded RVGL showed a statistically significant increase of siGLO/NeuN-positive cell number when compared to those treated with empty RVGL (*** $P < 0.001$). The neurons treated with the siGLO-loaded-SL also showed a significant increase of siGLO/NeuN-positive cell number when compared to empty RVGL-treated cells (* $P < 0.05$). However, a significantly lower number of siGLO/NeuN-positive cells was observed when compared to the neurons that were exposed to siGLO-loaded RVG liposomes (• $P < 0.05$).

Finally, we also probed the uptake of siGLO oligonucleotides enclosed in either RVG or stealth liposomes in the NeuN-immunolabelled primary neuronal cell cultures, with empty RVG liposomes used as a negative control for the green fluorescence signal (**Figure 2.5C**). The results showed an increased uptake of siGLO in NeuN-positive neurons exposed to RVGL when compared to those exposed to SL as confirmed by image analysis (**Figure 2.5D**).

Collectively, these results indicate that both RVG and stealth liposomes were internalised and could efficiently deliver siRNAs to primary cortical neurons. However, a difference in the intracellular localization ability exists between RVGL and SL, the former showing a significantly higher uptake in all the tested conditions. The increased uptake of RVGL is ascribable to the presence of the RVG peptide, which triggers endocytosis through the binding with nicotinic acetylcholine receptors, present on the neuronal cell membranes [127].

3.5 Evaluation of liposome toxicity by Hoechst 33342 staining

To evaluate the toxicity of the liposomes, neurons were exposed to empty RVG, α-syn-specific siRNA-loaded-RVGL or -SL for 72 hours. Neurons subjected to congruent volume media adjunctions at the same time of liposome treatments were used as a control (**Figures 2.6A,B**).

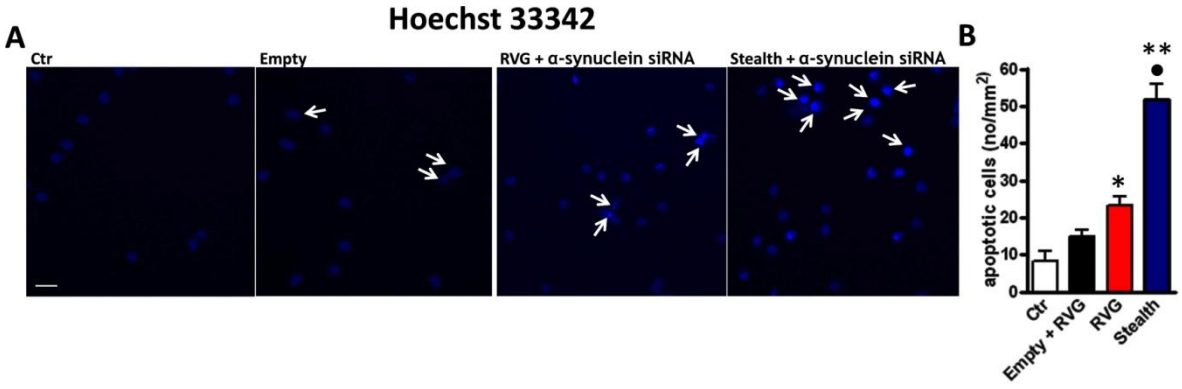

Figure 2.6. A. Representative photomicrographs showing Hoechst 33342 labeling in primary cortical neuron cultures in basal condition (ctr) or after a 72 h exposure to empty RVGL or RVGL as well as SL loaded with α-synuclein siRNA. Please note the presence of several nuclei with condensed chromatin (arrows) in the different experimental conditions, that is indicative of apoptotic cells. Scale bar: 50 μM.
B. The histogram is showing the number of apoptotic nells evaluated by counting the number of nuclei wim condensed chromatin per mm^2. A slight although statistically significant increase of apoptotic cells is evident in the neurons that were treated with RVG liposomes loaded with siRNA when compared to those treated with empty RVG liposomes (* $P < 0.05$). The use of SL loaded with siRNA was associated to a statistically significant increase in the number of apoptotic cells when compared to both empty RVG (** $P < 0.01$) or siRNA-loaded RVG liposomes (• $P < 0.05$).

Interestingly, we found that neurons exposed to siRNA-loaded stealth liposomes showed higher number of condensed nuclei that are indicative of apoptotic cells when compared to control, empty RVG or siRNA-loaded RVGL. These results indicate that although SL are able to efficiently deliver siRNAs into neuronal cells their use is

associated with toxicity. A possible explanation for the fact that SL resulted more toxic than RVGL may be that they might induce a more marked damage to neuronal cell membranes. Although the uptake of SL is lower than that of RVGL, in the former case it is mediated by non-specific mechanisms that might impinge on neuronal membrane homeostasis. This hypothesis is congruent with previous studies reporting the membrane toxicity of liposomal transfection reagents in primary neuronal cell cultures [128].

3.6 Evaluation of the efficiency of liposome-mediated α-syn gene silencing in mouse primary cortical and hippocampal neurons.

Finally, we evaluated whether RVG and stealth liposomes loaded with 25 nM of the siRNA sequence previously used to produce α-syn gene silencing in mouse primary neurons [129] could be used to efficiently silence this protein in cortical and hippocampal neuronal cell cultures. Neurons exposed to empty RVG liposomes or transfected with common siRNA-delivery agents such as INTERFERin and Lyovec were used as controls. Efficiency of α-syn gene silencing was probed by analyzing the α-syn-immunopositive area. Indeed, we previously described a discrepancy between mRNA and protein levels measured by real time PCR and western blotting, respectively, in neurons exposed to α-syn siRNAs [129]. Moreover, immunocytochemical analysis offers the possibility to probe α-syn expression, assess its distribution in neuronal cells and probe neuronal viability by Hoechst 33342, thus offering a valuable method to efficiently assess gene silencing and avoiding false results deriving from those neuronal cell cultures that may meet degeneration upon liposome exposure.

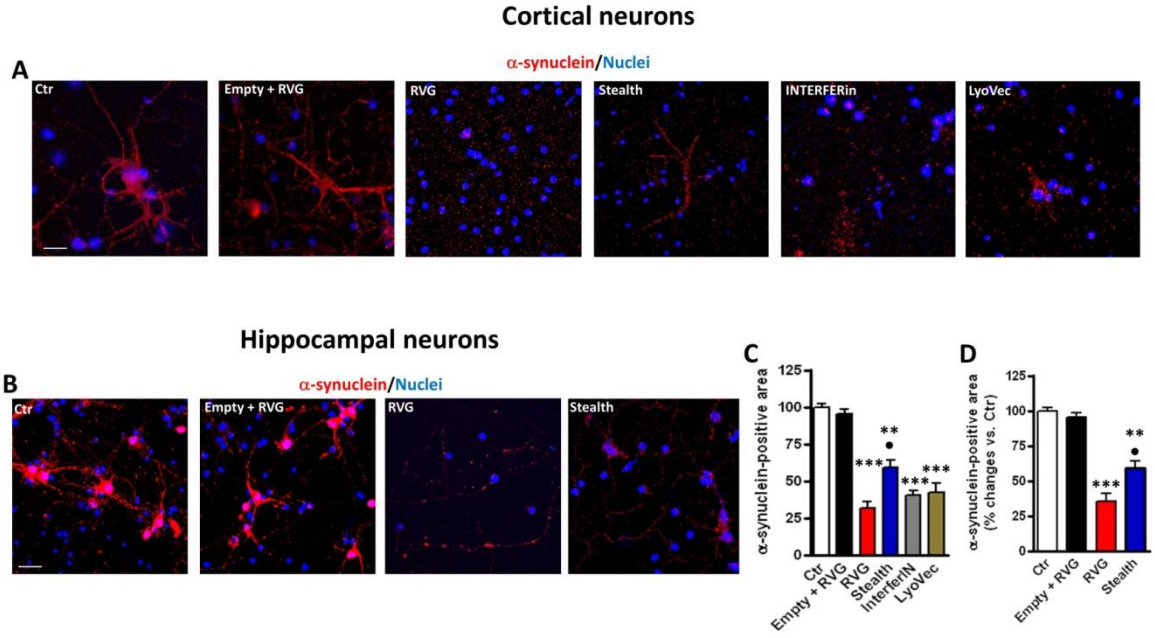

Figure 2.7. A. The images are showing alpha-synuclein immunolabeling in primary cortical neurons in basal conditions (Ctr), exposed to empty RVG liposomes or subjected to alpha-synuclein gene silencing by using a siRNA concentration of 25 nM delivered by RVGL, SL, Interferin or Lyovec.

B. Representative photomicrographs showing primary hippocampal neuronal cell cultures in basal conditions (Ctr), exposed to empty RVG liposomes and RVGL or SL loaded with 25 nM alpha-synuclein siRNA.

C. The graph is showing the mean ± s.e.m. of alpha-synuclein immunopositive area in the primary mouse cortical neurons represented in panel A. Please note the marked reduction of alpha-synuclein-immunopositive area in the neurons subjected to gene silencing by RVG liposomes, InterferIN, and Lyovec when compared to empty RVG-exposed neurons (*** $P < 0.001$). In the cultures exposed to alpha-synuclein siRNA-loaded SL the the immunopositive area was significantly higher when compared to the cells where gene silencing was mediated by the other transfection agents (• $P < 0.05$) although it was still statistically significantly different to that of empty RVG-treated neurons (** $P < 0.01$)

D. The histogram is showing the mean ± s.e.m. of alpha-synuclein immunopositive area in the primary mouse hippocampal neurons represented in panel B.

We found a marked reduction in the α-syn-immunopositive signal in primary cortical

neurons exposed to siRNA-RVGL compared either to control or empty RVG liposomes (**Figures 2.7A,C**). Of note, the efficiency of α-syn gene silencing afforded with siRNA-RVGL was comparable to that observed when siRNA was transfected either with Lyovec or INTERFERin. Conversely, stealth liposomes loaded with siRNA were only able to induce a 40 % reduction of α-syn levels when compared either to control or empty RVG treated cells, this difference was statistically significant compared to the response in siRNA-RVGL exposed neurons.

These data were confirmed by using primary hippocampal neuronal cell cultures that are usually affected by LB pathology in DLB (**Figures 2.7B,D**). We found a marked decrease of α-syn-immunopositive signal in the hippocampal neurons exposed to siRNA-RVGL when compared to control or empty RVG liposomes. However, siRNA-SL resulted in a lower reduction of α-syn levels when compared to siRNA-RVGL, in accordance with the results obtained from primary cortical neurons.

Since the use of SL was associated with higher toxicity when compared to that of RVGL it might be plausible that their lower ability to induce α-syn gene silencing might depend on the fact that the impairment of cell viability is responsible for the reduction of siRNA efficiency.

These results indicate that RVG liposomes loaded with α-syn siRNA are able to induce an efficient and reproducible reduction of the protein in mouse neuronal cells and could likely be tested as promising and efficient delivery agents for siRNA *in vivo* mouse models.

4. Conclusions

The anionic liposomes decorated with the brain targeting RVG peptide were capable of efficiently loading, protecting and delivering anti-α-syn siRNA to primary cortical and hippocampal cells *in vitro*. Once released inside the neuronal cells, the siRNA significantly reduced the levels of α-syn without affecting cell viability. The rationale behind this research was to produce a formulation stable in serum and suitable for non-invasive administration *in vivo*. Moreover, the design of the nanocarrier followed a straightforward approach exploiting simple solutions to overcome the most common drawbacks in siRNA delivery. In summary, a simple formulation with marked *in vitro* efficacy was produced, with potential to overcome the complex barriers encountered in the *in vivo* environment.

Chapter III
Folate-modified anionic liposomes for increased delivery of siRNA to U87 cells

Glioma is recognised as the most aggressive and fatal form of brain cancer. Current therapeutic approaches for glioma consist of surgery and chemotherapy, but they have a poor rate of success and they are associated to major drawbacks such as invasiveness of the intracranial surgical procedure, and poor brain tumor accumulation of the anticancer drugs. Folic acid-modified nanoparticles have been explored for their potential of increasing the distribution of chemotherapeutic agents in systemic tumors. In the present work, anionic, PEGylated liposomes decorated with folic acid have been prepared and tested as nanocarriers for the delivery of siRNA to human glioblastoma cells (U87). For efficient siRNA loading, the cationic protein protamine was included in the formulation to form a liposome-encapsulated siRNA-protamine complex. The folate-targeted vesicles have shown to be able to protect the siRNA from RNAses and transfect 65% of the treated cancer cells, while no uptake was mediated by the untargeted nanoparticles. The involvement of a folate receptor-mediated endocytosis mechanism was confirmed by the competition of free folic acid with the folate-modified liposomes for cell uptake. Overall, the folate-targeted siRNA-protamine liposomes were able to increase the siRNA delivery to glioblastoma cells in vitro. Thus, the present work demonstrate the feasibility of using a folate mojety to deliver nucleic acids to brain cancer cells. Further studies including a functional siRNA in the formulation will be carried out to investigate the silencing efficacy towards a target gene involved in glioblastoma proliferation or chemoresistance.

1. Introduction

Gliomas are glial cells-derived intracranial tumors which collectively account for 80% of the total primary brain tumors. Basing on the cell type which originates the malignancy, gliomas are referred to as astrocytomas, oligodendrogliomas or ependiomas [130]. Moreover, depending on the degree of malignancy and on the presence or absence of specific pathological features, a grade (I to IV) can be assigned to the gliomas according to the classification of the World Health Organization [131]. Glioblastoma multiforme (GBM), a grade IV astrocytoma accounting for more than half of the total reported gliomas, is the most aggressive form of primary brain tumor, characterized by a tragic median survival time after diagnosis of only 15 months [131,132]. From a clinical point of view, GBM can be subdivided into primary GBM, which arises de novo and represent the great majority of cases (>90%), and secondary GBM deriving from the progression of a lower grade astrocytoma [133]. Both the primary and secondary GBM subtypes are characterized by the presence of necrotic areas surrounded by undifferentiated cells, a dramatic microvascular proliferation, resistance to apoptosis, and genomic aberrations [133]. Compared to the other brain tumors, GBM spreads and infiltrates into the surrounding brain parenchyma more aggressively, but rarely metastasises outside the central nervous system (CNS) [132,134]. The invasiveness of GBM, together with its fast progression and the inaccessibility of the tumor for the majority of chemotherapeutic agents, pose serious difficulties for the treatment of such condition, and lead to a poor prognosis and high rate of relapse [135]. The standard of care for the treatment of GBM consists in the surgical resection followed by radiotherapy with concurrent temozolomide (TMZ) chemotherapy, followed by 6 cycles of maintenance TMZ [136]. Alternatively to TMZ, after surgical removal of the tumor, a carmustine implant (Gliadel wafer) can

be placed within the formed cavity to achieve a prolonged, local release of the drug. However, an increased risk of local neurotoxicity, edema and infections have been linked to this treatment [98]. As the standard therapies are not providing a long term suppression of the tumor growth, the patients will inexorably develop a recurrent disease. Bevacizumab, a monoclonal antibody that targets vascular endothelial growth factor-A (VEGF-A), has been approved in the US (but not in Europe) and is currently used as a treatment for recurrent glioblastoma [137]. Despite the slight improvements in terms of survival time, the cited treatments are still highly invasive and harmful for the surrounding brain tissue, and they lack a long term efficacy. An additional limitation of the currently employed chemotherapeutic agents is their inefficient crossing of the blood–brain barrier (BBB), and insufficient accumulation in the tumor cells [98,138]. In fact, GBM induces structural and functional modifications of the brain endothelium, which is usually referred to as "blood-brain tumor barrier" (BBTB) [97]. The developed BBTB has variable features depending on the examined brain area, ranging from a completely disrupted structure in the main tumor site, to slightly leaky in the peripheral regions, to an intact epithelium resembling the BBB in distant regions where isolated tumor cells can be found (**Figure 3.1**) [139]. Thus, even though chemotherapeutics may accumulate in the main tumor area as a consequence of the leaky nature of the BBTB, the presence of drug efflux pumps and multidrug resistance-associated proteins prevents their uptake into cancer cells. A possible strategy to increase drug access in tumor cells is exploiting the receptor-mediated transport systems.

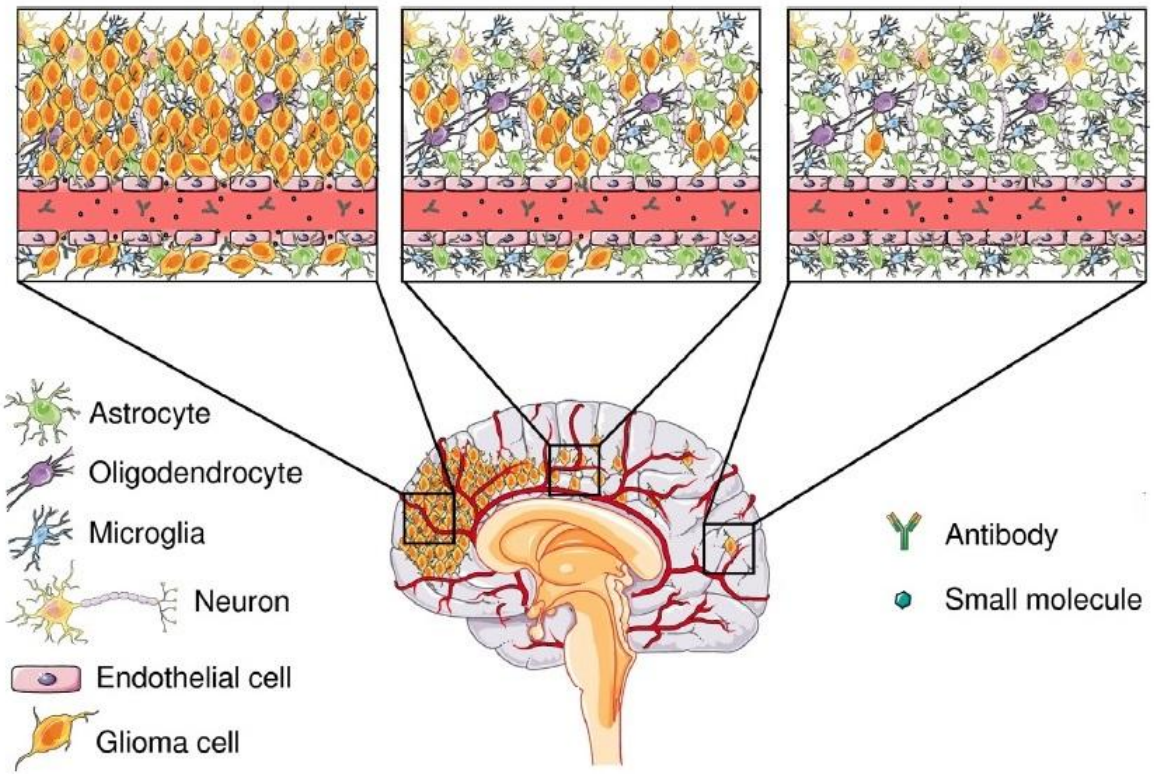

Figure 3.1. Schematic representation of the BBTB heterogeneity in different areas of a glioblastoma-affected brain. Reproduced from [98] with the permission of Elsevier.

Indeed, glioma cells show overexpression of several membrane receptors as compared to the normal brain parenchyma, suggesting that a selective enhancement of drug delivery to the cancer tissue is feasible. Among the others, the expression of the folate receptor alpha (FRα) in healthy tissues has shown to be limited, while an abundant presence was detected in several tumor types [140,141]. In fact, in the last decades, the use of folate-conjugate drugs or folate-targeted nanoparticles for active targeting to lung, ovarian, kidney and other types of systemic cancers has been extensively investigated [142,143]. Of note, despite the expression of FRα in more than 90% of the brain tumors has been documented, the potential of folate-targeted delivery to glioma has not been exhaustively explored yet [142]. Recently, a promising strategy involving the use of two different targeting agents for BBB crossing and cancer cell uptake has been reported by several authors [144,145].

However, being the folic acid an essential nutrient, a clear identification of the mechanisms governing its supply to the healthy CNS may lead to novel applications as a single targeting molecule. Indeed, it has recently been described how folates can be efficiently transported inside the brain parenchyma through the blood-cerebrospinal fluid barrier in the choroid plexus, and only in minor quantities through the BBB [146,147]. Thus, a folate-decorated nanocarrier could be a valuable candidate for the delivery of drugs and macromolecules to those CNS malignancies located in proximity of the choroid plexus.

In the last decade, in addition to small molecules and antibodies, therapeutic RNAi has emerged as a novel potential treatment for brain cancer. In 2008, a report from the first human trial of a RNAi-based therapy for brain cancer was reported [148]. In this work, after surgical removal of the tumor, the patients were treated with a local dose of short interfering RNAs (siRNAs) targeting tenascin C, an extracellular matrix glycoprotein involved in tumor cell adhesion and proliferation. Despite the promising results outlined by this and other pre-clinical studies, the use of siRNAs as therapeutic agents is still hampered by their poor pharmacokinetic properties. Indeed, siRNAs are prone to degradation by circulating RNAses, they are not able to passively cross the cell membrane and lack an efficient transport system [51]. Moreover, the presence of the BBTB poses an additional barrier to siRNA delivery to brain cancer. As for the systemic delivery, the encapsulation of siRNAs within a targeted nanocarrier or their conjugation with a suitable homing device have shown promising results for the delivery to primary brain cancers [149,150]. Indeed, in the case of siRNAs, achieving a distribution in the interstitial fluid surrounding the cancer cells is not sufficient, as they need to reach the cytoplasm to trigger the RNAi. Thus, strategies aiming at

increasing the intracellular accumulation of such agents are required to obtain a powerful biological response using a low nucleic acid dose.

In the present chapter, the preliminary results about the preparation and physico-chemical characterization of folate-modified liposomes are described, and their ability to deliver siRNAs to glioblastoma cells in vitro is evaluated. The final formulation was developed keeping in mind the possibility for an in vivo translation, thus a simple production process, involving only anionic and neutral phospholipds, was used. A targeted nanocarrier exposing a negatively charged surface was obtained, and the encapsulation of siRNAs was achieved by introducing protamine, a cationic, natural protein able to condense the nucleic acid and form positively charged complexes. As the main focuses of this work were the preparation and the investigation of the uptake process of folate-modified liposomes by tumor cells, a non-silencing siRNA (bearing a fluorescent moiety in the case of the uptake studies) was used for the formulations. The U87 cells, derived from a human glioblastoma, were chosen as an in vitro model to test the transfection ability of the folate-targeted liposomes. Moreover, a competition for the uptake of targeted liposomes was observed when the cells were co-incubated with an excess of free folic acid, supporting the hypothesis that the cell uptake occurred through a folate receptor-mediated endocytosis.

2. Experimental

2.1. Materials

Distearoylphosphatidylcholine (DSPC) was purchased from Avanti (Alabaster, USA). Distearoylphosphatidylethanolamine-polyethyleneglycol-2000 (DSPE-PEG) and distearoylphosphatidylethanolamine-polyethyleneglycol-2000-folic acid (DSPE-PEG-

FOL) were purchased from Nanocs (New York, USA). Cholesterol, protamine, chloroform, agarose, non-silencing siRNA and fluorescent siRNA labeled with FAM, were purchased from Sigma (MO, USA). Lipofectamine2000 was purchased from ThermoScientific (Ireland).

2.2. Complexation of protamine with siRNA

Protamine and siRNA (negative control or fluorescent negative control) were mixed at given ratios and diluted with RNAse free water to a siRNA concentration of 130 nM. The solution was incubated for 30 minutes at room temperature under gentle stirring to allow formation of the complexes. The formation of protamine-siRNA complexes was monitored by 1% agarose gel electrophoresis in Tris borate EDTA (TBE) buffer at 90 V.

2.3. Liposomes preparation

Liposomes were prepared using a modified thin-film hydration method. Briefly, for the preparation of stealth protamine-liposomes (SPL) a mixture of DSPC (3.70 mg), cholesterol (1.05 mg) and DSPE-PEG (1.10 mg) was used. For the preparation of folate-modified protamine-liposomes (FPL), the lipid amounts were the following: DSPC (3.70 mg), cholesterol (1.05 mg), DSPE-PEG (0.20 mg) and DSPE-PEG-FOL (0.63 mg). The lipid mixtures were dissolved in chloroform, which was then removed under a stream of nitrogen to obtain a thin lipid film. The lipid film was hydrated under mechanical stirring with 1 ml of the preformed protamine-siRNA complexes (130 nM siRNA) at 65°C. Obtained liposomes were probe sonicated to reduce size and lamellarity and obtain a monodisperse population.

2.4. Physico-chemical characterization

Size and surface charge measurements were carried out using dynamic light scattering (DLS) and electrophoretic light scattering (ELS), respectively. SL and FL were diluted up to 1 mL with deionized water and their size, polydispersity index (PDI) and Z potenzial were assessed by DLS and ELS using a Malvern Zetasizer Nano ZS. A total of five readings for size and charge were taken per sample and the refractive index (1.33) and viscosity (0.8872 mPa s) of water were used for data analysis.

2.5. Vesicles stability in serum

SPL and FPL were prepared at 0.58 mg/ml total lipid concentration and were incubated in 10% fetal bovine serum (FBS) at 37°C under gentle agitation. At given time points, 200 µl of the incubation mixture was withdrawn and diluted with 800 µl distilled water. Size and polydispersity index were measured by DLS immediately after the dilution.

2.6. Nucleases protection assay

To monitor the degradation of liposomal siRNA by serum nucleases, SPL and FPL were prepared at a final siRNA concentration of 0.58 µM, and incubated with 10% FBS at 37°C. At stated time points 120 µl aliquot was removed, heated at 80°C for 5 minutes to inactivate RNAses, mixed with SDS (0.2%) to disrupt liposomes and stored at -20°C until gel electrophoresis was performed. All the samples were mixed with a 10X Blue juice, gel loading buffer (Invitrogen, CA, USA) and were added to the wells of 1% agarose electrophoretic gel, prepared with Tris borate EDTA (TBE) buffer and containing 6 µl of SafeView™ (NBS Biologicals Ltd., England) per 100 ml solution. The electrophoresis was carried out 90 V for 45 min in TBE buffer. Unbound siRNA was

used as a control. The bands were visualised by UV, using DNR Bioimaging Systems MiniBis Pro and Gel capture US B2 software.

2.7. Cell culture

The human glioblastoma cells (U87) were grown in DMEM, supplemented with 10% foetal bovine serum (FBS) (Sigma, Germany), 100 units/ml penicillin, and 100 µg/ml streptomycin (complete medium). The cells were routinely passed by treatment with a 0.05% Trypsin–EDTA solution (GIBCO, United Kingdom), and maintained in a humidified chamber at 37 °C with 5% CO2.

2.7.1. Cellular uptake assay

U87 cells (105 cells/well), were seeded in complete growth media 24 h prior to transfection in 24-well plates. Liposomes were prepared as previously described using FAM-labelled siRNA (Sigma). After 24 h, SPL or FPL were diluted in complete growth media and added to the cells to achieve a siRNA concentration of 25 nM or 50 nM. The cells were then incubated at 37°C in normal conditions. After 24 h, cells were washed with PBS to remove uninternalised vesicles and trypsinised. Detached cells were diluted by the addition of PBS and transferred into polystyrene round-bottom tubes (Becton Dickinson). After centrifugation (1000 rpm for 5 min) the supernatant was discarded and pellets were re-suspended in 1000 µl cold PBS and kept under ice until the FACS analysis, performed by a FACScalibur (Becton Dickinson). For each sample 10,000 cells were measured out according to the FACScalibur manual. Fluorescein-positive cells were analysed by Dot Plot and by Histogram Plot (data not shown). Untreated cells, empty liposomes or naked FAM-labelled siRNA were used as

negative controls. Lipofectamine 2000 (Lf) was used as a positive transfection control. The Lf:siRNA vector was prepared according to the manufacturer's protocol.

2.7.2. MTT

The MTT assay was used to assess the cell viability after transfection with the liposomes. U87 cells (10^4 cells/ well), were seeded 24 h prior to transfection in 96-well plates. Liposomes were prepared as detailed previously using non-silencing siRNA (Sigma). After 24 hours, transfection was carried out using 25 nM or 50 nM siRNA complete media for 24 h. After this time period the media was removed and replaced with 100 µl serum-free and antibiotic-free media and 20 µl MTT reagent (5 mg/ml solution in PBS). Cells were incubated for 4 h at 37°C after which 100 ml DMSO was added to each well. Absorbance was measured at 570 nm using a PerkinElmer Victor2 1420 UV plate reader. The results are expressed as the percentage cell viability relative to untreated controls

2.7.3. Competitive uptake assay

U87 cells (2.5 x 104 cells/well), were seeded in 24-well plates either in complete medium (F-) or in complete medium containing folic acid (1mM) (F+). After 24 h, the medium was replaced with fresh F+ or F- medium and the cells were treated with SPL or FPL to a final siRNA concentration of 50 nM. After 4 or 24h of incubation, the medium was removed, cells were washed with PBS and lysed by the addition of a Triton X/SDS lysis buffer. The lysed cells were transferred to a 96 well plate and the fluorescent signal of FAM-labeled siRNA was detected using a PerkinElmer Victor2 1420 plate reader (excitation 485 nm, emission 535 nm). Samples were normalised to the total protein concentration obtained by a BCA assay of the lysed cells. The

background fluorescence of the untransfected cells was subtracted from the results of SPL and FPL-treated cells.

3. Results and discussion

3.1. Preparation of siRNA-protamine liposomes

In order to drive the encapsulation of siRNAs within the aqueous core of negatively charged liposomal vesicles, the complexation of siRNA with protamine was primarily carried out. The term protamine is generally referred to a class of low molecular weight, cationic proteins that are involved in the condensation of DNA in the nucleus of the sperm [151]. Several protamine/siRNA mass ratios were investigated, with the aim of identifying the minimum amount of protamine sufficient to form a positively charged, stable complex with siRNAs. The complex-forming ability of the different protamine/siRNA mixtures was checked by gel electrophoresis (as reported in Chapter II - RVG-modified liposomes for siRNA delivery to primary neuronal cells: evaluation of alpha synuclein knockdown efficacy) and by measuring the Z potential of the complex. A protamine/siRNA ratio of 1 was sufficient to produce a complex which included all the siRNA and possessed a Z potential of 22±4 mV, thus, this ratio was selected to produce the lipsomal formulation.

Liposomes were prepared according to the thin film hydration method, operating in a way that the siRNA-protamine complex loading happened simultaneously to the formation of the lipid vesicles. This procedure was adapted from Buyens et al, who previously exploited the technique to achieve high entrampent efficiencies of siRNA into cationic liposomes [125]. Briefly, the lipid film, obtained mixing the appropriate lipids for the production of SPL or FPL, was hydrated with the protamine/siRNA solution, shaking the tubes at high speed above the transition temperature of the

main lipid. The liposomes were then subjected to sonication by a titanium probe sonicator. The use of a probe sonicator instead of a bath type sonicator was necessary to convey sufficient energy to the colloidal dispersion in order to reduce the size and lamellarity of vesicles. The harsh treatment applied, however, was not detrimental for the integrity of siRNA, as checked by gel electrophoresis (data not shown). The obtained SPL showed a mean diameter of 110 ± 3 nm, and a polydispersity index (PDI) of 0.204 ± 0.05, while the FPL, bearing the folic acid on their surface as a targeting agent, measured 117 ± 3 nm in diameter, with a PDI of 0.199 ± 0.02. The formulations were characterized in terms of Z potential, exhibiting a less negative surface charge in the case of FPL (-30.6 ± 2 mV) as compared to the SPL (-47.4 ± 4 mV). Taken together, the reduction of the absolute Z potential and the slight increase in size prove the presence of the folate moieties on the vesicles' surface.

3.2. Vesicles stability in the presence of serum

A preliminary assay to investigate the behavior of nanocarriers in serum-containing cell cultures and in vivo, consist in the determination of their mean diameter in presence of serum proteins. Indeed, any nanocarrier which is intended for systemic application should not undergo opsonization by serum proteins, which lead to an increase in size and -in vivo- to the rapid clearence by the mononuclear phagocyte system (MPS). PEGylation is widely used to confer stealth properties and avoid opsonization of nanoparticles. To test whether the chosen amount and chain length of PEG was sufficient to prevent serum protein absorption, SPL or FPL were co-incubated with 10% FBS and measurements of size were performed at given time points. The average diameter of the vesicles did not change significantly ($P>0.05$) for up to 24 hours of co-incubation (**Figure 3.2**). Interestingly, the folate moiety on the

liposomes surface did not induce the aggregation nor the absorption of serum proteins, making the FPL suitable for use in serum-enriched cell cultures.

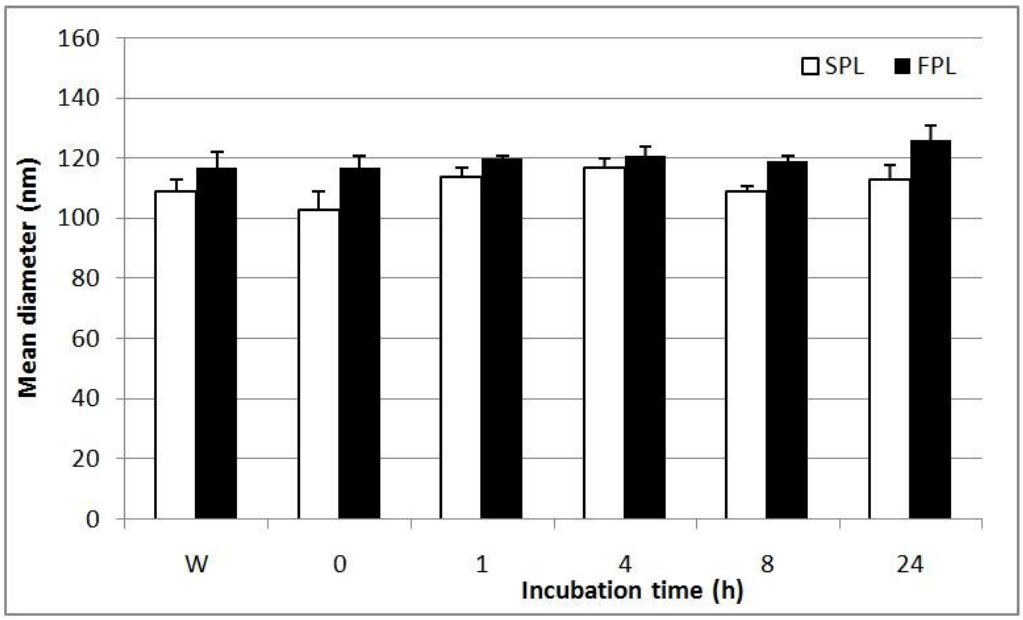

Figure 3.2. Mean diameter of liposomes (SPL or FPL) after co-incubation with FBS at 37°C. W: mean size measured in deionized water (to be used as a reference).

3.3. Nuclease protection assay

In addition to the stability of the vesicular structure, the siRNA integrity upon exposure to serum nucleases is an important feature when considering future in vivo experiments. The stability of SPL-encapsulated siRNA was assessed by agarose gel after different incubation times in 10% FBS. Prior to be loaded on the gel, the SPL-FBS mixtures were mixed with SDS with the dual aim of disrupting the lipid bilayer and, exploiting the anionic nature of the surfactant, dissociating the protamine-siRNA complex to allow the siRNA visualization on the agarose gel. The naked siRNA, used as a negative control, was completely degraded after only 10 minutes of FBS exposure (**Figure 3.3**). Conversely, the liposomal siRNA was efficiently protected from serum nucleases for up to 2 hours.

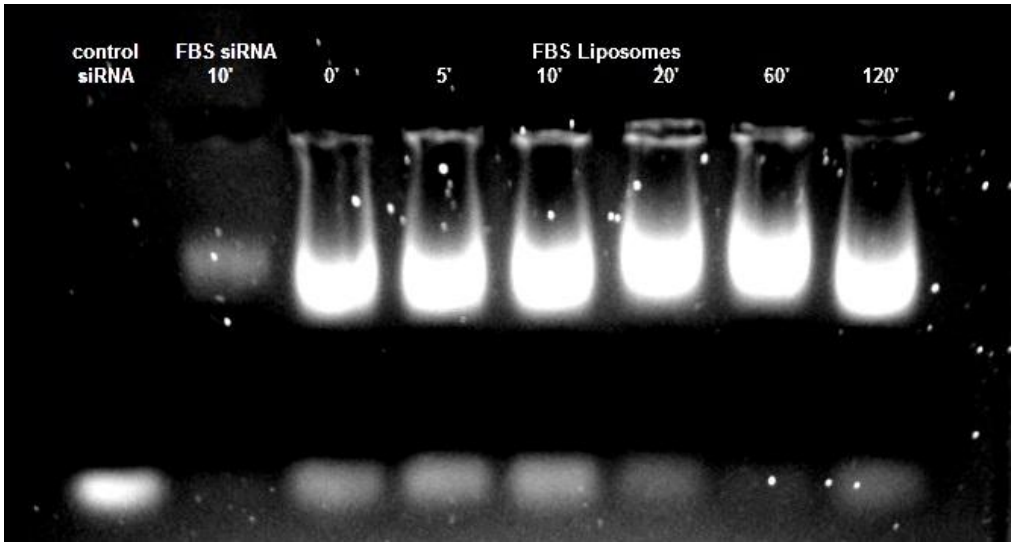

Figure 3.3. Gel electrophoresis of FBS co-incubated SPL after different exposure times (reported in minutes in the top of the figure). A naked siRNA was used as a positive control (first lane), and a naked siRNA co-incubated with FBS for 10 minutes was used as a negative control (second lane).

3.4. U87 cell uptake assay

The internalization of the liposome-encapsulated siRNA in human glioblastoma cells (U87) was assessed by flow cytometry. To detect the presence of siRNAs within the cells, the SPL, FPL or the control formulations were prepared using a FAM-labeled siRNA. The transfection time was kept constant to 24 hours, while the nanocarriers were used at two different concentrations (expressed as siRNA concentration) to investigate the influence of this parameter on the internalization rate. More in detail, 19 ± 2% of the cells treated with FPL (siRNA concentration = 25 nM) were efficiently transfected, as compared to a negligible uptake (< 0.5%) of the SPL (**Figure 3.4**). When the siRNA concentration was rised to 50 nM, the percentage of cells transfected by FPL grown to 65 ± 2%, while the SPL were able to be internalized by an extremely limited cell population (< 0.8%). Interestingly, the FRs were able to trigger the endocytosis of a larger amount of siRNA when exposed to higher concentration of

FPL, without an evident saturation effect despite the high concentration of folate (which corresponds to 75 μM when the siRNA concentration is 50 nM). This fact may be ascribable to the relatively long transfection time tested: during the 24 hours period, the FPLs may have been uptaken through a continuous internalization, unloading and recycling process of the FRs, preventing the detection of a clear saturation point of the receptors, that is known to happen in vitro at a folate concentration of 120 nM [140,152]. To draw more definite conclusions on the influence of FPL concentration on the uptake kinetics, the number of folate moieties bound to each liposome should be estimated, as well as the expression levels of FRs on the used cell line.

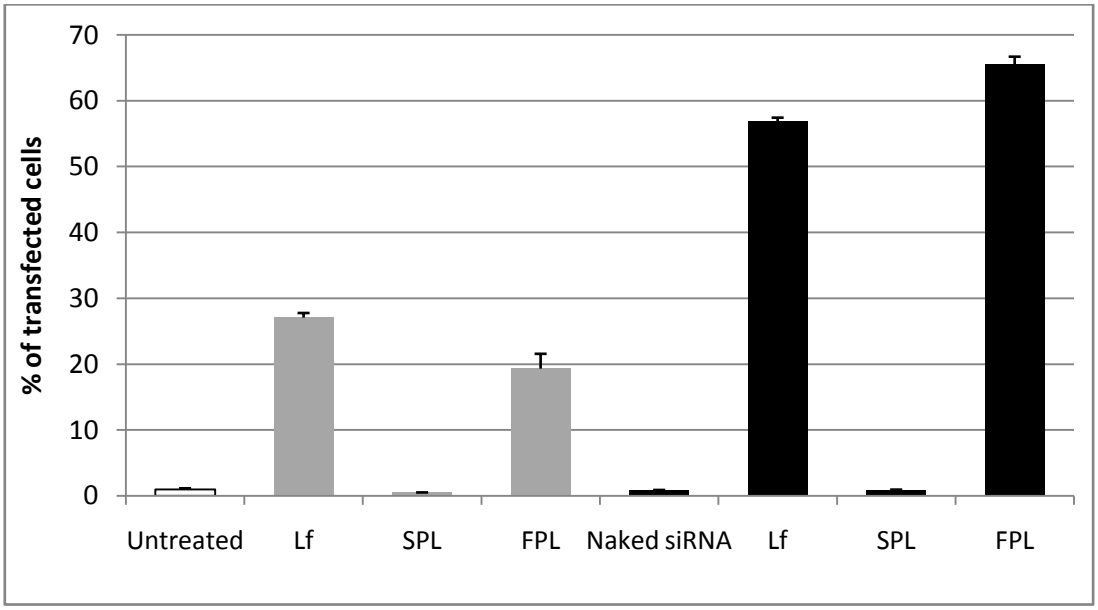

Figure 3.4. Histogram representing the percentage of transfected cells after 24 h exposure to the given formulation or control, as determined by FACS. Light grey bars: 25 nM siRNA, black bars: 50 nM siRNA. Lf: Lipofectamine 2000, SPL: stealth protamine-liposomes, FPL: folate protamine-liposomes. Data are expressed as mean ± standard deviation (n = 3).

3.5. Competitive uptake

The role played by the folate receptor in the uptake of the FPL was confirmed by a competitive uptake experiment. The cells were pre-incubated with free folic acid for 24 hours prior to be transfected either with SPL or FPL for 4 or 24 hours. The concentration of free folic acid was set below its limit of water solubility at 37°C, in order to avoid the addition of DMSO or other co-solvents to the cell medium. As expected, the pre-treatment with folic acid significantly reduces the uptake of FPL after 24 hours of transfection, due to the competition for the receptor mediated endocytosis (**Figure 3.5B**). Conversely, the difference in internalization of FPL between the pre-treated cells and the cells cultured in normal medium was not significant after 4 hours of incubation, which are probably not sufficient to allow a transport of a considerable amount of vesicles within the cells (**Figure 3.5A**). Moreover, the uptake of the SPL was the same (no statistically significant difference) if the cells were pre-treated with folic acid or not, demonstrating that the components of the vesicles other than the folic acid moiety (only present in the FPL) do not interact with the FRs. Surprisingly enough, the SPL-treated cells showed a detectable degree of transfection. This result was not in agreement with the results obtained from the FACS, where only a negligible internalization of the SPL was shown. A possible explanation could be linked to the less intensive washing steps in the case of the multiplate assay as compared to the FACS protocol, where a centrifugation and resuspension step of washed cells was included.

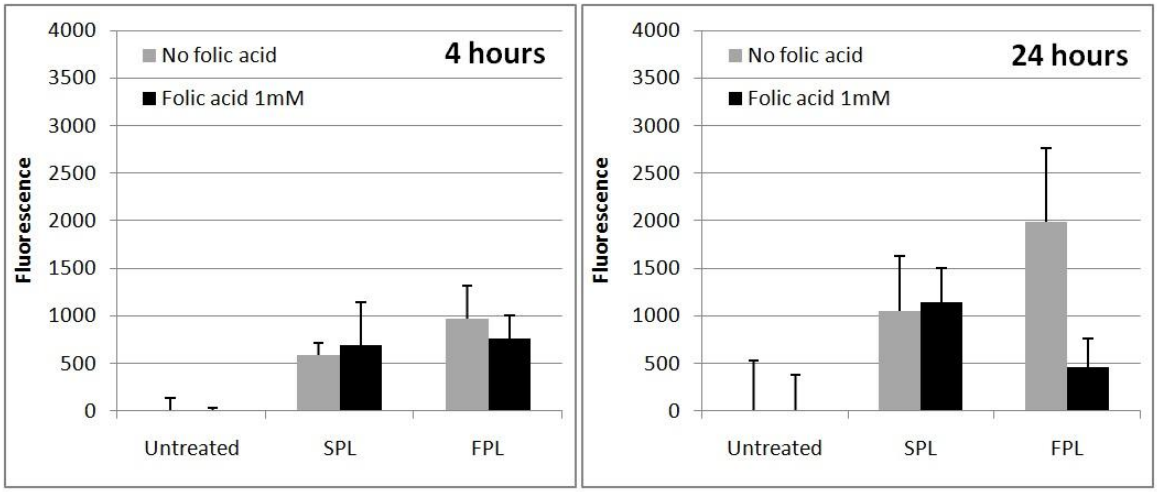

Figure 3.5. Competitive uptake assay. Grey bars represent the fluorescence of cells cultured in normal medium, while black bars represent the fluorescence of cells pre-treated with 1mM free folic acid. A) transfection time: 4 hours; B) transfection time: 24 hours. Data are expressed as mean ± standard deviation (n = 3).

3.6. MTT assay

The toxicity of the liposomal formulations on cells was evaluated by a MTT assay (**Figure 3.6**). Both the SPL and FPL showed some toxicity when applied on U87 cells at a siRNA concentration of 25 nM, reducing the amount of live cells to 86 ± 6% and 89 ± 5% as compared to an untreated population. Increasing the concentration of the formulations to 50 nM produced a more marked effect on cell viability, which was reduced to 72 ± 7% in the case of SPL and 77 ± 9% for the FPL-treated cells. The toxicity mediated by the nanocarriers is probably ascribable to the formulation itself rather than the siRNA, which consisted of a non-silencing sequence. Interestingly, no significant difference can be detected between the SPL and the FPL, suggesting that the folate-modified PEG lipid does not contribute to the noxious effect of the other components. Moreover, the toxicity of the developed formulations showed to be comparable (no statistically significant difference) to the one exerted by

Lipofectamine 2000, used at the same siRNA concentration of the liposomal nanocarriers.

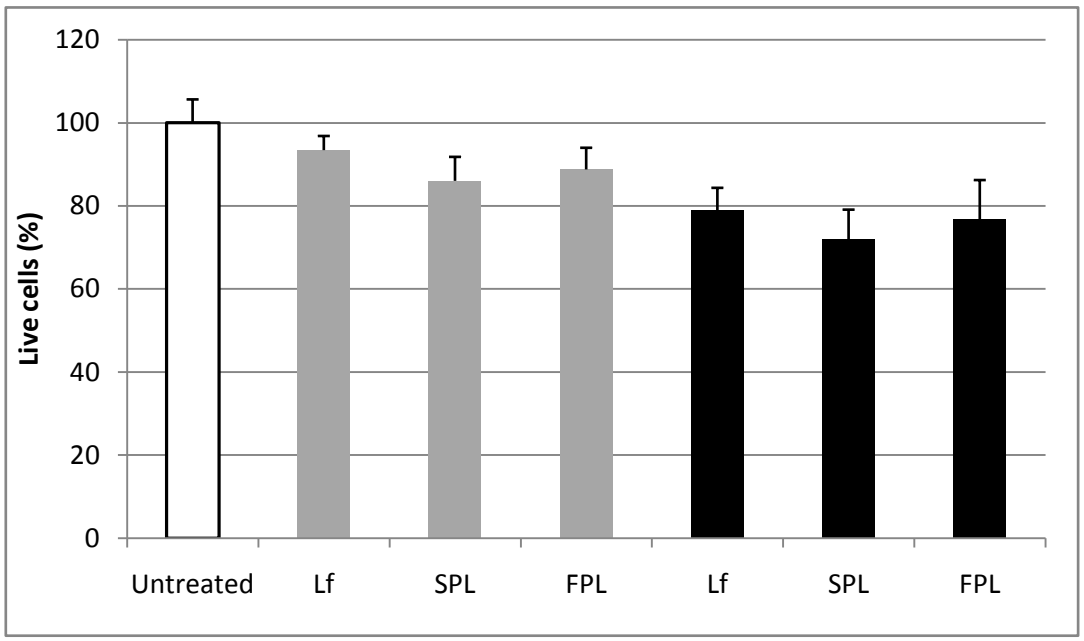

Figure 3.6. MTT assay. Light grey bars: 25 nM siRNA, black bars: 50 nM siRNA. Lf: Lipofectamine 2000, SPL: stealth protamine-liposomes, FPL: folate protamine-liposomes. Data are expressed as mean ± standard deviation (n = 3).

4. Conclusions and future perspectives

The work presented in this section comprises the preliminary assays required for the development of a nanocarrier for targeted siRNA delivery. Briefly, the design and the production of protamine-siRNA loaded liposomes is described, as well as their physico-chemical characterization. The developed nanocarriers showed to possess the essential features required for a future in vivo use, such as serum stability and a sufficient, although not optimal, protection of siRNAs from enzymatic degradation. The surface decoration with folic acid was chosen to induce a receptor-mediated uptake on brain cancer cells, exploiting a well-known homing device for a relatively less investigated target tumor. The inclusion of folic acid on the surface of liposomes significantly enhanced the uptake of siRNAs by glioblastoma cells, and the effect was

reversed by the competition of free folic acid added to the culture medium. These results may be intended as a premise for future investigations on the folate-mediated delivery of siRNA for the treatment of brain cancer. In this regard, a specific siRNA targeting a gene involved in GMB progression should be selected and included in the formulations. For instance, it has been reported that genes involved in the signalling pathways of receptor tyrosine kinase, retinoblastoma and p53 are mutated, deleted or amplified in over 75% of gliomas, providing a wide range of potential targets for RNAi-based therapy [153]. Moreover, a gene involved in the resistance of glioma to chemoterapeutics, such as multidrug resistance protein 1 (MDR 1), could be silenced to increase the sensitivity of tumor cells towards conventional therapies [154]. In this last scenario, the use of liposomes would allow the targeted co-delivery of siRNA and a cytotoxic agent, taking advantage of a convenient, single administration. In addition to the gene knockdown efficacy, the safety of the liposomal formulation towards normal brain cells should be assessed. In fact, our results showed that the prepared liposomes mediate a slight toxicity on the glioblastoma cells, which must be carefully evaluated to elucidate the components and/or the physico-chemical properties correlated to the effect.

Section II - Liposomes for subcutaneous drug delivery

The results described in this section have been published as:

Schlich M, Lai F, Murgia S, Valenti D, Fadda AM, Sinico C *Needle-free jet injection of intact phospholipid vesicles across the skin: a feasibility study*
Biomed Microdevices. **2016** Aug;18(4):67. doi: 10.1007/s10544-016-0098-3

and are reproduced with the permission of Elsevier.

Chapter IV
Needle-free jet injection of intact phospholipid vesicles across the skin: a feasibility study

Needle-free liquid jet injectors are devices developed for the delivery of pharmaceutical solutions through the skin. In this paper, we investigated for the first time the ability of these devices to deliver intact lipid vesicles. Diclofenac sodium loaded phospholipid vesicles of two types, namely liposomes and transfersomes, were prepared and fully characterized. The lipid vesicles were delivered through a skin specimen using a jet injector and the collected samples were analyzed to assess vesicle structural integrity, drug retention and release kinetics after the injection. In this regard, data concerning size, size distribution, surface charge of vesicles and bilayer integrity and thickness, before and after the injections, were measured by dynamic light scattering experiments, cryo-electron microscopy, and X-ray scattering techniques. Finally, the effect of vesicle fast jet injection through the skin on drug release kinetics was checked by in vitro experiments. The retention of the morphological, physico-chemical, and technological features after injection, proved the integrity of vesicles after skin crossing as a high-speed liquid jet. The delivery of undamaged vesicular carriers beneath the skin is of utmost importance to create a controlled release drug depot in the hypoderm, which may be beneficial for several localized therapies. Overall results reported in this paper may broaden the range of application of liquid jet injectors to lipid vesicle based formulations thus combining

beneficial performance of painless devices with those of liposomal drug delivery systems.

1. Introduction

Liquid jet injectors are devices that use a high-speed stream of fluid to deliver molecules across the skin into the intradermal, subcutaneous or intramuscular region without the use of a needle [155]. After more than 60 years of development, these devices are currently in clinical use for mass immunization and delivery of macromolecules such as insulin and growth hormones as well as small molecules including, for instance, penicillin, lidocaine, midazolam, steroids, alprostadil and bleomycin [156]. Basically, in the commercial liquid jet injectors, a piston pushed by a power source (compressed gas or spring) forces liquid medication at high speed (>100 m s^{-1}) through a tiny nozzle that is held against the skin. The high-speed stream of fluid, exiting the nozzle, puncture the skin and deliver drugs at different levels depending on the injector main parameters (i.e. nozzle diameter and stream velocity) as well as on liquid medication characteristics, mainly viscosity. Typically, the diameter of the nozzle and relative liquid jet, in commercial injectors, is smaller (30–560 μm) than the outer diameter of a standard hypodermic needle (810 μm for a 21G needle) [157,158]. The main advantage of using liquid jet injectors versus a standard syringe, is the reduction of needle phobia, and the absence of accidental needle-stick injury. Recently, liquid jet injectors have been used for subcutaneous injection of polymeric nanoparticles based on the biodegradable poly(lactide-co-glycolide) (PLGA)[159]. This study demonstrates the ability of injected PLGA particles to release coumarin-6 in the skin for prolonged periods. In fact, drugs delivered by needle-free jet injectors in form of solutions are generally quickly absorbed into

systemic circulation, thus rapidly cleared from the site of administration [160]. On the other hand, the encapsulation of drugs in nano/micro-carriers results in a prolonged location around the site of administration, which may be beneficial for localized therapies. An additional benefit of delivering drug-loaded nanoparticles to the hypoderm or into the muscle by liquid jet injectors, is the possibility of reaching poorly perfused areas for the local treatment of inflammation and pain, selecting the injection site accordingly [161]. Non-steroidal anti-inflammatory drugs (NSAIDs), including diclofenac, are usually applied on the skin surface in gels or patches to reach deep tissue below the skin for the relief of pain symptoms in muscular strains, sprains and contusions. Local application could be beneficial also in the treatment of rheumatic and osteoarthritic diseases but the difficulty of overcoming the barrier of the skin and subsequent cutaneous clearance make the drug pharmacokinetics complex [162]. During the past decades, there has been a lot of interest in lipid vesicles as a tool to improve drug skin permeation and to control its release rate [163]. However, when applied on the skin, vesicular systems provide variable effects according to their composition (i.e. liposomes, niosomes, ethosomes, elastic and deformable vesicles), structure and entrapped drug, and therefore, a variety of possible mechanisms have been proposed to explain vesicle skin penetration and permeation. They include the intact vesicular penetration, the penetration enhancing effect, the adsorption and fusion of vesicles on the skin surface and the vesicle penetration through the transappendageal route. Thus, some of the proposed mechanisms suggest that the integrity of lipid vesicles is maintained across the skin, while others hypothesize a disruption of the vesicular structure [164].While both the scenarios allow the penetration of the active molecule in the deeper skin layers, an intact vesicle, able to cross the skin barrier with the lowest cargo leakage possible, is

required to provide a sustained release over time. However, several conflicting results on this research topic have been published and the definite mechanism whereby vesicle skin drug delivery is achieved still represents a controversial point of view [163,165]. The key innovation of this work is the combination of two technologies such as liposomes and jet injectors. Indeed, in this study, different phospholipid vesicle formulations, such as conventional liposomes and transfersomes, were loaded with diclofenac sodium as a model drug and tested for their integrity and controlled release properties after subcutaneous administrations by means of a liquid jet injector. In fact, the high pressure given by the jet injector and the shock of fast impact on the skin could be detrimental for the structural and functional integrity of lipid vesicles, which are formed and maintained in shape by rather labile intermolecular forces. Thus, the possibility of obtaining a subcutaneous depot of loading drug intact vesicles through the administration by a needle-free liquid jet injector, overcoming the issues associated to the skin permeation, was here investigated for the first time. The rationale behind this new approach is to improve both the efficacy and the safety of localized therapy combining the performance of painless liquid injection devices with those of liposomal drug delivery systems.

2. Experimental

2.1. Materials

Purified soy phosphatidylcholine (Phospholipon® 90G, P90G) was kindly supplied by Lipoid GmbH (Germany). Polysorbate-80 (Tween 80) and diclofenac sodium (DCF) were purchased from Galeno (Prato, Italy). Ethanol and all the other products were of analytical grade and were purchased from Sigma–Aldrich (Milan, Italy).

2.2. Vesicle preparation

Conventional and elastic liposomes (transfersomes) were prepared using a thin film hydration method [166]. Briefly, the P90G (in addition to the surfactant in case of elastic liposomes) was dissolved in ethanol into a round bottomed flask. An appropriated amount of diclofenac sodium was added to the ethanol solution to obtain a drug concentration of 0.5 % (w/v) in the final vesicle preparations. The organic solvent was removed by rotary evaporation (Rotavapor, Buchi, Germany) and the lipid-drug mixture was deposited as a thin film. Final traces of solvent were removed under vacuum, overnight. The dried lipid films were hydrated either with distilled water (conventional liposomes) or with 7 % (v/v) ethanol /distilled water solution (elastic liposomes) by rotation at 80 rpm for 30 min at 40 °C, to achieve a final lipid concentration of 42.5 mg/ml (for liposomes and transfersomes) and a surfactant concentration of 7.8 mg/ml (for transfersomes). Resulting vesicles were vortexed for 1 min and then allowed to swell for 1 h at room temperature. 5 ml of liposomal suspensions were then sonicated for 120 s in cycles of 3 s on and 2 s off using a titanium probe ultrasonic disintegrator (Soniprep 150, MSE Crowley, UK).

2.3. Vesicle characterization

The average diameter and polydispersity index (PI) of both conventional and elastic liposomes were measured by dynamic light scattering (DLS) using a Zetasizer nano (Malvern Instrument, UK). Zeta potential was determined using the Zetasizer nano by means of the M3-PALS (Phase Analysis Light Scattering) technique. All the samples were analyzed 24 h after preparation. The DLS analysis of jet injected samples was carried out immediately after the administration. Small-angle X-ray scattering (SAXS) was recorded with a S3-MICRO SWAXS camera system (HECUS x-ray Systems, Graz,

Austria). Cu Kα radiation of wavelength 1.542 Å was provided by a GeniX x-ray generator, operating at 50 kVand 1 mA. A 1D-PSD-50M system (HECUS x-ray Systems, Graz, Austria) containing 1024 channels (54.0 μm wide) was used for detection of scattered x-rays in the small-angle region. The working q range ($Å^{-1}$) was $0.003 \leq q \leq 0.600$, where $q = 4\pi\sin(\theta)\lambda^{-1}$ is the scattering wave vector. For the analysis, thin-walled 2 mm glass capillaries were filled with the liposome dispersions. The diffraction patterns were recorded for 3 h and analyzed using the GAP (Global Analysis Program) software [167]. The GAP allows fitting the SAXS pattern of bilayer-based structures (i.e. vesicles and lamellar phases) [168]. Particularly, the membrane thickness (d_B) was defined as $2(z_H + 2\sigma_H)$, where z_H and σ_H, obtained from SAXS curve fitting, respectively represent the head group to bilayer center distance and the polar head amplitude. The latter parameter was kept fixed at 5 Å [169]. The morphology of the nanoparticles was observed by cryo-transmission electron microscopy (cryo-TEM) at 120 kV acceleration voltage using an FEI Tecnai T12 G^2 transmission electron microscope at about −175 °C in the low-dose imaging mode to minimize electronbeam radiation-damage. Images were digitally recorded with a Gatan US1000 high-resolution CCD camera [170].

2.4. Encapsulation efficiency

Conventional and elastic liposomal dispersions were purified from the non-incorporated drug by exhaustive dialysis, 24 h after preparation. Dispersions were loaded into a dialysis tubing (Spectra/Por® membranes: 12– 14 kDa MW cut-off, 3 nm pore size; Spectrum Laboratories Inc., USA) and dialyzed against distilled water (for conventional liposomes), or a 7 % (v/v) ethanol /distilled water solution containing Tween 80 at the same concentration used in the preparation (for

transfersomes). Dialysis of each sample (1 ml) was carried out in 500 ml of solvent, at 25 °C for 2 h which was appropriate to allow the dissolution and consequent removal of free diclofenac (DCF). Drug loading efficiency (E%) was determined by high performance liquid chromatography (HPLC) after disruption of dialized (D) and not purified (NP) vesicles with methanol. The following equation was used:

$$E\% = \frac{DCF\ in\ D\ \times 100}{DCF\ in\ NP}$$

Diclofenac content of D and NP vesicles was quantified at 283 nm using a chromatograph Alliance 2690 (Waters, Italy). The column was a Sunfire C18 (3.5 μm, 4.6 × 150 mm, Waters). The mobile phase was a mixture of 20 % water and 80 % acetonitrile (v/v), delivered at a flow rate of 0.5 ml/min. A standard calibration curve (R^2 of 0.999) was built up by using working, standard solutions (1.0–0.01 mg/ml). The diclofenac retention time (tr) was 4 min, and the minimum detectable amount was 2 ng/μl.

2.5. Jet injection of vesicles dispersions

Liposome jet injections into the skin were performed by means of a commercial jet injector, Comfort-in (Eternity Healthcare Inc., Vancouver, BC, Canada), developed for subcutaneous injection of insulin, with a jet diameter of 178 μm, following a procedure reported in literature [171]. Full-thickness skin was excised from new born Goland-Pietrain hybrid pigs (1–1.5 kg) died of natural causes, provided by a local slaughterhouse. A previous study has shown that this animal model provided reliable information enabling to predict drug ability to permeate through human skin [172]. The subcutaneous fat was carefully removed and the skin was cut into 3 × 3 cm^2 samples, randomized and stored at −80 °C. One day before the experiments it was

pre-equilibrated in physiological solution (0.9 %, w/v of NaCl) at 32 °C. Briefly, a skin specimen supported by a wire mesh, was placed on a disposable glass vial (10 ml volume). The nozzle chamber of the jet injector was filled with 500 µl of vesicles dispersion and the injection was performed holding the nozzle at right angle to the skin, placing them in direct contact. The same procedure without the skin specimen was carried out for jet injections into an empty vial.

2.6. In vitro release study

In vitro release studies of diclofenac sodium from different vesicle formulations were performed through a cellulose membrane (Spectra/Por® membranes: 12–14 kDa MW cutoff, 3 nm pore size; Spectrum Laboratories Inc., USA) using vertical Franz diffusion cells (Rofarma, Milan)[173]. The receiver compartment had a volume of 6.5 ml and an effective diffusion area of 0.636 cm2. The receptor compartment was filled with a 20 % (v/v) ethanol/distilled water mixture, which was constantly stirred with a small magnetic bar and thermostated at 37 °C throughout the experiments. 0.5 ml of each vesicle suspension were placed on the membrane surface and the experiment was run for 8 h. Two diclofenac sodium solutions either in distilled water or in 7 % (v/v) ethanol/distilled water were also studied as controls of respective formulations. At scheduled time intervals, 1 ml of the receptor solution was withdrawn and replaced with fresh medium to ensure sink conditions. The amount of diclofenac sodium in withdrawn samples was analyzed by HPLC. At the end of the experiments, samples of the donor phase were analyzed and checked for diclofenac sodium content: the total recovery from the donor and receptor compartments was always more than 95 % of the applied dose.

2.7. Statistical analysis of data

Data analysis was carried out with the software package R, version 2.10.1. Results are expressed as the mean ± standard deviation. Multiple comparisons of means (Tukey test) were used to substantiate statistical differences between groups, while Student's t-test was used for comparison between two samples. Significance was tested at the 0.05 level of probability (P).

3. Results and discussion

Delivery of diclofenac loaded intact vesicles through the skin by jet injection was assessed by comparison of physicochemical and technological properties of vesicles before (Pre) and after the injection. Two different conditions of jet injection were examined (Vial and Skin). In the former case (Vial) the injection was performed directly in a glass disposable vial to analyze exclusively the effect of high pressure given by the device on vesicles' integrity. In the latter case (Skin), the syringe was directed against a skin specimen, and the injected dispersion was collected in a glass vial underneath and analyzed to study the influence of forced skin crossing on vesicle structure. Two different class of vesicles, namely conventional liposomes and transfersomes, were prepared. As with liposomes, transfersomes mainly consist of phospholipids, but also contain a surfactant, which was Tween 80 in this study, capable of increasing bilayer deformability. When applied on the skin surface, transfersomes can squeeze between the corneocytes and reach the deep skin layers more easily than conventional liposomes, due to their elasticity [174]. Based on this fact, the choice of testing high deformable and elastic vesicles was aimed to investigate if these features might be beneficial for bearing the impact with the injector plunger and the skin. More in details, data concerning size, size distribution

and surface charge of vesicles before and after the injections were analyzed and compared. Moreover, bilayer integrity and thickness was checked by means of X-ray scattering techniques and cryo-TEM, while in vitro drug release experiments were performed to further investigate vesicle stability as well as to evaluate the effectiveness as delivery system.

3.1. Effect of jet injection on vesicle physico-chemical properties

The method of preparation of small unilamellar vesicles (both liposomes and transfersomes) showed high reproducibility in terms of hydrodynamic radius and polydispersity index. The vesicle mean diameter, which was measured 24 h from the preparation to allow the system to stabilize after the sonication process, was approximately 55 nm and 46 nm, for conventional liposomes and Transfersomes respectively (**Table 4.1**). The vesicular systems were found to be sufficiently homogeneous with over 98% of the signal collected by the DLS belonging to the population with the cited dimensions. DLS experiments carried out on vesicles injected through the skin and in the glass vial showed no significant differences ($P > 0.05$) in average size and PDI compared to the uninjected formulation (**Figure 4.1**).

	Size (nm)	**PDI**	**Z potential (mV)**	**EE (%)**
Liposomes	54.5±5	0.284±0.020	-53.6±6.2	73±4
Transfersomes	46.4±2	0.251±0.020	-30.2±1.4	68±5

Table 4.1. Main characteristics of liposomes and transfersomes before injection (Pre). Data are expressed as mean ± standard deviation (n = 6).

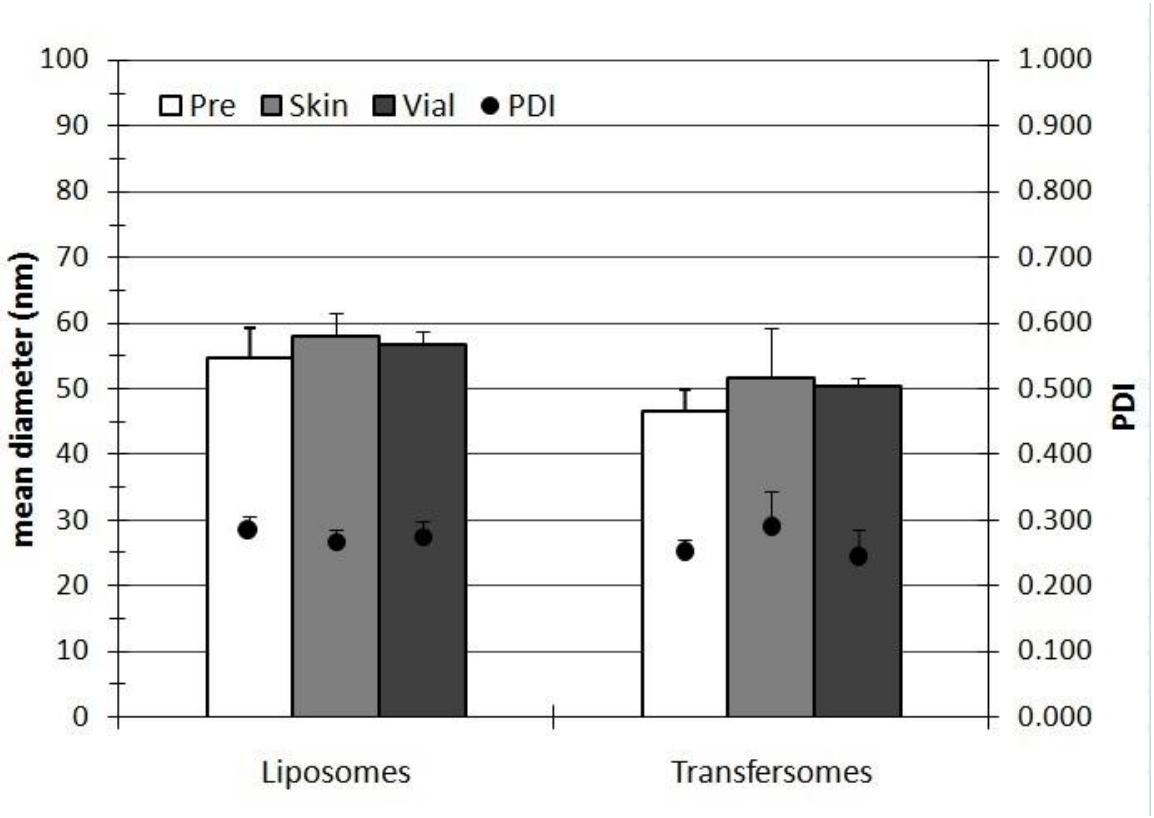

Figure 4.1. Mean diameter (histogram bars) and polydispersity index (dots) (PDI) of liposomes and transfersomes before (Pre) and after the injection in an empty vial (Vial) or through the skin (Skin). Differences between Pre, Skin and Vial liposomes as well as Pre, Skin and Vial transfersomes are not statistically significant ($P > 0.05$). Error bars represent the mean ± standard deviation of at least six independent experimental determinations.

Both conventional liposomes and transfersomes retained their average size, showing neither aggregation nor size reduction as a consequence of the jet injection. The Zeta Potential of transfersomes was significantly ($P < 0.05$) less negative than that of liposomes, although the presence of the non-ionic surfactant Tween 80 into the bilayer composition should not affect the surface charge. Such decrease in Zeta potential value of transfersomes is probably related to the presence of the bulk headgroup of Tween 80, whose position, which is expected to be on the surface of vesicles due to its polar nature, may decrease the density of charged phospatidylcholine molecules thus reducing the negative charge. Besides the position

of tween 80, also the orientation of the phosphatidylcholine head groups could contribute to the negative potential values. Indeed, the choline group plane may lie below the phosphate group plane. The same differences can be observed in the corresponding jet injected samples (Vial and Skin, **Table 4.2**), thus suggesting the retention of the lipid (liposomes) and lipid-surfactant (transfersomes) organization on the surface of vesicles after the injection.

Sample	**Z potential (mV)**
Lipo-Pre	-51 ± 4
Lipo-Vial	-48 ± 4
Lipo-Skin	-49 ± 3
Transf-Pre	-30 ± 3
Transf-Vial	-32 ± 2
Transf-Skin	-31 ± 2

Table 4.2. Zeta potential of liposomes and transfersomes before (Lipo-Pre, Transf-Pre) and after the injection in an empty vial (Lipo-Vial, Transf-Vial) or through the skin (Lipo-Skin, Transf-Skin). Data are expressed as mean ± standard deviation (n = 6).

Scattering profiles obtained from SAXS experiments on the liposome and the transfersome systems under investigation are reported in **Figure 4.2**. All the liposomes formulations displayed a broad diffusive scattering pattern with a barely visible shoulder at low q suggesting the presence of tiny amounts of oligolamellar structures in a dispersion of mostly unilamellar liposomes. Differently, transfersomes exhibited the pure diffusive scattering pattern classically attributed to unilamellar vesicles, with no evidence of Bragg or quasi-Bragg peaks, representative for oligo- or multilamellar vesicles. In all cases, the analysis performed by GAP reveals structural parameters (**Table 4.3**) in agreement with similar systems[175].

Remarkably, within the liposome or transfersome series, the scattering profiles perfectly overlap, indicating that the use of the jet injector and the passage through

the skin did not cause significant alterations in the vesicles bilayer or in the systems lamellarity.

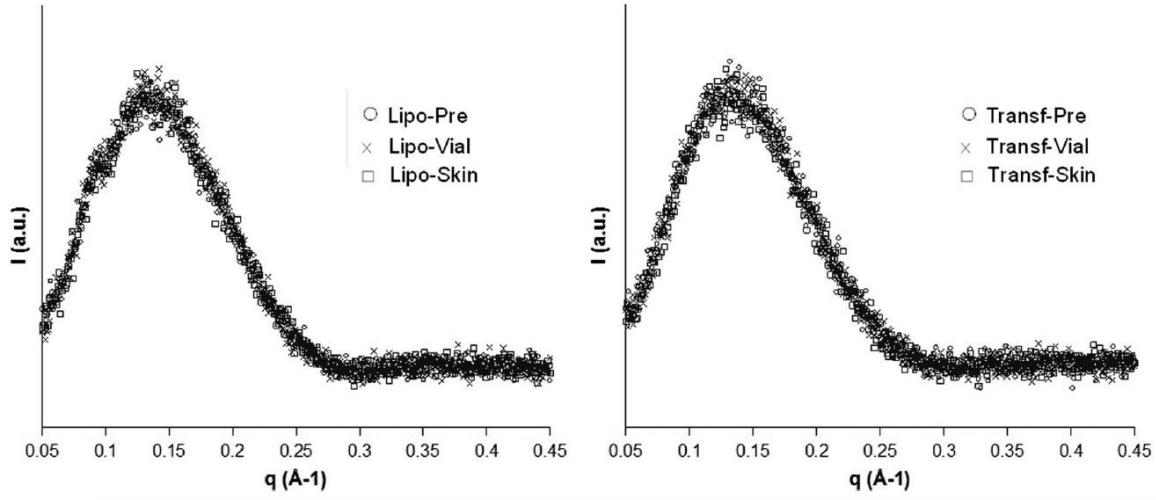

Figure 4.2. SAXS patterns of liposomes (left) and transfersomes (right) before (Pre,○) and after the injection in an empty vial (Vial, X) or through the skin (Skin, □).

Sample	**Z_H (Å)**	**d_b (Å)**
Lipo-Pre	15.1 ± 0.1	50 ± 1
Lipo-Vial	15.2 ± 0.1	50 ± 1
Lipo-Skin	15.2 ± 0.1	50 ± 1
Transf-Pre	15.0 ± 0.1	50 ± 1
Transf-Vial	15.0 ± 0.1	50 ± 1
Transf-Skin	15.0 ± 0.1	50 ± 1

Table 4.3. Bilayer thickness (d_b) and head group to bilayer center distance (z_H) of liposomes and transfersomes before (Lipo-Pre, Transf- Pre) and after the injection in an empty vial (Lipo-Vial, Transf-Vial) or through the skin (Lipo-Skin, Transf-Skin), obtained from GAP analysis. Data are expressed as mean ± standard deviation (n =3)

Results from DLS and SAXS analysis were also confirmed through the direct visual inspection of the samples as seen by cryo-TEM. In **Figure 4.3** are reported some micrographs representative for the transfersomes freshly prepared (A, B) and after

injection through the skin (C, D) showing that in both cases samples are characterized by a population of unilamelar vesicles endowed of low polydispersity.

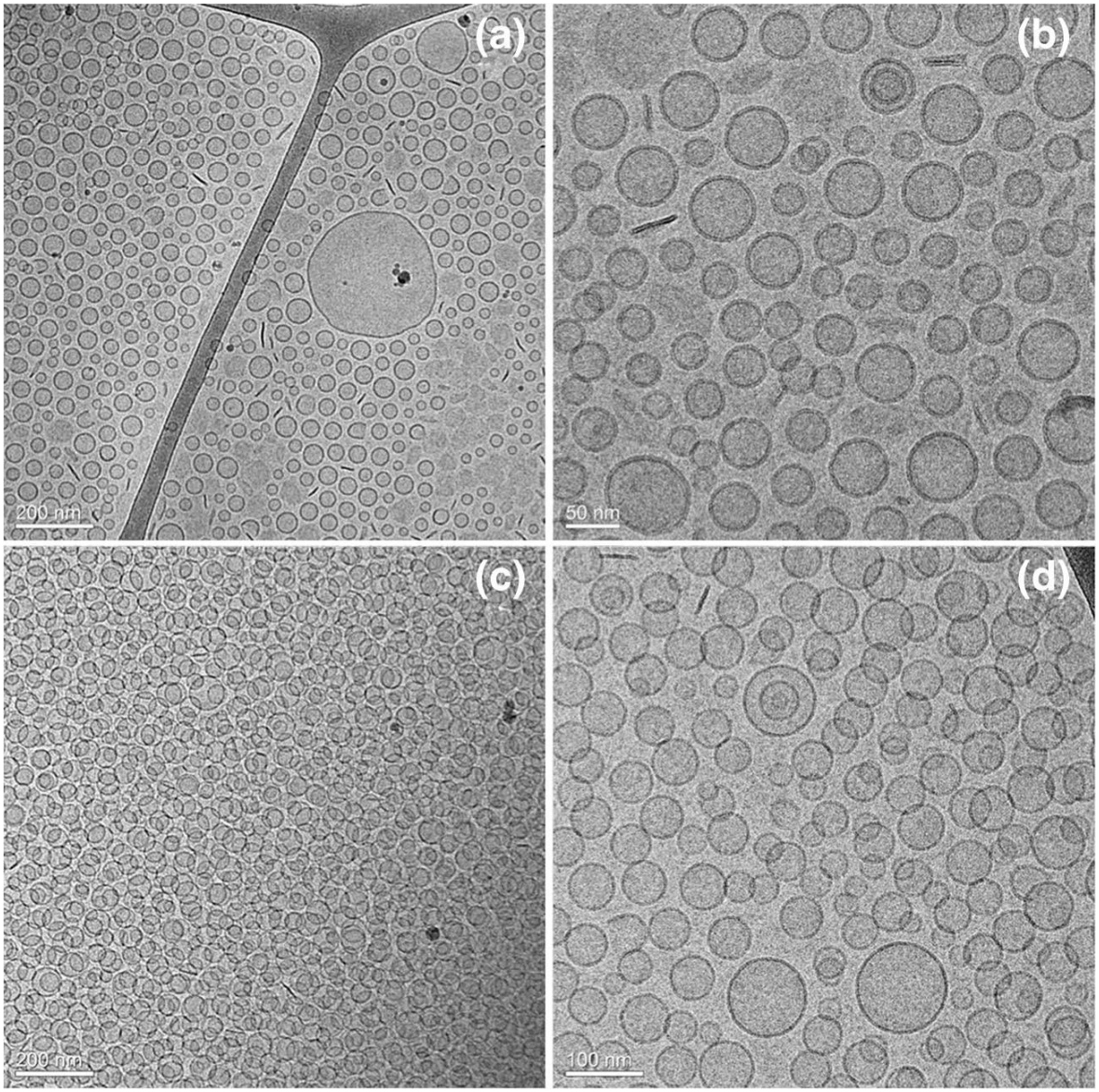

Figure 4.3. Cryo-TEM micrographs of transfersomes obtained immediately after preparation (a, b) and after injection through the skin (c, d). Scale bars are 200 (a, c), 100 (d), and 50 (b) nm.

3.2. Drug retention in jet injected vesicles

On the basis of size, z-potential and SAXS measurement results, we can reasonably state the structural integrity of vesicles and substantial absence of effects of the jet

injection, alone (Vial) or in combination with the skin crossing (Skin), on these features. To investigate the drug retention of vesicles following the jet injection, the encapsulation efficiencies of liposomes and transfersomes before and after the shot were evaluated. Transfersomes showed an encapsulation efficiency of diclofenac sodium slightly lower than liposomes, resulting in 68 ± 5 % and 73 ± 4 %, respectively. Since the presence of ethanol and/ or surfactant can increase the drug dissolution and encapsulation efficiency, this is an unexpected result that could be ascribed to the higher permeability of the bilayered membrane [174]. Of most interest is the conservation of encapsulation efficiency after the jet injection of both liposomes and transfersomes (**Figure 4.4**), proving that no changes occur in drug retention capability of vesicles when exposed to fast jet injection and skin crossing.

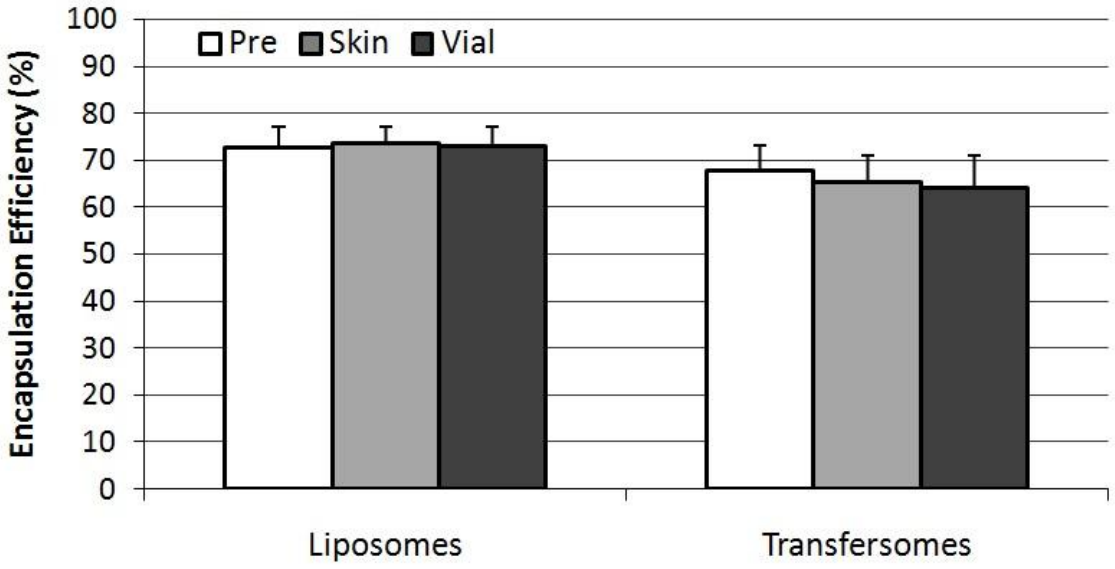

Figure 4.4. Encapsulation efficiency of liposomes and transfersomes before (Pre) and after the injection in an empty vial (Vial) or through the skin (Skin). Differences between Pre- Skin- and Vial-Liposomes, as well as Pre- Skin- and Vial-Transfersomes are not statistically significant ($P > 0.05$). Bars represent the mean ± standard deviation of at least six independent experimental determinations.

3.3. In vitro drug release study

The concept of lipid vesicles as potential carriers for controlled drug release has been extensively discussed in past years [176,177]. When administered locally, the liposomal formulation allows for prolonged retention of the encapsulated drug at the injected site by limiting its diffusion and degradation ('depot' function). In this study we performed in vitro diclofenac sodium release experiments from both liposomes and transfersome, before and after injection. With this experiment, we aimed to confirm the controlled release of our vesicular systems exploiting a well-known in vitro model, and to check the effect of vesicle fast jet injection through the skin on drug release kinetics. Comparison between not-injected (Pre) and skin-jet injected samples (Skin) showed no significant differences ($P > 0.05$), resulting in the release of 27 ± 5 % and 31 ± 2 % of the dose for liposomes, and 25 ± 2 % and 23 ± 4 % for transfersomes (**Figure 4.5**).

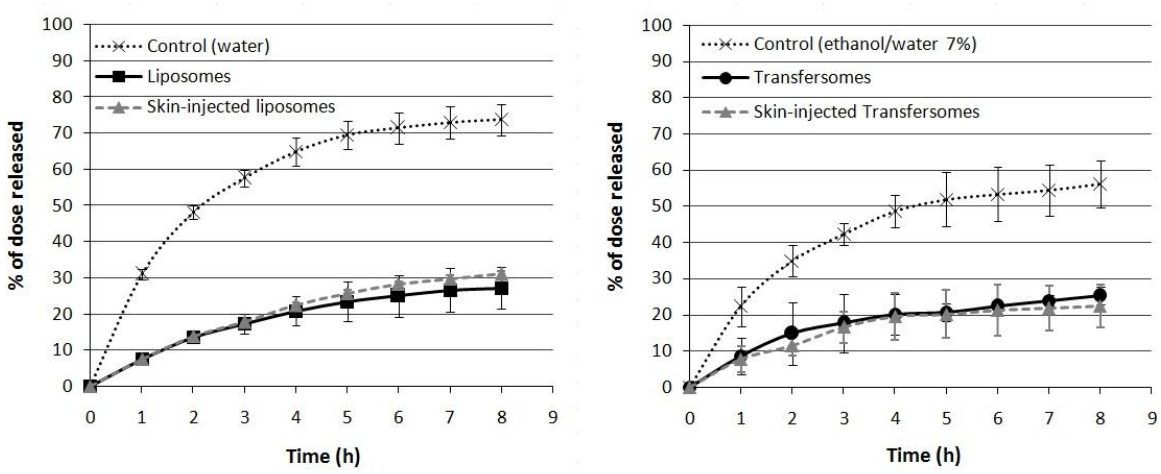

Figure 4.5. In vitro release (%) of diclofenac sodiumthrough cellulose membrane fromliposomes and transfersomes (pre and after skin injection) and control solutions (water or ethanol/water 7 % v/v). Data are expressed as mean ± standard deviation (n = 3)

All the tested formulations showed a prolonged release profile, that is evident by comparison of their results with the ones given by the control solutions of diclofenac sodium (in water or in ethanol/water 7 % v/v), which turned out in a faster release of the drug. Such results assess the possibility of administration of both conventional liposomes and transfersomes in the hypoderm through commercial jet injectors, obtaining an efficient subcutaneous drug reservoir with a long lasting release profile. Such system can be of major interest to produce a localized sustained effect in the site of injection (e.g. near to an inflamed joint) reducing the amount of drug absorbed in the systemic circulation over time, and avoiding high peak concentration of conventional dosage forms with immediate release. Moreover, the drug release rate could be modulate by varying the vesicle structure (i.e. uni- or multilamellar), size and lipid composition and/or the depth of the injection, using devices which differ for stream rate, nozzle diameter etc.

4. Conclusions

Liposomes and transfersomes loaded with diclofenac sodium were prepared and fully characterized. Both the vesicular systems were found capable of maintaining their physicochemical properties, as well as the in vitro drug release profile, after the injection through the skin by a needle-free liquid jet injector. It is, to our knowledge, the first time that a commercially available needle-free medical device is used for the subcutaneous delivery of liposomes and transfersomes, assessing the integrity of vesicles after skin crossing as a high-speed liquid jet. Results reported in this paper may broaden the range of application of liquid jet injectors to lipid vesicle-based formulations, and pave the way to the design of novel liposomal medications for subcutaneous delivery.

General conclusions

Shortly after the first report by Bangham in 1965, liposomes have been proposed as drug delivery systems. In over 40 years of research in this field, liposomes have been extensively investigated as carriers for the delivery of a wide range of pharmaceutically active compounds and macromolecules, with the aim of modifying and improving their biopharmaceutical properties. In fact, the inclusion in liposomes can affect significantly the distribution of the loaded drug, modifying the toxicity and efficacy profile and allowing a site specific delivery exploiting the concept of targeting. Moreover, the flourishing research of the last decades in the field led to the availability of a great variety of production methods and components, enabling the fine tuning of vesicles properties to achieve very specific goals, such as prolonged release or distribution to difficult-to-access organs and tissues.

In this thesis, liposomes have been used for two main purposes, namely the targeted delivery of siRNAs to neuronal or brain cancer cells, and the combination with a needle-free jet injector for the administration of anti inflammatory drugs in the subcutaneous tissue.

As for the first section, liposomes were decorated with appropriate targeting agents (a virus-derived peptide or folic acid) and demonstrated an increased uptake of siRNA by the target cells. In addition, the inclusion of siRNAs within the vesicle core led to the protection of the nucleic acid from the nuclease digestion, and to a knockdown of the target gene comparable to the one achieved by commercial transfection agents.

The second section presents the first report (to the best of our knowledge) of a combined use of a commercial needle-free jet injector with a liposomal formulation. In this work, the feasibility of the administration of liposomal suspension through the

cited medical device was assessed by monitoring the physico-chemical properties of the vesicles before and after the administration through the skin *ex-vivo.* The positive results reported include the needle-free injector among the possible administration methods for liposomes, thus broadening the applications of such delivery systems.

The different topics debated in the two sections of this thesis reflect the great versatility of liposomes, which, despite the vast literature available and an extensive research carried out in the last decades, still have a great potential to be unveiled.

References

[1] G. Meister, T. Tuschi, Mechanisms of gene silencing by double-stranded RNA, Nature. 431 (2004) 343–349. doi:10.1038/nature02873.

[2] G. Stefani, F.J. Slack, Small non-coding RNAs in animal development, Nat. Rev. Mol. Cell Biol. 9 (2008) 219–230. doi:10.1038/nrm2347.

[3] B. Zhang, X. Pan, G.P. Cobb, T.A. Anderson, Plant microRNA: A small regulatory molecule with big impact, Dev. Biol. 289 (2006) 3–16. doi:10.1016/j.ydbio.2005.10.036.

[4] C. Wilkins, R. Dishongh, S.C. Moore, M. a Whitt, M. Chow, K. Machaca, RNA interference is an antiviral defence mechanism in Caenorhabditis elegans., Nature. 436 (2005) 1044–1047. doi:10.1038/nature03957.

[5] S.W. Ding, O. Voinnet, Antiviral Immunity Directed by Small RNAs, Cell. 130 (2007) 413–426. doi:10.1016/j.cell.2007.07.039.

[6] N. Agrawal, P.V.N. Dasaradhi, A. Mohmmed, P. Malhotra, R.K. Bhatnagar, S.K. Mukherjee, RNA interference: biology, mechanism, and applications., Microbiol. Mol. Biol. Rev. 67 (2003) 657–85. doi:10.1128/MMBR.67.4.657.

[7] C. Napoli, C. Lemieux, R. Jorgensen, Introduction of a Chimeric Chalcone Synthase Gene into Petunia Results in Reversible Co-Suppression of Homologous Genes in trans., Plant Cell. 2 (1990) 279–289. doi:10.1105/tpc.2.4.279.

[8] G.L. Sen, H.M. Blau, A brief history of RNAi: the silence of the genes, Faseb J. 20 (2006) 1293–1299. doi:10.1096/fj.06-6014rev.

[9] A. Fire, S. Xu, M.K. Montgomery, S.A. Kostas, S.E. Driver, C.C. Mello, Potent and specific genetic interference by double-stranded RNA in Caenorhabditis elegans, Nature. 391 (1998) 806–811.

[10] S.M. Elbashir, J. Harborth, W. Lendeckel, A. Yalcin, K. Weber, T. Tuschl, Duplexes of 21-nucleotide RNAs mediate RNA interference in cultured mammalian cells, Nature. 411 (2001) 494–498. doi:10.1038/35078107.

[11] R.W. Carthew, E.J. Sontheimer, Origins and mechanisms of miRNAs and siRNAs, Cell. 136 (2009) 642–655. doi:10.1016/j.cell.2009.01.035.Origins.

[12] X. Li, R.W. Carthew, A microRNA mediates EGF receptor signaling and promotes photoreceptor differentiation in the Drosophila eye, Cell. 123 (2005) 1267–1277. doi:10.1016/j.cell.2005.10.040.

[13] V.N. Kim, MicroRNA biogenesis: coordinated cropping and dicing., Nat. Rev. Mol. Cell Biol. 6 (2005) 376–85. doi:10.1038/nrm1644.

[14] K. Ui-Tei, Y. Naito, K. Nishi, A. Juni, K. Saigo, Thermodynamic stability and Watson-Crick base pairing in the seed duplex are major determinants of the

efficiency of the siRNA-based off-target effect, Nucleic Acids Res. 36 (2008) 7100–7109. doi:10.1093/nar/gkn902.

[15] L. He, G.J. Hannon, MicroRNAs: small RNAs with a big role in gene regulation., Nat. Rev. Genet. 5 (2004) 522–531. doi:10.1038/nrg1415.

[16] A. Grimson, K.K.-H. Farh, W.K. Johnston, P. Garrett-Engele, L.P. Lim, D.P. Bartel, MicroRNA Targeting Specificity in Mammals: Determinants Beyond Seed Pairing, Mol. Cell. 27 (2007) 91–105. doi:10.1016/j.molcel.2007.06.017.

[17] H. Siomi, M.C. Siomi, On the road to reading the RNA-interference code, Nature. 457 (2009) 396–404. doi:10.1038/nature07754.

[18] D.E. Golden, V.R. Gerbasi, E.J. Sontheimer, An Inside Job for siRNAs, Mol. Cell. 31 (2008) 309–312. doi:10.1016/j.molcel.2008.07.008.An.

[19] Y. Tomari, P.D. Zamore, Y. Tomari, P.D. Zamore, Perspective : machines for RNAi Perspective : machines for RNAi, Genes Dev. (2005) 517–529. doi:10.1101/gad.1284105.

[20] J.K.W. Lam, M.Y.T. Chow, Y. Zhang, S.W.S. Leung, siRNA Versus miRNA as Therapeutics for Gene Silencing, Mol. Ther. Acids. 4 (2015) e252. doi:10.1038/mtna.2015.23.

[21] D.D. Rao, J.S. Vorhies, N. Senzer, J. Nemunaitis, siRNA vs. shRNA: Similarities and differences, Adv. Drug Deliv. Rev. 61 (2009) 746–759. doi:10.1016/j.addr.2009.04.004.

[22] D. Grimm, Small silencing RNAs: state-of-the-art., Adv. Drug Deliv. Rev. 61 (2009) 672–703. doi:10.1016/j.addr.2009.05.002.

[23] J. Perkel, RNAI Therapeutics: A Two-Year Update, Science (80-.). 326 (2009) 454–456.

[24] D.W. Bartlett, M.E. Davis, Insights into the kinetics of siRNA-mediated gene silencing from live-cell and live-animal bioluminescent imaging, Nucleic Acids Res. 34 (2006) 322–333. doi:10.1093/nar/gkj439.

[25] K. Raemdonck, R.E. Vandenbroucke, J. Demeester, N.N. Sanders, S.C. De Smedt, Maintaining the silence: reflections on long-term RNAi, Drug Discov. Today. 13 (2008) 917–931. doi:10.1016/j.drudis.2008.06.008.

[26] G. Sui, C. Soohoo, E.B. Affar, F. Gay, Y. Shi, W.C. Forrester, Y. Shi, A DNA vector-based RNAi technology to suppress gene expression in mammalian cells., Proc. Natl. Acad. Sci. U. S. A. 99 (2002) 5515–20. doi:10.1073/pnas.082117599.

[27] E. Lund, S. Güttinger, A. Calado, J.E. Dahlberg, U. Kutay, Nuclear export of microRNA precursors., Science (80-.). 303 (2004) 95–98. doi:10.1126/science.1090599.

[28] S. Zou, K. Scarfo, M.H. Nantz, J.G. Hecker, Lipid-mediated delivery of RNA is more efficient than delivery of DNA in non-dividing cells, Int. J. Pharm. 389 (2010) 232–243. doi:10.1016/j.ijpharm.2010.01.019.

[29] O. Snøve, J.J. Rossi, Toxicity in mice expressing short hairpin RNAs gives new

insight into RNAi, Genome Biol. 7 (2006) 231. doi:10.1186/gb-2006-7-8-231.

[30] R. Yi, B.P. Doehle, Y. Qin, I.G. Macara, B.R. Cullen, Overexpression of exportin 5 enhances RNA interference mediated by short hairpin RNAs and microRNAs., RNA. 11 (2005) 220–226. doi:10.1261/rna.7233305.

[31] D. Grimm, K.L. Streetz, C.L. Jopling, T.A. Storm, K. Pandey, C.R. Davis, P. Marion, F. Salazar, M.A. Kay, Fatality in mice due to oversaturation of cellular microRNA/short hairpin RNA pathways, Nature. 441 (2006) 537–541. doi:nature04791 [pii]10.1038/nature04791 [doi].

[32] J.C. Giering, D. Grimm, T. a Storm, M. a Kay, Expression of shRNA from a tissue-specific pol II promoter is an effective and safe RNAi therapeutic., Mol. Ther. 16 (2008) 1630–1636. doi:10.1038/mt.2008.144.

[33] M. John, R. Constien, A. Akinc, M. Goldberg, Y.-A. Moon, M. Spranger, P. Hadwiger, J. Soutschek, H.-P. Vornlocher, M. Manoharan, M. Stoffel, R. Langer, D.G. Anderson, J.D. Horton, V. Koteliansky, D. Bumcrot, Effective RNAi-mediated gene silencing without interruption of the endogenous microRNA pathway., Nature. 449 (2007) 745–7. doi:10.1038/nature06179.

[34] W.G. Kaelin, Use and Abuse of RNAi to Study Mammalian Gene Function, Science (80-.). 337 (2012) 421–422.

[35] H.-S. Chang, C.-H. Lin, Y.-C. Chen, W.C.Y. Yu, Using siRNA technique to generate transgenic animals with spatiotemporal and conditional gene knockdown., Am. J. Pathol. 165 (2004) 1535–1541. doi:10.1016/S0002-9440(10)63411-6.

[36] M.T. Hemann, J.S. Fridman, J.T. Zilfou, E. Hernando, P.J. Paddison, C. Cordon-Cardo, G.J. Hannon, S.W. Lowe, An epi-allelic series of p53 hypomorphs created by stable RNAi produces distinct tumor phenotypes in vivo., Nat. Genet. 33 (2003) 396–400. doi:10.1038/ng1091.

[37] K. Kotnik, E. Popova, M. Todiras, M.A. Mori, N. Alenina, J. Seibler, M. Bader, Inducible transgenic rat model for diabetes mellitus based on shRNA-mediated gene knockdown, PLoS One. 4 (2009). doi:10.1371/journal.pone.0005124.

[38] J.E. Zuckerman, M.E. Davis, Clinical experiences with systemically administered siRNA-based therapeutics in cancer, Nat. Rev. Drug Discov. 14 (2015) 843–856. doi:10.1038/nrd4685.

[39] L. Aagaard, J.J. Rossi, RNAi therapeutics: principles, prospects and challenges., Adv. Drug Deliv. Rev. 59 (2007) 75–86. doi:10.1016/j.addr.2007.03.005.

[40] P. Gonzalez-Alegre, Therapeutic RNA interference for neurodegenerative diseases: From promise to progress., Pharmacol. Ther. 114 (2007) 34–55. doi:10.1016/j.pharmthera.2007.01.003.

[41] G. Ozcan, B. Ozpolat, R.L. Coleman, A.K. Sood, G. Lopez-Berestein, Preclinical and clinical development of siRNA-based therapeutics, Adv. Drug Deliv. Rev. 87 (2015) 108–119. doi:10.1016/j.addr.2015.01.007.

[42] K.A. Howard, RNA Interference from Biology to Therapeutics, 2012.

[43] F.M. Van De Water, O.C. Boerman, A.C. Wouterse, J.G.P. Peters, F.G.M. Russel, R. Masereeuw, Intravenously Administered Short Interfering Rna Accumulates in the Kidney and Selectively Suppresses Gene Function in Renal Proximal Tubules Abstract :, Pharmacology. 34 (2006) 1393–1397. doi:10.1124/dmd.106.009555.that.

[44] F. Liu, L.M. Shollenberger, C.C. Conwell, X. Yuan, L. Huang, Mechanism of naked DNA clearance after intravenous injection, J. Gene Med. 9 (2007) 613–619. doi:10.1002/jgm.

[45] J.M. Layzer, A.P. Mccaffrey, A.K. Tanner, Z. a N. Huang, M. a Kay, In vivo activity of nuclease-resistant siRNAs, Rna. 10 (2004) 766–771. doi:10.1261/rna.5239604.The.

[46] D.R. Yazbeck, K.-L. Min, M.J. Damha, Molecular requirements for degradation of a modified sense RNA strand by Escherichia coli ribonuclease H1., Nucleic Acids Res. 30 (2002) 3015–25. doi:10.1093/nar/gkf429.

[47] M.M. Frank, L.F. Fries, The role of complement in inflammation and phagocytosis, Immunol. Today. 12 (1991) 322–326. doi:10.1016/0167-5699(91)90009-I.

[48] D.E. Owens, N.A. Peppas, Opsonization, biodistribution, and pharmacokinetics of polymeric nanoparticles, Int. J. Pharm. 307 (2006) 93–102. doi:10.1016/j.ijpharm.2005.10.010.

[49] B. Ballarín-González, F. Dagnaes-Hansen, R. a Fenton, S. Gao, S. Hein, M. Dong, J. Kjems, K. a Howard, Protection and Systemic Translocation of siRNA Following Oral Administration of Chitosan/siRNA Nanoparticles., Mol. Ther. Nucleic Acids. 2 (2013) e76. doi:10.1038/mtna.2013.2.

[50] D. Haussecker, Current issues of RNAi therapeutics delivery and development, J. Control. Release. 195 (2014) 49–54. doi:10.1016/j.jconrel.2014.07.056.

[51] J. Wang, Z. Lu, M.G. Wientjes, J.L.-S. Au, Delivery of siRNA Therapeutics: Barriers and Carriers, AAPS J. 12 (2010) 492–503. doi:10.1208/s12248-010-9210-4.

[52] M. Gooding, M. Malhotra, J.C. Evans, R. Darcy, C.M. O'Driscoll, Oligonucleotide conjugates – Candidates for gene silencing therapeutics, Eur. J. Pharm. Biopharm. 107 (2016) 321–340. doi:10.1016/j.ejpb.2016.07.024.

[53] N.S. Petrova, M.A. Zenkova, E.L. Chernolovskaya, Structure - Functions Relations in Small Interfering RNAs, in: Pract. Appl. Biomed. Eng., 2012: pp. 187–228.

[54] T.M. Rana, Illuminating the silence: understanding the structure and function of small RNAs, Nat. Rev. Cell Biol. 8 (2007) 23–36. doi:10.1038/nrm2085.

[55] A. Gallas, C. Alexander, M.C. Davies, S. Puri, S. Allen, Chemistry and formulations for siRNA therapeutics., Chem. Soc. Rev. 42 (2013) 7983–97. doi:10.1039/c3cs35520a.

[56] C. Wolfrum, S. Shi, K.N. Jayaprakash, M. Jayaraman, G. Wang, R.K. Pandey, K.G. Rajeev, T. Nakayama, K. Charrise, E.M. Ndungo, T. Zimmermann, V. Koteliansky, M. Manoharan, M. Stoffel, Mechanisms and optimization of in vivo delivery of

lipophilic siRNAs., Nat. Biotechnol. 25 (2007) 1149–1157. doi:10.1038/nbt1339.

[57] F. Iversen, C. Yang, F. Dagnæs-Hansen, D.H. Schaffert, J. Kjems, S. Gao, Optimized siRNA-PEG conjugates for extended blood circulation and reduced urine excretion in mice, Theranostics. 3 (2013) 201–209. doi:10.7150/thno.5743.

[58] M. Hamidi, A. Azadi, P. Rafiei, Pharmacokinetic consequences of pegylation., Drug Deliv. 13 (2006) 399–409. doi:10.1080/10717540600814402.

[59] G. Cesarone, O.P. Edupuganti, C.P. Chen, E. Wickstrom, Insulin receptor substrate 1 knockdown in human MCF7 ER+ breast cancer cells by nuclease-resistant IRS1 siRNA conjugated to a disulfide-bridged D-peptide analogue of insulin-like growth factor 1, Bioconjug. Chem. 18 (2007) 1831–1840. doi:10.1021/bc070135v.

[60] J. Barquinero, H. Eixarch, M. Pérez-Melgosa, Retroviral vectors: new applications for an old tool., Gene Ther. 11 Suppl 1 (2004) S3–S9. doi:10.1038/sj.gt.3302363.

[61] C.X. Li, A. Parker, E. Menocal, S. Xiang, L. Borodyansky, J.H. Fruehauf, Delivery of RNA interference, Cell Cycle. 5 (2006) 2103–2109. doi:10.4161/cc.5.18.3192.

[62] S.R. Choudhury, E. Hudry, C.A. Maguire, M. Sena-Esteves, X.O. Breakefield, P. Grandi, Viral vectors for therapy of neurologic diseases, Neuropharmacology. (2015). doi:10.1016/j.neuropharm.2016.02.013.

[63] S. Nayak, R.W. Herzog, Progress and prospects: immune responses to viral vectors., Gene Ther. 17 (2010) 295–304. doi:10.1038/gt.2009.148.Progress.

[64] W.S.M. Wold, K. Toth, Adenovirus Vectors for Gene Therapy, Vaccination and Cancer Gene Therapy, Curr. Gene Ther. 13 (2013) 421–433.

[65] J.L. Santiago-Ortiz, D. V. Schaffer, Adeno-associated virus (AAV) vectors in cancer gene therapy, J. Control. Release. 240 (2016) 287–301. doi:10.1016/j.jconrel.2016.01.001.

[66] S. David, B. Pitard, J.-P. Benoît, C. Passirani, Non-viral nanosystems for systemic siRNA delivery., Pharmacol. Res. 62 (2010) 100–14. doi:10.1016/j.phrs.2009.11.013.

[67] E. Fattal, G. Barratt, Nanotechnologies and controlled release systems for the delivery of antisense oligonucleotides and small interfering RNA., Br. J. Pharmacol. 157 (2009) 179–94. doi:10.1111/j.1476-5381.2009.00148.x.

[68] S. Zhang, B. Zhao, H. Jiang, B. Wang, B. Ma, Cationic lipids and polymers mediated vectors for delivery of siRNA, J. Control. Release. 123 (2007) 1–10. doi:10.1016/j.jconrel.2007.07.016.

[69] H.M. Aliabadi, B. Landry, C. Sun, T. Tang, H. Uludağ, Supramolecular assemblies in functional siRNA delivery: Where do we stand?, Biomaterials. 33 (2012) 2546–2569. doi:10.1016/j.biomaterials.2011.11.079.

[70] S.S. Kim, H. Garg, A. Joshi, N. Manjunath, Strategies for targeted nonviral

delivery of siRNAs in vivo, Trends Mol. Med. 15 (2009) 491–500. doi:10.1016/j.molmed.2009.09.001.

[71] O. Zelphati, L.S. Uyechi, L.G. Barron, F.C. Szoka, Effect of serum components on the physico-chemical properties of cationic lipid/oligonucleotide complexes and on their interactions with cells, Biochim. Biophys. Acta - Lipids Lipid Metab. 1390 (1998) 119–133. doi:10.1016/S0005-2760(97)00169-0.

[72] H. Lv, S. Zhang, B. Wang, S. Cui, J. Yan, Toxicity of cationic lipids and cationic polymers in gene delivery, J. Control. Release. 114 (2006) 100–109. doi:10.1016/j.jconrel.2006.04.014.

[73] O. Nag, V. Awasthi, Surface Engineering of Liposomes for Stealth Behavior, Pharmaceutics. 5 (2013) 542–569. doi:10.3390/pharmaceutics5040542.

[74] A.A. Mokhtarieh, S. Cheong, S. Kim, B.H. Chung, M.K. Lee, Asymmetric liposome particles with highly efficient encapsulation of siRNA and without nonspecific cell penetration suitable for target-specific delivery, Biochim. Biophys. Acta - Biomembr. 1818 (2012) 1633–1641. doi:10.1016/j.bbamem.2012.03.016.

[75] A. Ewe, O. Panchal, S.R. Pinnapireddy, U. Bakowsky, S. Przybylski, A. Temme, A. Aigner, Liposome-polyethylenimine complexes (DPPC-PEI lipopolyplexes) for therapeutic siRNA delivery in vivo, Nanomedicine Nanotechnology, Biol. Med. 13 (2017) 209–218. doi:10.1016/j.nano.2016.08.005.

[76] T.G. Iversen, T. Skotland, K. Sandvig, Endocytosis and intracellular transport of nanoparticles: Present knowledge and need for future studies, Nano Today. 6 (2011) 176–185. doi:10.1016/j.nantod.2011.02.003.

[77] S. Xu, B.Z. Olenyuk, C.T. Okamoto, S.F. Hamm-Alvarez, Targeting receptor-mediated endocytotic pathways with nanoparticles: Rationale and advances, Adv. Drug Deliv. Rev. 65 (2013) 121–138. doi:10.1016/j.addr.2012.09.041.

[78] J.P. Luzio, M.D.J. Parkinson, S.R. Gray, N. a Bright, The delivery of endocytosed cargo to lysosomes., Biochem. Soc. Trans. 37 (2009) 1019–1021. doi:10.1042/BST0371019.

[79] W. Liang, J.K.W. Lam, Endosomal Escape Pathways for Non-Viral Nucleic Acid Delivery Systems, in: Mol. Regul. Endocytosis, 2012: pp. 429–456. doi:10.5772/46006.

[80] A. Akinc, M. Thomas, A.M. Klibanov, R. Langer, Exploring polyethylenimine-mediated DNA transfection and the proton sponge hypothesis, J. Gene Med. 7 (2005) 657–663. doi:10.1002/jgm.696.

[81] I.S. Zuhorn, U. Bakowsky, E. Polushkin, W.H. Visser, M.C.A. Stuart, J.B.F.N. Engberts, D. Hoekstra, Nonbilayer phase of lipoplex-membrane mixture determines endosomal escape of genetic cargo and transfection efficiency, Mol. Ther. 11 (2005) 801–810. doi:10.1016/j.ymthe.2004.12.018.

[82] W. Li, F. Nicol, F.C. Szoka, GALA: A designed synthetic pH-responsive amphipathic peptide with applications in drug and gene delivery, Adv. Drug Deliv. Rev. 56 (2004) 967–985. doi:10.1016/j.addr.2003.10.041.

[83] Safety Study of CALAA-01 to Treat Solid Tumor Cancers, Clinicaltrials.gov. (n.d.). https://clinicaltrials.gov/ct2/show/NCT00689065.

[84] M.E. Davis, J.E. Zuckerman, C.H.J. Choi, D. Seligson, A. Tolcher, C. a Alabi, Y. Yen, J.D. Heidel, A. Ribas, Evidence of RNAi in humans from systemically administered siRNA via targeted nanoparticles., Nature. 464 (2010) 1067–70. doi:10.1038/nature08956.

[85] C. Lorenzer, M. Dirin, A.-M. Winkler, V. Baumann, J. Winkler, Going beyond the liver: Progress and challenges of targeted delivery of siRNA therapeutics, J. Control. Release. 203 (2015) 1–15. doi:10.1016/j.jconrel.2015.02.003.

[86] L.C. Gomes-Da-Silva, S. Simões, J.N. Moreira, Challenging the future of siRNA therapeutics against cancer: The crucial role of nanotechnology, Cell. Mol. Life Sci. 71 (2014) 1417–1438. doi:10.1007/s00018-013-1502-2.

[87] A.M. O'Mahony, B.M.D.C. Godinho, J.F. Cryan, C.M. O'Driscoll, Non-viral nanosystems for gene and small interfering RNA delivery to the central nervous system: formulating the solution., J. Pharm. Sci. 102 (2013) 3469–84. doi:10.1002/jps.23672.

[88] N.J. Abbott, L. Rönnbäck, E. Hansson, Astrocyte–endothelial interactions at the blood–brain barrier, Nat. Rev. Neurosci. 7 (2006) 41–53. doi:10.1038/nrn1824.

[89] E. Garcia-Garcia, K. Andrieux, S. Gil, P. Couvreur, Colloidal carriers and blood-brain barrier (BBB) translocation: A way to deliver drugs to the brain?, Int. J. Pharm. 298 (2005) 274–292. doi:10.1016/j.ijpharm.2005.03.031.

[90] F. Lai, A.M. Fadda, C. Sinico, Liposomes for brain delivery., Expert Opin. Drug Deliv. 10 (2013) 1003–22. doi:10.1517/17425247.2013.766714.

[91] H.L. Wong, X.Y. Wu, R. Bendayan, Nanotechnological advances for the delivery of CNS therapeutics., Adv. Drug Deliv. Rev. 64 (2012) 686–700. doi:10.1016/j.addr.2011.10.007.

[92] Y. Chen, L. Liu, Modern methods for delivery of drugs across the blood-brain barrier, Adv. Drug Deliv. Rev. 64 (2012) 640–665. doi:10.1016/j.addr.2011.11.010.

[93] J. V. Georgieva, D. Hoekstra, I.S. Zuhorn, Smuggling Drugs into the Brain: An Overview of Ligands Targeting Transcytosis for Drug Delivery across the Blood-Brain Barrier, Pharmaceutics. 6 (2014) 557–583. doi:10.3390/pharmaceutics6040557.

[94] E. Soddu, G. Rassu, P. Giunchedi, B. Sarmento, E. Gavini, From naturally-occurring neurotoxic agents to CNS shuttles for drug delivery, Eur. J. Pharm. Sci. 74 (2015) 63–76. doi:10.1016/j.ejps.2015.04.005.

[95] P. Kumar, H. Wu, J.L. McBride, K.-E. Jung, M.H. Kim, B.L. Davidson, S.K. Lee, P. Shankar, N. Manjunath, Transvascular delivery of small interfering RNA to the central nervous system., Nature. 448 (2007) 39–43. doi:10.1038/nature05901.

[96] R. Daneman, The blood-brain barrier in health and disease, Ann. Neurol. 72 (2012) 648–672. doi:10.1002/ana.23648.

[97] D.R. Groothuis, The blood-brain and blood-tumor barriers: a review of strategies for increasing drug delivery, Neuro. Oncol. 2 (2000) 45–59.

[98] O. van Tellingen, B. Yetkin-Arik, M.C. de Gooijer, P. Wesseling, T. Wurdinger, H.E. de Vries, Overcoming the blood–brain tumor barrier for effective glioblastoma treatment, Drug Resist. Updat. 19 (2015) 1–12. doi:10.1016/j.drup.2015.02.002.

[99] D. Karra, R. Dahm, Transfection techniques for neuronal cells., J. Neurosci. 30 (2010) 6171–6177. doi:10.1523/JNEUROSCI.0183-10.2010.

[100] A.M. Krichevsky, K.S. Kosik, RNAi functions in cultured mammalian neurons., Proc. Natl. Acad. Sci. U. S. A. 99 (2002) 11926–11929. doi:10.1073/pnas.182272699.

[101] J.T. Bendor, T.P. Logan, R.H. Edwards, The Function of α-Synuclein, Neuron. 79 (2013) 1044–1066. doi:10.1016/j.neuron.2013.09.004.

[102] P.J. Mclean, H. Kawamata, S. Ribich, B.T. Hyman, Membrane Association and Protein Conformation of α-Synuclein in, J. Biol. Chem. 275 (2000) 8812–8816. doi:10.1074/jbc.275.12.8812.

[103] H.A. Lashuel, C.R. Overk, A. Oueslati, E. Masliah, The many faces of α-synuclein: from structure and toxicity to therapeutic target., Nat. Rev. Neurosci. 14 (2013) 38–48. doi:10.1038/nrn3406.

[104] A. Bellucci, N.B. Mercuri, A. Venneri, G. Faustini, F. Longhena, M. Pizzi, C. Missale, P. Spano, Parkinson's disease: From synaptic loss to connectome dysfunction, Neuropathol. Appl. Neurobiol. 42 (2016) 77–94. doi:10.1111/nan.12297.

[105] A. Bellucci, M. Zaltieri, L. Navarria, J. Grigoletto, C. Missale, P. Spano, From α-synuclein to synaptic dysfunctions: New insights into the pathophysiology of Parkinson's disease, Brain Res. 1476 (2012) 183–202. doi:10.1016/j.brainres.2012.04.014.

[106] D.M. Maraganore, Rationale for Therapeutic Silencing of Alpha-Synuclein in Parkinson ' s Disease, J. Mov. Disord. 4 (2011) 1–7.

[107] C.G. Specht, R. Schoepfer, Deletion of the alpha-synuclein locus in a subpopulation of C57BL/6J inbred mice., BMC Neurosci. 2 (2001) 11. doi:10.1186/1471-2202-2-11.

[108] M.G. Spillantini, A.R. Crowther, R. Jakes, M. Hasegawa, M. Goedert, a-Synuclein in filamentous inclusions of Lewy bodies from Parkinson ' s disease and dementia with Lewy bodies, PNAS. 95 (1998) 6469–6473.

[109] H. Braak, K. Del Tredici, U. Rüb, R. a. . de Vos, E.N.. Jansen Steur, E. Braak, Staging of brain pathology related to sporadic Parkinson's disease, Neurobiol. Aging. 24 (2003) 197–211. doi:10.1016/S0197-4580(02)00065-9.

[110] A. Eslamboli, M. Romero-Ramos, C. Burger, T. Bjorklund, N. Muzyczka, R.J. Mandel, H. Baker, R.M. Ridley, D. Kirik, Long-term consequences of human alpha-synuclein overexpression in the primate ventral midbrain., Brain. 130

(2007) 799–815. doi:10.1093/brain/awl382.

[111] V.N. Uversky, Neuropathology, biochemistry, and biophysics of alpha-synuclein aggregation., J. Neurochem. 103 (2007) 17–37. doi:10.1111/j.1471-4159.2007.04764.x.

[112] M.K. Sapru, J.W. Yates, S. Hogan, L. Jiang, J. Halter, M.C. Bohn, Silencing of human alpha-synuclein in vitro and in rat brain using lentiviral-mediated RNAi., Exp. Neurol. 198 (2006) 382–90. doi:10.1016/j.expneurol.2005.12.024.

[113] J. Lewis, H. Melrose, D. Bumcrot, A. Hope, C. Zehr, S. Lincoln, A. Braithwaite, Z. He, S. Ogholikhan, K. Hinkle, C. Kent, I. Toudjarska, K. Charisse, R. Braich, R.K. Pandey, M. Heckman, D.M. Maraganore, J. Crook, M.J. Farrer, In vivo silencing of alpha-synuclein using naked siRNA., Mol. Neurodegener. 3 (2008) 19. doi:10.1186/1750-1326-3-19.

[114] A.L. McCormack, S.K. Mak, J.M. Henderson, D. Bumcrot, M.J. Farrer, D. a Di Monte, Alpha-synuclein suppression by targeted small interfering RNA in the primate substantia nigra., PLoS One. 5 (2010) e12122. doi:10.1371/journal.pone.0012122.

[115] O.S. Gorbatyuk, S. Li, K. Nash, M. Gorbatyuk, A.S. Lewin, L.F. Sullivan, R.J. Mandel, W. Chen, C. Meyers, F.P. Manfredsson, N. Muzyczka, In vivo RNAi-mediated alpha-synuclein silencing induces nigrostriatal degeneration., Mol. Ther. 18 (2010) 1450–7. doi:10.1038/mt.2010.115.

[116] J. Yang, H. Liu, X. Zhang, Design, preparation and application of nucleic acid delivery carriers, Biotechnol. Adv. 32 (2014) 804–817. doi:10.1016/j.biotechadv.2013.11.004.

[117] J.M. Cooper, P.B.O. Wiklander, J.Z. Nordin, R. Al-Shawi, M.J. Wood, M. Vithlani, A.H. V Schapira, J.P. Simons, S. El-Andaloussi, L. Alvarez-Erviti, Systemic exosomal siRNA delivery reduced alpha-synuclein aggregates in brains of transgenic mice., Mov. Disord. 29 (2014) 1476–85. doi:10.1002/mds.25978.

[118] L. Alvarez-erviti, Y. Seow, H. Yin, C. Betts, S. Lakhal, M.J.A. Wood, Delivery of siRNA to the mouse brain by systemic injection of targeted exosomes, Nat. Biotechnol. 29 (2011) 341–345. doi:10.1038/nbt.1807.

[119] P.D. Robbins, A.E. Morelli, Regulation of Immune Responses by Extracellular Vesicules, Nat. Immunol. 14 (2014) 195–208. doi:10.1038/nri3622.Regulation.

[120] P. Vader, E.A. Mol, G. Pasterkamp, R.M. Schiffelers, Extracellular vesicles for drug delivery, Adv. Drug Deliv. Rev. (2016). doi:10.1016/j.addr.2016.02.006.

[121] M.A. De Luca, F. Lai, F. Corrias, P. Caboni, Z. Bimpisidis, E. Maccioni, A.M. Fadda, G. Di Chiara, Lactoferrin- and antitransferrin-modified liposomes for brain targeting of the NK3 receptor agonist senktide: Preparation and in vivo evaluation, Int. J. Pharm. 479 (2015) 129–137. doi:10.1016/j.ijpharm.2014.12.057.

[122] B. Ozpolat, A.K. Sood, G. Lopez-Berestein, Liposomal siRNA nanocarriers for cancer therapy., Adv. Drug Deliv. Rev. 66 (2014) 110–6. doi:10.1016/j.addr.2013.12.008.

[123] W. Li, F.C. Szoka, Lipid-based nanoparticles for nucleic acid delivery., Pharm. Res. 24 (2007) 438–49. doi:10.1007/s11095-006-9180-5.

[124] M. Kapoor, D.J. Burgess, S.D. Patil, Physicochemical characterization techniques for lipid based delivery systems for siRNA., Int. J. Pharm. 427 (2012) 35–57. doi:10.1016/j.ijpharm.2011.09.032.

[125] K. Buyens, J. Demeester, S.S. De Smedt, N.N. Sanders, Elucidating the encapsulation of short interfering RNA in PEGylated cationic liposomes., Langmuir. 25 (2009) 4886–91. doi:10.1021/la803973p.

[126] H. Huo, Y. Gao, Y. Wang, J. Zhang, Z. Wang, T. Jiang, S. Wang, Polyion complex micelles composed of pegylated polyasparthydrazide derivatives for siRNA delivery to the brain, J. Colloid Interface Sci. 447 (2015) 8–15. doi:10.1016/j.jcis.2015.01.043.

[127] M. Lafon, Rabies virus receptors, J. Neurovirol. 11 (2005) 82–87. doi:10.1080/13550280590900427.

[128] M. Bauer, B.W. Kristensen, M. Meyer, T. Gasser, H.R. Widmer, J. Zimmer, M. Ueffing, Toxic effects of lipid-mediated gene transfer in ventral mesencephalic explant cultures, Basic Clin. Pharmacol. Toxicol. 98 (2006) 395–400. doi:10.1111/j.1742-7843.2006.pto_310.x.

[129] M. Zaltieri, J. Grigoletto, F. Longhena, L. Navarria, G. Favero, S. Castrezzati, M.A. Colivicchi, L. Della Corte, R. Rezzani, M. Pizzi, F. Benfenati, M.G. Spillantini, C. Missale, P. Spano, A. Bellucci, α-synuclein and synapsin III cooperatively regulate synaptic function in dopamine neurons., J. Cell Sci. 128 (2015) 2231–43. doi:10.1242/jcs.157867.

[130] J. a Schwartzbaum, J.L. Fisher, K.D. Aldape, M. Wrensch, Epidemiology and molecular pathology of glioma., Nat. Clin. Pract. Neurol. 2 (2006) 494–503; quiz 1 p following 516. doi:10.1038/ncpneuro0289.

[131] D.N. Louis, H. Ohgaki, O.D. Wiestler, W.K. Cavenee, P.C. Burger, A. Jouvet, B.W. Scheithauer, P. Kleihues, The 2007 WHO Classification of Tumours of the Central Nervous System, Acta Neuropathol. 114 (2007) 97–109. doi:10.1007/s00401-007-0243-4.

[132] J.P. Thakkar, T. a. Dolecek, C. Horbinski, Q.T. Ostrom, D.D. Lightner, J.S. Barnholtz-Sloan, J.L. Villano, Epidemiologic and Molecular Prognostic Review of Glioblastoma, Cancer Epidemiol. Biomarkers Prev. 23 (2014) 1985–1996. doi:10.1158/1055-9965.EPI-14-0275.

[133] C. Alifieris, D.T. Trafalis, Glioblastoma Multiforme: Pathogenesis and Treatment., Pharmacol. Ther. 152 (2015) 1–20. doi:10.1016/j.pharmthera.2015.05.005.

[134] M.. Castro, R. Cowen, I.. Williamson, a David, M.. Jimenez-Dalmaroni, X. Yuan, a Bigliari, J.. Williams, J. Hu, P.. Lowenstein, Current and future strategies for the treatment of malignant brain tumors, Pharmacol. Ther. 98 (2003) 71–108. doi:10.1016/S0163-7258(03)00014-7.

[135] L.P. Serwer, C.D. James, Challenges in drug delivery to tumors of the central

nervous system: An overview of pharmacological and surgical considerations, Adv. Drug Deliv. Rev. 64 (2012) 590–597. doi:10.1016/j.addr.2012.01.004.

[136] R. Stupp, W.P. Mason, M.J. van den Bent, M. Weller, B. Fisher, M.J.B. Taphoorn, K. Belanger, A.A. Brandes, C. Marosi, U. Bogdahn, J. Curschmann, R.C. Janzer, S.K. Ludwin, T. Gorlia, A. Allgeier, D. Lacombe, J.G. Cairncross, E. Eisenhauer, R.O. Mirimanoff, Radiotherapy plus Concomitant and Adjuvant Temozolomide for Glioblastoma, N. Engl. J. Med. 352 (2005) 987–996. doi:10.1056/NEJMoa043330.

[137] M. Gil-Gil, M. Gil-Gil, C. Mesia, M. Rey, J. Bruna, Bevacizumab for the Treatment of Glioblastoma, Clin. Med. Insights Oncol. (2013) 123. doi:10.4137/CMO.S8503.

[138] N.S. Ningaraj, Drug delivery to brain tumours: challenges and progress, Expert Opin. Drug Deliv. 3 (2006) 499–509. doi:10.1517/17425247.3.4.499.

[139] L.G. Dubois, L. Campanati, C. Righy, I. Dâ€™Andrea-Meira, T.C.L. de S. e Spohr, I. Porto-Carreiro, C.M. Pereira, J. BalÃ§a-Silva, S.A. Kahn, M.F. DosSantos, M. de A.R. Oliveira, A. Ximenes-da-Silva, M.C. Lopes, E. Faveret, E.L. Gasparetto, V. Moura-Neto, Gliomas and the vascular fragility of the blood brain barrier, Front. Cell. Neurosci. 8 (2014) 1–13. doi:10.3389/fncel.2014.00418.

[140] N. Parker, M.J. Turk, E. Westrick, J.D. Lewis, P.S. Low, C.P. Leamon, Folate receptor expression in carcinomas and normal tissues determined by a quantitative radioligand binding assay, Anal. Biochem. 338 (2005) 284–293. doi:10.1016/j.ab.2004.12.026.

[141] S.D. Weitman, K.M. Frazier, B.A. Kamen, The folate receptor in central nervous system malignancies of childhood, J Neurooncol. 21 (1994) 107–112.

[142] P.S. Low, S.A. Kularatne, Folate-targeted therapeutic and imaging agents for cancer, Curr. Opin. Chem. Biol. 13 (2009) 256–262. doi:10.1016/j.cbpa.2009.03.022.

[143] Y. Lu, P.S. Low, Folate-mediated delivery of macromolecular anticancer therapeutic agents, Adv. Drug Deliv. Rev. 64 (2012) 342–352. doi:10.1016/j.addr.2012.09.020.

[144] Y.C. Chen, C.F. Chiang, L.F. Chen, P.C. Liang, W.Y. Hsieh, W.L. Lin, Polymersomes conjugated with des-octanoyl ghrelin and folate as a BBB-penetrating cancer cell-targeting delivery system, Biomaterials. 35 (2014) 4066–4081. doi:10.1016/j.biomaterials.2014.01.042.

[145] J.Q. Gao, Q. Lv, L.M. Li, X.J. Tang, F.Z. Li, Y.L. Hu, M. Han, Glioma targeting and blood-brain barrier penetration bydual-targeting doxorubincin liposomes, Biomaterials. 34 (2013) 5628–5639. doi:10.1016/j.biomaterials.2013.03.097.

[146] M. Grapp, A. Wrede, M. Schweizer, S. Hüwel, H.-J. Galla, N. Snaidero, M. Simons, J. Bückers, P.S. Low, H. Urlaub, J. Gärtner, R. Steinfeld, Choroid plexus transcytosis and exosome shuttling deliver folate into brain parenchyma., Nat. Commun. 4 (2013) 2123. doi:10.1038/ncomms3123.

[147] J.R. Araújo, P. Gonçalves, F. Martel, Characterization of uptake of folates by rat

and human blood-brain barrier endothelial cells, BioFactors. 36 (2010) 201–209. doi:10.1002/biof.82.

[148] E. Wyszko, K. Rolle, S. Nowak, R. Zukiel, M. Nowak, R. Piestrzeniewicz, I. Gawrońska, M.Z. Barciszewska, J. Barciszewski, A multivariate analysis of patients with brain tumors treated with ATN-RNA., Acta Pol. Pharm. 65 (2008) 677–684.

[149] L. Wei, X.Y. Guo, T. Yang, M.Z. Yu, D.W. Chen, J.C. Wang, Brain tumor-targeted therapy by systemic delivery of siRNA with Transferrin receptor-mediated core-shell nanoparticles, Int. J. Pharm. 510 (2016) 394–405. doi:10.1016/j.ijpharm.2016.06.127.

[150] J. Jung, A. Solanki, K.A. Memoli, K. Kamei, H. Kim, M. Drahl, L.J. Williams, H.-R. Tseng, K.-B. Lee, Selective inhibition of human brain tumor cell proliferation via multifunctional quantum dot-based siRNA delivery, Angew. Chemie. 49 (2010) 103–107. doi:10.1002/anie.200905126.Selective.

[151] M.L. Meistrich, B. Mohapatra, C.R. Shirley, M. Zhao, Roles of transition nuclear proteins in spermiogenesis., Chromosoma. 111 (2003) 483–488. doi:10.1007/s00412-002-0227-z.

[152] C.M. Paulos, J. a Reddy, C.P. Leamon, M.J. Turk, P.S. Low, Ligand binding and kinetics of folate receptor recycling in vivo: impact on receptor-mediated drug delivery., Mol. Pharmacol. 66 (2004) 1406–1414. doi:10.1124/mol.104.003723.

[153] M. Malhotra, A. Toulouse, B. Godinho, D. McCarthy, J.F. Cryan, C. O'Driscoll, RNAi therapeutics for brain cancer: Current advancements in RNAi delivery strategies, Mol. BioSyst. 11 (2015) 2635–2657. doi:10.1039/C5MB00278H.

[154] P. Zhao, H. Wang, H. Gao, C. Li, Y. Zhang, Reversal of multidrug resistance by magnetic chitosan-Fe(3)O(4) nanoparticle-encapsulated MDR(1) siRNA in glioblastoma cell line., Neurol. Res. 35 (2013) 821–828. doi:10.1179/1743132813Y.0000000218.

[155] A. Arora, M.R. Prausnitz, S. Mitragotri, Micro-scale devices for transdermal drug delivery., Int. J. Pharm. 364 (2008) 227–36. doi:10.1016/j.ijpharm.2008.08.032.

[156] S. Mitragotri, Current status and future prospects of needle-free liquid jet injectors., Nat. Rev. Drug Discov. 5 (2006) 543–548. doi:10.1038/nrd2076.

[157] J. Baxter, S. Mitragotri, Needle-free liquid jet injections: mechanisms and applications., Expert Rev. Med. Devices. 3 (2006) 565–74. doi:10.1586/17434440.3.5.565.

[158] J. Schramm-baxter, S. Mitragotri, Needle-free jet injections : dependence of jet penetration and dispersion in the skin on jet power, J. Control. Release. 97 (2004) 527–535. doi:10.1016/j.jconrel.2004.04.006.

[159] Y. Michinaka, S. Mitragotri, Delivery of polymeric particles into skin using needle-free liquid jet injectors., J. Control. Release. 153 (2011) 249–54. doi:10.1016/j.jconrel.2011.03.024.

[160] M. Harris, R. Joy, G. Larsen, M. Valyi, E. Walker, L.W. Frick, R.M. Palmatier, S. a.

Wring, J.S.G. Montaner, Enfuvirtide plasma levels and injection site reactions using a needle-free gas-powered injection system (Biojector), Aids. 20 (2006) 719–723. doi:10.1016/j.athoracsur.2005.12.029.

[161] D. Leng, H. Chen, G. Li, M. Guo, Z. Zhu, L. Xu, Y. Wang, Development and comparison of intramuscularly long-acting paliperidone palmitate nanosuspensions with different particle size, Int. J. Pharm. 472 (2014) 380–385. doi:10.1016/j.ijpharm.2014.05.052.

[162] C.F. Goh, M.E. Lane, Formulation of diclofenac for dermal delivery, Int. J. Pharm. 473 (2014) 607–616. doi:10.1016/j.ijpharm.2014.07.052.

[163] D. Cosco, C. Celia, F. Cilurzo, E. Trapasso, D. Paolino, Colloidal carriers for the enhanced delivery through the skin, Expert Opin. Drug Deliv. 5 (2008) 737–55. doi:10.1517/17425247.5.7.737.

[164] M.M.A. Elsayed, O.Y. Abdallah, V.F. Naggar, N.M. Khalafallah, Deformable liposomes and ethosomes as carriers for skin delivery of ketotifen, Pharmazie. 62 (2007) 133–137. doi:10.1691/ph.2007.2.6082.

[165] C. Sinico, A.M. Fadda, Vesicular carriers for dermal drug delivery, Expert Opin. Drug Deliv. 6 (2009) 813–825.

[166] G. Gregoriadis, Liposome Technology, 2007.

[167] G. Pabst, M. Rappolt, H. Amenitsch, P. Laggner, Structural information from\nmultilamellar liposomes at full hydration: Full q-range fitting with high quality x-ray\ndata, Phys Rev E. 52 (2000) 4000–4009.

[168] M. Carboni, A.M. Falchi, S. Lampis, C. Sinico, M.L. Manca, J. Schmidt, Y. Talmon, S. Murgia, M. Monduzzi, Physicochemical, Cytotoxic, and Dermal Release Features of a Novel Cationic Liposome Nanocarrier, Adv. Healthc. Mater. 2 (2013) 692–701. doi:10.1002/adhm.201200302.

[169] J. Pan, S. Tristram-Nagle, N. Kucerka, J.F. Nagle, Temperature dependence of structure, bending rigidity, and bilayer interactions of dioleoylphosphatidylcholine bilayers., Biophys. J. 94 (2008) 117–24. doi:10.1529/biophysj.107.115691.

[170] Y. Talmon, The study of nanostructured liquids by cryogenic-temperature electron microscopy - A status report, J. Mol. Liq. 210 (2015) 2–8. doi:10.1016/j.molliq.2015.03.054.

[171] J.R. Schramm-Baxter, S. Mitragotri, Needle-free jet injections: dependence of jet penetration and dispersion in the skin on jet power, J. Control. Release. 97 (2004) 527–535.

[172] F. Cilurzo, P. Minghetti, C. Sinico, Newborn pig skin as model membrane in in vitro drug permeation studies: a technical note., AAPS PharmSciTech. 8 (2007) E94. doi:10.1208/pt0804094.

[173] C. Sinico, D. Valenti, M. Manconi, F. Lai, A.M. Fadda, Cutaneous delivery of 8-methoxypsoralen from liposomal and niosomal carriers, J. Drug Deliv. Sci. Technol. 16 (2006) 115–120.

[174] G. Cevc, G. Blume, Hydrocortisone and dexamethasone in very deformable drug carriers have increased biological potency, prolonged effect, and reduced therapeutic dosage, Biochim. Biophys. Acta - Biomembr. 1663 (2004) 61–73. doi:10.1016/j.bbamem.2004.01.006.

[175] C. Caddeo, M. Manconi, A.M. Fadda, F. Lai, S. Lampis, O. Diez-Sales, C. Sinico, Nanocarriers for antioxidant resveratrol: Formulation approach, vesicle self-assembly and stability evaluation, Colloids Surfaces B Biointerfaces. 111 (2013) 327–332. doi:10.1016/j.colsurfb.2013.06.016.

[176] T.M. Allen, P.R. Cullis, Liposomal drug delivery systems: From concept to clinical applications, Adv. Drug Deliv. Rev. 65 (2013) 36–48. doi:10.1016/j.addr.2012.09.037.

[177] B. Ozbakir, B.J. Crielaard, J.M. Metselaar, G. Storm, T. Lammers, Liposomal corticosteroids for the treatment of inflammatory disorders and cancer., J. Control. Release. 190 (2014) 624–36. doi:10.1016/j.jconrel.2014.05.039.